FACILITY SITING AND LAYOUT OPTIMIZATION FOR RISK REDUCTION OF OFFSHORE OPERATIONS

A Dissertation

by

JOSHUA PAUL RICHARDSON

Submitted to the Office of Graduate and Professional Studies of
Texas A&M University
in partial fulfillment of the requirements for the degree of

DOCTOR OF PHILOSOPHY

Chair of Committee,	M. Sam Mannan
Committee Members,	Mahmoud El-Halwagi
	James Holste
	Halit Uster
Head of Department,	M. Nazmul Karim

August 2015

Major Subject: Chemical Engineering

ABSTRACT

An MINLP optimization model has been created that optimizes the layout of a set of sections with fixed footprint areas bound to an offshore platform of a given size based on safety considerations due to fire, explosion, and toxic scenarios. Process parameters are used to estimate the probability of an event as well as the magnitude of the possible impact on other sections, which can be weighted in importance in the objective. The magnitude of the impact is directly dependent on several factors: the spacing between the sections, the congestion in the general vicinity of the section, escape routes, and domino effects of fire and explosion.

Explosion modeling is carried out both for vapor cloud explosions ignited within the area that they are created, and dispersed flammable clouds with footprints based on weather conditions, congestion, and process conditions. Modeling uses an approximation to the TNO multi-energy method which takes into account the amount of congestion and confinement in the area and the size of the flammable cloud.

Fire modeling is used to ascertain the adequacy of layout of both sections and muster points that the sections are assigned to. Modeling is done using three different correlations for different fire scenarios: pool fire, fireball, and jet fire. Toxic effects of combustion products and escape-hindering effects of smoke production are also incorporated into the model, accounting for weather conditions and local congestion.

Toxic modeling is based on the same dispersion modeling estimation as the explosion and fire scearios use and focuses on the effect of hydrogen sulfide leaks causing incapacitation, escape difficulties due to eye irritation and disorientation, and death.

Dispersion modeling to determine effects of smoke, dispersed gas clouds, and toxic vapors is carried out in three-dimensions using the CFD software FLACS and the anticipated congestion model (ACM), a method that has not yet been applied to generalized dispersion. The results are correlated to an expression as a function of flow

rate, congestion, windspeed, and their interactions that can be used in the optimization formulation.

Mitigations are also considered; blast walls and fire walls, both ideal (non-failing) and with failure mechanisms, are incorporated into the model as a key component considered during the layout.

It is shown that the model is a positive step into an area that has sparsely been considered, contributing a framework for the integrated consideration and minimization of several key risk factors in the offshore realm that, as yet, have been unexplored from the numerical optimization viewpoint.

DEDICATION

This work is dedicated to my sanity, which sadly passed away during the course of my Ph.D. work. I miss you, buddy.

ACKNOWLEDGMENTS

I would like to acknowledge my gratitude to the many people that assisted me and gave me moral support during my graduate studies at Texas A&M, both in direct regard to academics and for the ones that helped me through the tough times and the calm, the good and bad, and during the times that I didn't think I had the will to keep going. I'm glad I had so many incredible people to take this trip with.

I wouldn't be where I am right now without the guidance of my adviser, Dr. Sam Mannan. It is a testament to the motivation that he has given me and high standard to which he has held me that I've been able to make it this far. Through the broad range of experiences that I've been lucky enough to have while at the Center, I have become a more well-rounded and skilled person, and I owe a debt of gratitude to Dr. Mannan for giving me this opportunity.

I also thank my committee members – Dr. Mahmoud El-Halwagi, Dr. Jim Holste, and Dr. Halit Uster, as well as my past committee member Dr. Carl Laird and my two-time substitute committee member Dr. Charles Glover, all of whom I respect greatly and am indebted to for taking the time to be on my committee.

Within the Center, I wish to thank my team leader, Dr. Yi Liu for helping me out greatly with my research, providing helpful advice, and assisting with the editing and revision of my papers and dissertation. I also thank the rest of the postdocs, past and present (too many to name!) for their interest in my research and for their support.

To all the other students that have come through the Center while I've been here, whether you graduated before I really got started, or whether I'm out the door as you're coming in; whether we knew each other well, or only talked a little: although it's been a long few years, I wouldn't trade the experience for anything and it's all because of your friendship and the good times we've all shared. And I think that's the highest compliment I can give to anyone.

Finally, to my family, who has given me more support and love than I know what to do with: it's over!

NOMENCLATURE

Sets

F	a set of floors that sections may be allocated to
J	a set of sections to be placed in the layout, generally an intermediate section in impact modeling
K	a set of sections to be placed in the layout, generally the affecting section in impact modeling
L	a set of floors that sections may be allocated to, used in comparisons with set F
M	a set of monitor regions for dispersion, used on left side of variables and parameters
M	a set of muster points that are allocated to the platform
R	a set of release directions for dispersion, used on left side of variables and parameters
S	a set of sections to be placed in the layout, generally the affected section in impact modeling

Scalars and Parameters

AR_S	the maximum aspect ratio between the longest and shortest side of a section, s
$Area_S$	the footprint area per floor that a section, s, occupies
CC_K	characteristic congestion in section k
CC_B	characteristic background congestion
$cost_S$	scaling factor for the objective function, synonymous with the number of personnel within a section s
$FloorSpacing$	the height of a floor and the separation distance between the deck of one floor and another
LBx_S	the lower bound on the x-direction size of section s
LBy_S	the lower bound on the y-direction size of section s
M	a “Big-M” scalar for use in the non-overlap
$MaxWalls$	maximum number of blast walls that can be allocated
N	maximum number of personnel a muster point can

	accommodate
P_{rated}	rated yield pressure for a blast wall
$P_{1\% dest}$	overpressure at which 1% destruction, calculated from probit function, occurs
$Personnel_S$	number of personnel allocated to section s
$SectionCost_S$	the relative cost of a section, s, that is used in the objective function as a scaling factor
sep	a minimum separation distance between two sections
$Stories_S$	the number of floors that a section, s, occupies
${}_{R,M}tac$	base flow coefficient for a release in the R-direction in the M-direction monitor region
${}_{R,M}te$	base congestion coefficient for a release in the R-direction in the M-direction monitor region
${}_{R,M}tfi$	proportional wind coefficient for a release in the R-direction in the M-direction monitor region
${}_{R,M}tg$	base wind coefficient for a release in the R-direction in the M-direction monitor region
UBx_S	the upper bound on the x-direction size of section s
UBy_S	the upper bound on the y-direction size of section s
W_X	the x-direction width of the platform
W_Y	the y-direction width of the platform

Variables

$a_{S,K,F}$	binary non-overlap variable defining whether section k exists to the +x-direction of section s (1) or not (0)
$b_{S,K,F}$	binary non-overlap variable defining whether section k exists to the –x-direction of section s (1) or not (0)
${}_{M}BR_{S,F}$	calculated blockage ratio in the M-direction of s on floor f
$BW_{s,k}$	binary variable denoting that a blast from section k is affected by any blast wall if 1, not affected if 0
${}_{M}BW_{S,K}$	binary variable denoting that an explosion from section k is affected by an allocated blast wall on section s in the M-direction if 1, not affected if 0

$c_{S,K,F}$	binary non-overlap variable defining whether section k exists to the +y-direction of section s (1) or not (0)
${}_{R,M}c'_{S,K,F}$	scaled explosion coefficient for a dispersed cloud explosion in section s on floor f in monitor region M due to an R-direction release from section k
${}_{R,M}Conc_{S,K,F}$	concentration of flammable gas in a monitor region M in which section s resides existing on floor f due to a release in the R-direction in section k
$d_{D,K,F}$	binary non-overlap variable defining whether section k exists to the –y-direction of section s (1) or not (0)
$DestructionProbability_{S,K}$	the probability that an explosion in section k will cause the destruction of section s
$down^*_{S,K,F,L}$	binary variable denoting whether section s existing on floor f is on a floor lower than section k on floor l
$down_{S,K,F}$	binary variable denoting whether section s existing on a floor f is below section k on any floor
$Dx_{S,K}$	the minimum separation distance between the midpoints of sections s and k in the x-direction
$Dy_{S,K}$	the minimum separation distance between the midpoints of sections s and k in the y-direction
${}_{R,M}E_{S,K,F}$	amount of energy in a section s in a monitor region M in which section s resides existing on floor f due to a release in the R-direction in section k
$EProbEscape_{S,K,M}$	component of escape failure related to the heat flux from a fire in section k on the escape route section s takes to muster point m
$EProbMuster_{S,K,M}$	component of escape failure related to the heat flux from a fire in section k on muster point m to which section s is allocated
$EProbSection_{S,K}$	component of escape failure probability related to the heat flux from a fire in section k directly on section s
$EscapeProbability_{S,K,M}$	the probability that a fire in section k will cause the failure to escape from section s to muster point m
$ex1_{S,M}$	the x-direction intermediate point of interest between a section s and muster m used in radiation modeling calculations
$ey1_{S,M}$	the y-direction intermediate point of interest between a

	section s and muster m used in radiation modeling
$F_{S,K,F}$	binary variable defining whether sections s and k both exist on floor f (1) or not (0)
Fa_S	binary variable for escape route choice x-to-y direction
Fb_S	binary variable for escape route choice y-to-x direction
Fc_S	binary variable for escape route choice direct
$Floor_S$	the floor that section s is assigned to
FO_F	binary variable defining whether a floor f is occupied (1) or unoccupied (0)
$I_{S,K,M}$	the radiative flux on the escape of personnel from section s to muster m from a fire in section k
Lx_S	the length in the x-direction of section s
Ly_S	the length in the y-direction of section s
$M_{S,K,F}$	generic term for non-overlap constraints a, b, c, and d
ma_M	binary variable assigning muster point m to the –x side of the platform
mb_M	binary variable assigning muster point m to the +x side of the platform
mc_M	binary variable assigning muster point m to the –y side of the platform
md_M	binary variable assigning muster point m to the +y side of the platform
$MProb_{S,K}$	mitigated probability of section s destruction due to an explosion in section k
mx_M	the x-direction coordinate of a muster point m
my_M	the y-direction coordinate of a muster point m
$P_{S,K}$	the overpressure on section s due to an explosion in section k
${}_{R,M}P_{J,S,F}$	the overpressure estimated on section j from a dispersed cloud explosion in section s that lies in monitor region M due to a release in section k in the R-direction
$P_{S,K(mitigated)}$	mitigated pressure on a section s due to a blast from section k, considering failing blast walls
$P_{S,K(nom)}$	nominal overpressure on a section s due to a blast from section k, considering failing blast walls

${}_{R,M}S_{S,K,F}$	binary variable for determining whether a release from section k in the R-direction causes a concentration exceeding the LFL in monitor region M in which section s resides
${}_{R,M}SD_{S,F}$	scaled dispersion mass fraction in monitor region M due to an R-direction release in section s on floor f
$SectionMuster_{S,M}$	binary variable for section s allocated to muster point m
t_{esc}	time to escape to muster
$ToxicProbability_{S,K}$	probability of death in section s due to a toxic release in section k
${}_{R}TProb_{S,K}$	probability of death in section s due to an R-direction toxic release in section k
$up^*_{S,K,F,L}$	binary variable denoting whether section s existing on floor f is on a floor higher than section k on floor l
$up_{S,K,F}$	binary variable denoting whether section s existing on a floor f is above section k on any floor
v_{esc}	escape velocity to muster
$V_{S,F}$	binary variable defining whether section s exists on floor f (1) or not (0)
${}_{M}W_{S}$	binary variable denoting a blast wall allocated to the M-direction of s (1) or not (0)
$X_{S,K,F}$	generic term for non-overlap constraints a, b, c, and d
x_S	the midpoint in the x-direction of section s
y_S	the midpoint in the y-direction of section s

Other

$a+c$	base flowrate coefficient for dispersion correlation
AIT	autoignition temperature of a material [K]
C	congestion ratio, multiplied by 100
C	concentration [ppm]
C_D	orifice coefficient for mass flow of leak
c_S	explosion severity constant from the modified TNO formulation
C_S	extinction coefficient [m^{-1}]

D	pool diameter [m]
e	base congestion coefficient for dispersion correlation
E_S	available explosion energy within a section s [J]
F	flow rate of material [kg/s]
$f+i$	proportional wind coefficient for dispersion correlation
F_R	total heat flux from the surface of a fireball [kW/m^2]
FR	flow rate of material [kg]
g	base wind coefficient for dispersion correlation
g	acceleration due to gravity [m/s^2]
H	pool fire plume height [m]
ΔH_C	heat of combustion [J/kg]
k	isentropic expansion factor
m	total mass [kg]
$\dot{m}$	mass flowrate [kg/s]
m''	mass burning velocity [kg/m^{2}s]
MIE	minimum ignition energy of a material [mJ]
P	probability derived from probit functions
P_{atm}	atmospheric pressure [Pa]
P_P	process pressure
$\dot{Q}$	heat release from burning [J/s]
R	reactivity of materials
$r_{S,K}$	euclidean distance between sections s and k [m]
S	shape factor for ignition considerations
T	process temperature [K]
t	time [s]
t_b	pool fire burning time [s]
t_e	exposure time for probit formulation [s]
u^*	effective wind speed [m/s]
u	wind speed [m/s]
W	wind speed [m/s]

x	concentration of material [ppm]
Y	probit value
χ	pool fire experimental correlation factor
ρ_{amb}	ambient density [kg/m^3]
ρ_P	process density [kg/m^3]
θ	flame angle [deg]

TABLE OF CONTENTS

Page

LIST OF TABLES

Page

LIST OF FIGURES

Page

1. INTRODUCTION AND MOTIVATION

Facility siting and layout is one of the principal considerations in any environment that equipment, people, resources, or labor has to be used. The motivation for this is largely economic, in that the optimal layout of resources can allow for a more efficient operation in a multitude of ways, which will then push down the cost of doing business.

In the process industries, it must also be taken into account that, due to the inherent hazards of the materials that are worked with, layout should be done with a keen eye on safety considerations. Whether it be toxic hydrogen sulfide in a refinery that can disperse and harm those on-site as well as those off-site, or an explosive cloud of natural gas in the confined and congested areas of an offshore platform, it is necessary not only to plan for the responses to these events in the rare case that they occur, but also to design processes such that the probability of such an event occurring is minimized. Proper facility layout is a powerful tool to help ensure that the probability and consequence of these events are minimized.

The consequences of poor siting and layout are well documented in the tragedies that have followed. Some of the most well-known incidents have been a direct result of poor choices of layout, and several have spurred the realization that a better understanding of the subject is needed to ensure safety to workers and the public. Perhaps the most infamous incident related to siting and layout was the Texas City Refinery explosion in March of 2005, where inadequate spacing between trailers and the isomerization process directly contributed to several fatalities. The trailers were as close as 121 feet from the release, and heavy damage to a trailer 600 feet from the explosion was reported [1]. The CSB investigation concluded that it was necessary to adopt a new regulation for the siting of temporary buildings and recommended that such a standard be issued [2]. This standard was produced by API in 2007 as RP 753 – Management of Hazards Associated with Location of Process Plant Portable Buildings [3], and is considered standard practice under OSHA Process Safety Management guidelines.

Several other high-profile incidents have been attributed to poor decisions for facility siting and layout. Of the twenty-eight that died in the 1974 Flixborough incident, eighteen died in the control room, many due to a roof collapse and others due to severe injuries sustained from broken glass caused by the explosion overpressure of a vapor cloud of about 50 tons of cyclohexane [4]. Of the same profile was the Phillips 66 Pasadena, Texas incident in 1989 which leveled the entire site, killing 24, many of whom were in occupied control rooms and other buildings [5].

Offshore installments have not been exempt from layout issues either. The two most infamous offshore incidents – Piper Alpha in 1988 and Deepwater Horizon in 2010 could both be said to have inherent problems with their layouts. For Piper Alpha, which left behind 167 fatalities, design flaws were exacerbated by the fact that the electrical classification of the platform did not require production areas to be decoupled from accommodation areas such as the control room or living quarters, and thus the control room was placed on top of the production module and the quarters was placed directly next to it with no consideration given to spacing [6]. Not only did this have the effect of killing many people in the subsequent fire (mostly due to smoke inhalation and asphyxiation, not burning), it also had the effect of 'decapitating' the platform due to lack of redundancies in command and control. The layout of the platform was such that the escape routes were inadequate for the incident, also lacking redundancy, leaving many with their only feasible route off of the platform blocked by the destruction from the fire and explosion. Also contributing was the fact that the platform was not well-designed for a low-probability catastrophic incident, as it was much more cost-effective to design for the smaller, more frequent incidents that occur on a platform.

Though many improvements had been made between 1988 and 2010, the Deepwater Horizon incident shows that the problem of facility layout is still as complicated and important as ever. One of the contributing factors in the difficulty of evacuation from the drilling platform was the predetermined evacuation routes being blocked by debris from the explosion or otherwise inaccessible [7]. There were reports from employees that survived the incident that flooring panels were missing making it

difficult to proceed, stairwells were collapsed, and walkways were completely destroyed. Even those in the highly occupied quarters area had to fight wreckage and debris on their way to muster. Flames and smoke were also a large problem for workers in certain parts of the platform, but those affected were able to make it to their secondary muster through alternate routes, perhaps showing that in some ways the consideration for escape routes was effective in the face of such a disaster.

1.1 Literature Review

A literature review is presented in this section for general offshore operations, layout of these offshore facilities, numerical methods for layout, and identification of gaps between practice and this research as well as between other research and this research. This provides a general overview of the problem and the motivation for this research. More detailed literature review appears in the chapters that follow as it becomes necessary.

1.1.1 Offshore Operations

In order to understand the nuance to and differences in layout and siting for an offshore platform, it is first necessary to have some level of understanding exactly what operations are performed and what hazards are present. According to the Handbook of Offshore Operations [8], the following areas are important to consider in topsides layout:

- Wellhead Area: Potential for uncontrolled flow and high pressures leads to the need for adequate ventilation and separation from other sources of ignition. Should be separated as best as possible from quarters and other occupied areas and be designed with egress in mind, as the area can become tightly spaced. Firewalls may be necessary.
- Fired process units: Source of ignition and can also be a source of fuel if the units are run on or contain hydrocarbons. Firewalls may be necessary, and a safety spacing of 15 feet is recommended.

- Unfired process units: Source of fuel. Separate from sources of ignition.
- Hydrocarbon storage: Source of fuel that is particularly important in the feeding of unplanned combustion incidents, since there is typically a relatively large amount of fuel located in one small area. Hydrocarbon tanks should be located on the top level, if possible, to minimize the impact of fire impingement on equipment above the tanks.
- Machinery areas: A source of ignition, and possibly fuel if the machinery is run on hydrocarbon fuel. May be spaced near the quarters if the machinery is not a source of fuel (as the quarters is also a source of ignition)
- Quarters and utilities: As a source of ignition and also the site of a large population, the quarters must be separated as best as possible from fuel sources. Secondary considerations are separation from noise and vibration. Escape routes are key, and should not lead personnel into dangerous situations.
- Pipelines: Uncontrolled flows may originate in the pipeline area, and so ignition should be separated from this source of fuel.
- Flares and vents: Both flares and vents are potential sources of both fuel and ignition.

1.1.2 Offshore Facility Layout

There are many factors that are taken into account in the practical layout of an offshore platform, of which safety is at the forefront along with design considerations that allow the platform to carry out its function. These range from the broad considerations for separation of ignition and fuel and weather conditions, to the minutia of design specifications for handrails and placement of staircases. The main contributing factors to the difference in between onshore layout and offshore layout are as follows:

- Lack of adequate space for separation of units, exclusion zones
- Congestion and confinement created by this lack of space
- Three-dimensional modeling of hazards and layout

- Design for human safety factors such as escape routes and muster points

Each of these factors presents unique and often conflicting challenges in the layout of an offshore facility – for example, space can be made for separation of units to reduce congestion and enhance exclusion zones, but this would require a larger platform at higher cost and a greater weight, both of which are undesirable consequences [9]. An alternative may be to space equipment with a large longitudinal spacing while minimizing transverse dimension, but this may lead to low stability and poor balance in the transverse direction. This becomes a concern in the case of floating production storage and offloading units [8]. Likewise, the multi-story layout of platforms allows equipment to be spaced ideally for transport between modules, but also adds to congestion, leads to considerations for the upward propagation of fire, and spaces all equipment closer together so that an incident has the potential for greater damage. The quarters may be separated to an entirely different platform connected to the main platform by a bridge, but this is not always possible in deeper water [10], and not always economically feasible in certain areas or under certain circumstances [11].

The problem, primarily due to the tradeoffs associated with most safety decisions made in layout, is that minute details can make a large difference in the risk level of a platform. Compounding this problem is the human factor – though undeniably necessary and indispensable, it is inevitable that humans will make mistakes in complex problems. Though there are many guidelines, heuristics, and a wealth of experience in offshore operations, incidents continue to happen and improvements are commonly found in the aftermath of incidents.

A computational method for the improvement of layout for offshore operations based on safety considerations, utilizing strategies for estimating the effect of different catastrophic events on the platform and personnel, with an aim of minimizing the risk can circumvent this human factor and deliver an optimal solution based on the input model, free of bias and considering all pertinent information. A brief introduction to the optimization of facility layout is given in the following section.

1.1.3 Numerical Methods for Facility Layout

Facility layout optimization using numerical methods has been an area of interest since at least 1957, when Koopmans and Beckmann published their work on assignment problems and the location of economic activities [12], proposing a method to account for the benefit of an economic activity that depends on the activity in another location using the quadratic assignment problem, which spurred a world of new research and interest into the objective-based design of facility layouts, whether based on manufacturing facilities, process plants, or in the very siting of facilities themselves.

It was not until 1996, when Penteado and Ciric published their MINLP model for process plant layout with respect to safety considerations [13] that process safety was incorporated into facility layout optimization. The objective function minimizes four financial factors – piping costs and land costs, both strictly economical, cost of protective devices, the first safety factor, and the financial risk of a process safety incident. The piping and land costs are based on the rectilinear length of piping between process units and the total footprint of the facility, respectively. The protective devices, used either to prevent an incident or minimize the impact of the incident, include concepts of waterspray or blast walls. Finally, the financial risk of a process safety incident is simply the monetary consequence of an incident scaled by the probability of that incident. The hazard faced by such a facility is explosion overpressure, as determined using the TNT method. The goal is to site several different units with circular footprints so as to minimize the total financial risk.

As the subject became more popular within process systems and chemical engineering academia shortly after Penteado and Ciric's paper, new formulations to the plant layout problem began to be published. Papageorgiou and Rotstein [14] created an MILP model in the same vein of the MINLP model of Penteado and Ciric, but using rectangular process units and a safe separation distance parameter between certain units. Thus, the safety factor came from a standard acceptable distance rather than from an explosion overpressure damage function. Georgiadis and Macchietto proposed a general programming model to the process plant layout problem [15], which could, as they

pointed out, be modified for safety considerations by excluding certain process units from certain zones in a method that would require some level of expertise and common sense in the field of plant design.

Multi-story optimization of facility layout has been a subject of research since the 1999 publication of a grid-based general MILP method for process plant layout published by Georgiadis, et. al. [15], focusing on minimizing piping and land costs, and the 2002 publication by Patsiatzis and Papageorgiou [16], which presented an MILP model for allocating equipment to multiple floorson a continuous basis based on an objective of minimizing total cost comprised of pumping costs and area costs, incorporating minimum safety distances between equipment.

These formulations, though they were not in any way associated with offshore facilities, nor was it indicated that offshore applications were aforethought, in a sense opened the door to the realm of offshore layout optimization. An MILP model proposed by Park, et. al. [17], explored the layout of an onshore multi-floor ethylene plant with simple consideration given to VCE effects balanced against piping costs and land costs. However, whereas an offshore platform may have equipment spanning several floors, this model allocates equipment to only one floor. This was improved by Ku, et. al. [18], in their application of the multi-floor layout to an FPSO, which allowed equipment to occupy multiple floors if needed. However, this study does not account for the effects of explosions, fire, or toxic release, instead opting to consider safety through minimum separation distance, and disregard the complexities of hazard management along multiple floors.

In recent years, work has been done on the facility layout problem specifically with respect to process safety by the Mary Kay O'Connor Process Safety Center at Texas A&M University. This work has included safety-based optimal layout of new process units in the case of fire and explosion [19] and toxic gas releases [20], using both continuous-plane methods and a grid-based method [21]. The approach for fire and explosion scenarios is MINLP and takes into account the TNT-scaled blast overpressure, fire radiation found using PHAST, and an interconnection cost as a balance. The results

of the model are validated using the FLACS software. The approach for toxic effects uses the DEGADIS model to approximate footprint using a Monte Carlo simulation to sample meteorological conditions that affect dispersion. Both continuous methods make use of the disjunctive formulation for non-overlap constraints as described in the work by Vazquez-Roman, et. al [22] and based on the computational optimization work of Grossman and Lee [23].

Table 1: Comparison of relevant optimization formulations for the facility layout problem (partially compiled by Ku, et al. [18])

Study	Year	Setting	Floors	Safety Considerations
Penteado and Ciric [13]	1996	EO Plant (onshore)	Single	Minimum spacing, explosion
Georgiadis, et al. [24]	1997	Batch Plant (onshore)	Multi	None (transportation cost)
Georgiadis, et al. [15]	1999	Batch Plant (onshore)	Multi	None (layout and transportation cost)
Patsiatzis and Papageorgiou [16]	2002	EO Plant (onshore)	Multi	None (layout cost objective)
Diaz-Ovalle, et al. [25]	2010	Chemical Plant (onshore)	Single	Worst-case toxic dispersion
Jung, et al. [21]	2010	Distillation unit (onshore)	Single	Explosion (grid-based plane methodology)
Jung, et al. [20]	2010	Loading facility (onshore)	Single	Toxic dispersion
Jung, et al. [19]	2011	Hexane distillation unit (onshore)	Single	Minimum spacing, fire and explosion
Park, et al. [17]	2011	EO Plant (onshore)	Multi	Explosion
Ku, et al. [26]	2012	LNG-FPSO (offshore)	Multi	Minimum spacing
Ku, et al. [18]	2013	LNG-FPSO (offshore)	Multi	Minimum spacing
This study	2015	Widely-applicable offshore	Multi	Vapor cloud explosion (local and dispersed cloud), fire, toxic dispersion, combustion effects (toxic products, smoke obscuration of sight), escape optimization, mitigation, congestion effects, weather effects

1.1.4 Gaps between Practice and This Research

In practice, the current method of offshore facility layout is much like that of onshore facility layout – the initial layout is created when the process and other parameters are well-defined, and much of the layout consideration is given to a logical progression of flows through the process, as well as to safety consideration. Size of the platform is dictated by the intended function of the platform, and space is generally minimized due to economic concerns.

Experience, as it should be, is highly valued in this process. Blast and fire surveys are conducted, and the process iterates between layout and new information input which creates a new layout. However, as always with human input, mistakes can be made. The advantage of a proper model for this application is that based on the inputs, an optimal solution can always (with certain caveats) be found. Thus, if the model is a quality model, the output should be useful. This research aims to provide that model to bridge the gap between the current practice and the optimization approach.

1.1.5 Gaps between Prior Research and This Research

Though much research has been done on the facility layout problem with respect to onshore process plants, offshore layout has not been to nearly the same extent. Several possible reasons for this exist. It may be because there is a feeling that since offshore platforms often perform nearly the same function as one another, there is not the same level of variability between platforms as there is between process plants. It may also be thought that the lack of space to lay out a platform actually makes the job easier since there are fewer options for placing units. Finally, it could also be thought that there are not as many options for addition of units to an offshore platform, while an onshore process plant is constantly in flux.

Each of these assertions is fallacious. Though it may be true that there is less variability in the operations of an offshore platform, there are still incidents occurring that can be attributed, at least in part, to facility layout. As can be seen between the Piper Alpha incident and the Deepwater Horizon event, there are still difficulties in keeping

employees safe, especially in the face of unforeseeable disaster. Though the lack of space on a platform lessens the options for placement of equipment and modules, it also makes it increasingly important that they are arranged properly, as the difference between complete destruction and protection of workers and assets is hidden in the many permutations of placement possible in the confined area of a platform. And though the flux in the layout of an offshore platform may not be of the same magnitude as that of a process plant, it is just as important to be able to plan what changes might be necessary and how they might be incorporated, because there is no simple option to add more space as there might be in an onshore plant.

In the case of multi-floor optimization, safety has not been taken into account in as much detail as economic and process flow considerations. Though simple explosion modeling has been examined, fire and toxic considerations have been largely ignored in the offshore formulation. The secondary effects of congestion have not been incorporated into existing models, and escape modeling, perhaps the area with the highest risk contribution in a catastrophic event, has not been examined. Indeed, there are many gaps to be filled in the current research landscape. This research aims not only to advance the understanding and formulation of offshore facility layout models with respect to safety considerations, as well as the models upon which the layout formulation relies upon, but to also create a foundation upon which further offshore facility layout optimization work can be built. Detailed information on the goals and objectives of this research follows in Chapter 2. Additional literature review on pertinent topics is presented in the following chapters as the need arises.

2. OBJECTIVES

The main objective of this research is to create an optimization formulation for the layout of an offshore platform with respect to minimization of combined risk, advancing the offshore layout problem by taking into account the following considerations:

- Account for the lack of space on an offshore platform as it relates to the added risk from catastrophic events and balance trade-offs that occur due to this lack of space
- Create a multi-floor model that resolves the differences in risk from catastrophic events at different points in space with different elevations
- Quantify effects of added congestion and confinement on explosions, fire, and dispersion
- Facilitate escape through optimal placement of sections and muster points associated with the sections to minimize the effects of heat radiation and smoke effects from fire
- Incorporate domino effect, where flammable gas may disperse to another section and be ignited, and account for directional effects of the ensuing blast
- Ensure that the optimization models solve in a reasonable amount of time, and create the model in such a way that efficiency is maximized
- Take into account relevant existing guidance in the field of offshore layout and design as useful
- Verify the findings using advanced risk analysis models such as CFD

2.1 Practical Objectives

Practically, offshore platforms should be in compliance with API RP 75 – Recommended Practice for Development of a Safety and Environmental Management Program for Offshore Operations and Facilities [27], which specifies implicitly that

layout should be taken into account during design. One of the references to API RP 75 is API 14J – Recommended Practice for Design and Hazards Analysis for Offshore Production Facilities [28], which includes more detail about the concept of layout for offshore production facilities. It states that among platform equipment arrangement factors, important considerations are:

- Separation of fuel and ignition sources
- Adequate space in between equipment
- Consideration of wind direction for venting of hydrocarbon vapors
- Escape routes
- Use of firewalls and barrier walls
- Ease of maintenance of equipment
- Streamlining of process flow

While acknowledging that the major problems in arrangement of equipment are the lack of space and the inherent difficulty that it causes in all of the recommended elements.

In practical terms, the objective of this research is to create a framework through which numerical optimization can be used to efficiently solve the problems posed by the unique nature of offshore platforms by taking into account all of the aforementioned elements recommended in practice.

2.2 Research Objectives

In order to satisfy the practical objectives, it is necessary to create a model that, although simplified, gives a complete understanding of the hazards and risks of an offshore platform during a catastrophic event. Original mathematical formulation of the constraints and decisions for how to model the hazard phenomena are the key considerations in this research. Translation of physical phenomena into mathematical constructs is not always straightforward and requires creative solutions, particularly in

the field of numerical optimization where highly complicated problems are not always tractable and simplifications must routinely be made in order to come to a solution.

It is expected that the model will provide a positive step into an area that has sparsely been considered, contributing a framework for the integrated consideration of several key risk factors in the offshore realm that, as yet, have been unexplored from the numerical optimization viewpoint, both standing alone as a work and providing a foundation for future work into facility layout optimization as well as other fields.

Finally, it must be proven that the results that are given by the model are superior to the results given in the current method of layout formulation based on the model criteria, i.e. the model must be better at reducing risk in fire, explosion, and toxic release scenarios than the current method of human design. To test this, the results will be tested against the calculated risk by the model in base cases as well as optimized cases, and the layouts will be compared quantitatively against risk analysis tools such as CFD for dispersion and explosion and integral models for fire hazard.

3. A MODEL TO OPTIMIZE LAYOUT FOR OFFSHORE EXPLOSION AND ESCAPE SCENARIOS

3.1 Practical Layout Concerns

Because there are many subtle factors that go into the design of an offshore platform, it is quite a challenge to create a model that will both accurately reflect that subtlety but also be possible to solve to an optimal solution. Thus, a balance of simplicity and complexity must be struck for the model.

3.2 Mathematical Modeling and Optimization Formulation

Of paramount importance is the mathematical model to be used in the optimization formulation. It must reflect not only physical reality, such as the fact that two pieces of matter cannot occupy the same space or that it is impossible that a section of a platform be outside of the domain of that platform, but also the inherent practical complexities of platform management, such as the fact that some sections will take up more than one level of the platform, or that it is necessary to have two routes of escape from any point in the layout. The following sections outline the necessary information and constraints needed to create the model.

3.2.1 Selected Sets, Scalars, and Parameters Used in the Base Model

The following sets, scalars, and parameters are used in this formulation, not including those used as process parameters, which are discussed in sections 3.3 – 3.6:

$\boldsymbol{s \in S}$**,** a set of sections to be placed in the layout
$\boldsymbol{f \in F}$**,** a set of floors that occupy the platform
$\boldsymbol{m \in M}$**,** a set of floors that occupy the platform
$\mathbf{W_x}$, the x-direction size of the platform footprint
$\mathbf{W_y}$, the y-direction size of the platform footprint
sep, a minimum separation distance between sections

FloorSpacing, the height of a floor, and the separation distance between the deck of one floor and another

$Stories_s$, the number of floors that a section, s, takes up

$Area_s$, the area that must be allotted to a section, s

AR_s, the maximum aspect ratio between the longest and shortest side of a section, s

$SectionCost_s$, the relative cost of a section, s, to be used in the objective function

N, a big M scalar

UBx_s: the upper bound on the x-direction size of section s

LBx_s: the lower bound on the x-direction size of section s

UBy_s: the upper bound on the y-direction size of section s

LBy_s: the lower bound on the y-direction size of section s

3.2.2 Selected Variables Used in the Base Model

The following variables are used in this formulation:

x_s: the midpoint in the x-direction of a section, s

y_s: the midpoint in the y-direction of a section, s

Lx_s: the length in the x-direction of a side of section s

Ly_s: the length in the y-direction of a side of section s

NF: total number of floors on the platform

$Floor_s$: the floor that section s is assigned to

FO_f: binary variable defines whether floor f is occupied (1) or unoccupied (0)

$V_{s,f}$: binary variable that defines the assignment of section s to floor f (1 if section s is assigned to floor f, 0 otherwise)

$F_{s,k,f}$: binary variable that determines whether sections s and k are assigned to the same floor f (1 if sections s and k are both assigned to floor f, 0 otherwise)

$a_{s,k,f}$: binary variable for the non-overlap constraint (sections s and k on the same floor f must not overlap to the left)

$b_{s,k,f}$: binary variable for the non-overlap constraint (sections s and k on the same floor f must not overlap to the right)

$c_{s,k,f}$: binary variable for the non-overlap constraint (sections s and k on the same floor f must not overlap below)

$d_{s,k,f}$: binary variable for the non-overlap constraint (sections s and k on the same floor f must not overlap above)

$Dx_{s,k}$: the minimum separation distance between the midpoints of sections s and k in the x-direction

$Dy_{s,k}$: the minimum separation distance between the midpoints of sections s and k in the y-direction

mx_m: the x-direction muster coordinate of muster m

my_m: the y-direction muster coordinate of muster m

$ex1_s$: an intermediate x-dimension point of interest used in fire modeling calculations

$ey1_s$: an intermediate y-dimension point of interest used in fire modeling calculations

$P_{s,k}$: the overpressure on section s as a result of an explosion in section k

$I_{s,k}$: the fire radiation intensity on section s as a result of a fire in section k

Fa_s, Fb_s, Fc_s: decision variables to determine which path to take from section s to its associated muster point

$DestructionProbability_{s,k}$: the probability that an explosion in section k will completely destroy section s

$EscapeProbability_{s,k}$: the probability that an fire in section k will render escape from section s to its associated muster point impossible

3.2.3 Constraints

The constraints used in this formulation are presented in the sections that follow:

3.2.3.1 Area, Aspect Ratio, and Side Length Expressions

The area, aspect ratio, and side length expressions ensure that the footprint area of the section is satisfied, while keeping the ratio of the sides in the x-direction and y-direction to a reasonable value, so that the section is not practically unusable. The AR_s

parameter sets the maximum aspect ratio for a section, and would be set as an input based on acceptable dimensions in practice.

$$Area_s = Lx_s * Ly_s$$
$$LBx_s \leq Lx_s \leq UBx_s$$
$$LBy_s \leq Ly_s \leq UBy_s$$

Where LBx_s and UBx_s are determined as a function of the footprint area and aspect ratio parameters:

$$UBx_s = \min(\sqrt{Area_s * AR_s}, Wx)$$
$$LBx_s = \frac{Area_s}{UBx_s}$$

With the y-dimension bounds calculated in a similar manner. The range of allowed side-lengths is illustrated in the figure below.

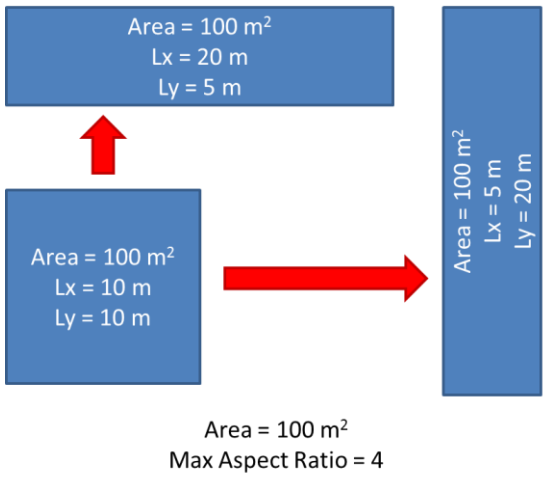

Figure 1: An example of possible footprints for a section of a given area and a defined maximum aspect ratio

This formulation is different from most existing process plant facility layout formulations in that most existing formulations use defined side lengths that may be flipped between the x- and y-directions, but still are rigid in the fact that no intermediate sizes are allowed. By using the area formulation, it is possible to have a more flexible layout based on the space allowed.

3.2.3.2 Separation Distance Expressions

The separation distance expressions define how far away from each other the midpoints of two sections must be in order to maintain a non-overlapping system. This takes into account the length of the side in the x- or y-direction and the minimum separation distance parameter.

$$Dx_{s,k} = \frac{Lx_s + Lx_k}{2} + sep$$

$$Dy_{s,k} = \frac{Ly_s + Ly_k}{2} + sep$$

This formulation is illustrated in the figure below:

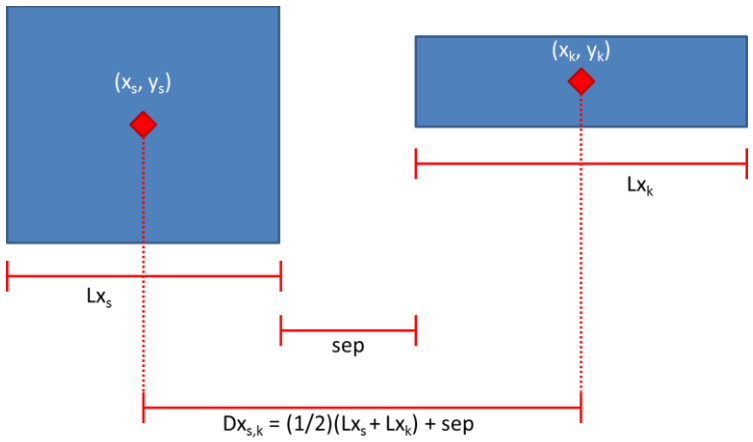

Figure 2: Visual representation of the minimum separation between midpoints constraint

3.2.3.3 Platform Boundary Constraints

The platform boundary constraints operate in the same way as the minimum separation distance constraints, except that the overlap constraint is with the edge of the platform rather than another section.

$$\frac{Lx_s}{2} \leq x_s \leq Wx - \frac{Lx_s}{2}$$
$$\frac{Ly_s}{2} \leq y_s \leq Wy - \frac{Ly_s}{2}$$

3.2.3.4 Non-Overlap Constraints

The binary variables for non-overlap constraints are modified from the convex hull relaxation of a disjunctive programming approach to non-overlapping. The non-overlapping constraints require the model to define where a section is in relation to another section, not only with respect to the x- and y- direction, but also with respect to which floors the sections occupy. This is an extension of the method found in the work of Jung, et. al. [20], where the sections were forced to be either left of, right of, above, or below each other. In this model, an additional possibility is introduced: the sections do not occupy the same floor, and thus can occupy the same x- and y-dimensional space without overlapping. The original constraints can be visualized as in the following figure:

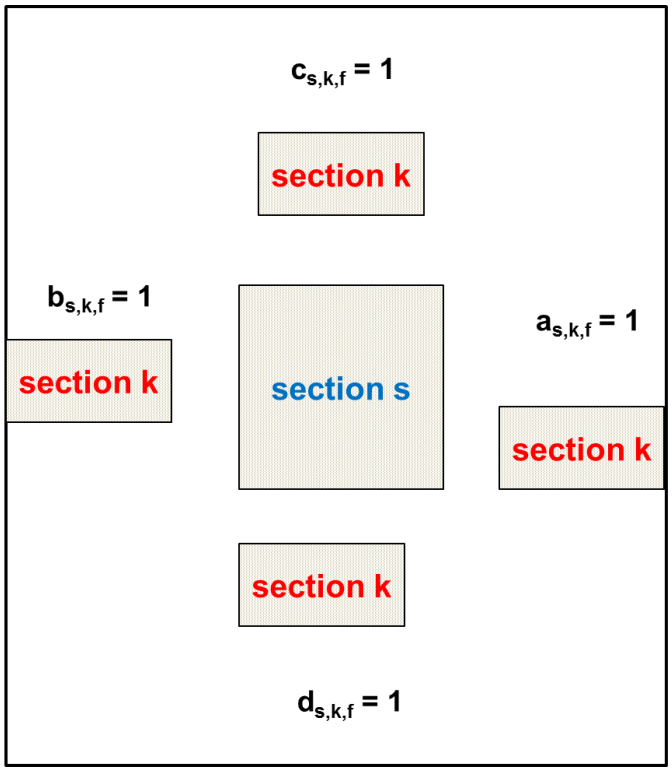

Figure 3: Relative facility placement for non-overlap constraint definition, modified from Jung et. al [20]

And be expressed mathematically as follows:

$$x_s \leq (1 - a_{s,k,f}) * M + (x_k - Dx_{s,k})$$
$$x_s \geq (x_k + Dx_{s,k}) - (1 - b_{s,k,f}) * M$$
$$y_s \leq (1 - c_{s,k,f}) * M + (y_k - Dy_{s,k})$$
$$y_s \geq (y_k + Dy_{s,k}) - (1 - d_{s,k,f}) * M$$
$$a_{s,k,f} + b_{s,k,f} + c_{s,k,f} + d_{s,k,f} = 1$$

Where M is a suitably chosen Big-M parameter. The first four expressions define where section s is placed in relation to section k, where a, b, c, and d define section s as left of, right of, below, and above, respectively. As only one binary variable can be true

(fixed by the fifth expression), three of the constraints collapse, and only one is held active.

However, because of the extra dimension being considered in this formulation, it is necessary to add an extra binary variable, $F_{s,k,f}$. The definition of this binary variable is explained in the next section and is true (value equal to one) when sections s and k occupy the same floor, and false when they do not. The fifth expression from above is now modified to:

$$a_{s,k,f} + b_{s,k,f} + c_{s,k,f} + d_{s,k,f} - F_{s,k,f} = 0$$

Forcing one of the constraints to be active if and only if s and k occupy the same floor. Thus, if F is false, there is no non-overlap constraint between s and k.

3.2.3.5 Floor Constraints

The first constraint that must be met is the assignment of a section to the proper number of floors using the $Stories_s$ parameter. Because there is the possibility of a single section (such as the quarters or wellhead area) requiring multiple floors, this constraint must be modified from the usual 'one facility allocated to one site' constraint to reflect the new 'one facility allocated to multiple floors' constraint:

$$\sum_{f} V_{s,f} = Stories_s$$

Where $V_{s,f}$ is a binary variable that is true if section s is assigned to floor f. In order to make the new non-overlapping constraints (previous section) work, it is imperative to know whether two sections occupy the same floor. This can be accomplished using the following system of constraints, first used by Patsiatzis and Papageorgieu [16]:

$$F_{s,k,f} \geq V_{s,f} + V_{k,f} - 1$$
$$F_{s,k,f} \leq 1 - V_{s,f} + V_{k,f}$$
$$F_{s,k,f} \leq 1 + V_{s,f} - V_{k,f}$$

Table 2: List of values for the floor definition series of constraints

s on floor?	k on floor?	Constraint 1	Constraint 2	Constraint 3	F value
Yes	Yes	$F_{s,k,f} \geq 1$	$F_{s,k,f} \leq 1$	$F_{s,k,f} \leq 1$	1
Yes	No	$F_{s,k,f} \geq 0$	$F_{s,k,f} \leq 0$	$F_{s,k,f} \leq 2$	0
No	Yes	$F_{s,k,f} \geq 0$	$F_{s,k,f} \leq 2$	$F_{s,k,f} \leq 0$	0
No	No	$F_{s,k,f} \geq -1$	$F_{s,k,f} \leq 1$	$F_{s,k,f} \leq 1$	0,1

In the case of neither s nor k occupying a given floor, the F value is not constrained and can be either true or false. In the formulation, since the F value is used to decide whether two sections are constrained and must not overlap with each other, and since the optimization is based upon maximum spacing when possible to lessen the risk of fire and explosion hazards, the F value will always optimize to zero if s and k do not occupy the same floor, simply because it is needed to come to the optimal solution.

3.2.3.6 Muster Expressions

Because one of the main points of focus in offshore operations is the ability to escape in the case of an emergency, muster points must be taken into account with a value equal to, if not greater than, that of the effect of fire and explosion on the individual sections themselves. Because it is necessary to spread the muster points across the platform for ease of access, four muster points are defined, each assigned to a different side of the platform:

$$ma_m + mb_m + mc_m + md_m = 1$$
$$\sum_m ma_m = 1, \sum_m mb_m = 1, \sum_m mc_m = 1, \sum_m md_m = 1$$

Where ma_m assigns a muster to the left side of the platform, mb_m assigns a muster to the right side of the platform, mc_m assigns a muster to the bottom side of the platform, and md_m assigns a muster to the top side of the platform. The constraints ensure that one muster point is only allocated to one side, and that each side is only allocated once. Once assigned to a side, the muster points may move along their assigned edge such that the musters on the left and right sides have their x-coordinates fixed and may vary in their y-coordinates, and the musters on the top and bottom have their y-coordinates fixed, and may vary in their x-coordinates:

$$mx_m \leq (1 - ma_m) * Wx$$
$$mx_m \geq (mb_m) * Wx$$
$$my_m \leq (1 - mc_m) * Wy$$
$$my_m \geq (md_m) * Wy$$

As illustrated in the following table:

Table 3: List of values for the muster assignment set of expressions

Muster Side	Expression 1	Expression 2	Expression 3	Expression 4
Left	$mx_m \leq 0$	$mx_m \geq 0$	$my_m \leq Wy$	$my_m \geq 0$
Right	$mx_m \geq Wx$	$mx_m \leq Wx$	$my_m \leq Wy$	$my_m \geq 0$
Bottom	$mx_m \leq Wx$	$mx_m \geq 0$	$my_m \leq 0$	$my_m \geq 0$
Top	$mx_m \leq Wx$	$mx_m \geq 0$	$my_m \leq Wy$	$my_m \geq Wy$

Each section must then be assigned to a single muster using the $SectionMuster_{s,m}$ binary variable which is defined as 1 if section s is assigned to muster m and 0 otherwise:

$$\sum_{m} SectionMuster_{s,m} = 1$$

And further, to assure that one muster isn't over-utilized by personnel trying to escape, another constraint is added:

$$\sum_{s} Personnel_s * SectionMuster_{s,m} = N$$

Where N is the maximum number of people that can be accommodated by a muster point.

3.2.4 Objective Function

The objective function is as follows:

$$\min z = \sum_{s} \sum_{k} cost_s * [P(Dest)_{s,k} + P(Esc)_{s,k}]$$

Which can be termed as the sum of the calculated probability that a section will be destroyed due to explosion, thus causing the loss of the personnel in that section, and the probability that escape from a section to its muster will be unsuccessful, also causing the loss of the personnel in that section. Each probability is scaled by a cost for that section, which can be defined by any criteria, but will be defined as the number of personnel assigned to the section in this formulation. In this way, the only objective taken into account by this model is that the probability that personnel are lost due to an explosion or blocked escape is minimized.

The methodology for determining the probabilities of destruction and failure of escape is given in the sections that follow.

3.3 Explosion Modeling

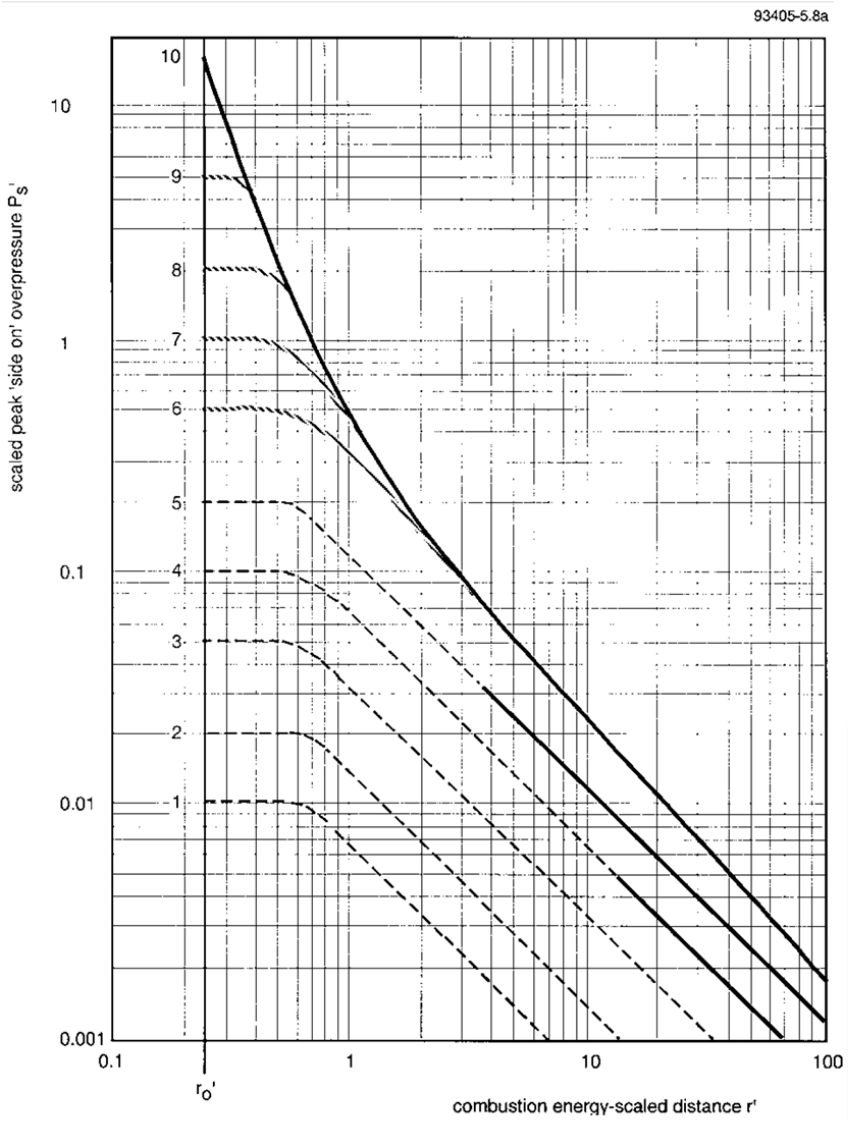

Figure 4: TNO scaled blast curves [29]

Explosion modeling is based on the TNO multi-energy model [29]. This model requires knowledge of the amount of confinement and congestion in an area, material that is ignited, amount of that material, and relative spacing of points of interest in order to find the overpressure at a given point.

For the figure above, the combustion energy scaled distance is the distance between the origin of the explosion and the point of interest, scaled by the amount of energy in the congested portion of the vapor cloud as such:

$$r' = \frac{r}{[\frac{E}{p_{atm}}]^{1/3}}$$

Where r is defined in meters, E is defined in joules, and pressure is defined in pascals. The scaled overpressure is simply the overpressure generated by the explosion scaled by the atmospheric pressure:

$$P_s' = \frac{P}{P_{atm}}$$

Normally the proper correlation from distance to overpressure is made by first determining the scaled distance of interest, then determining which blast level curve should be used, and finally reading from the chart the scaled overpressure and converting to a true overpressure. However, for the optimization formulation, using a graphical representation directly will not work, so each of the curves has been converted to a mathematical expression in order that a continuous function relating distance from the explosion and explosion overpressure at the point of interest can be found.

Noting that the curves appear linear on a log-log plot up until a certain minimum value of scaled distance, and further noting that for curves of power level 1-6, the slopes

are very nearly, if not totally, equal, an expression for this linear portion can be found of form:

$$y = cx^b$$

where b is the apparent slope of the log-log plot and c is the constant that defines the y-intercept on the log-log plot. The b exponent is the same for all power levels 1-6, and is defined as -1, as the apparent slope of the log-log plot is -1. The c coefficient is the scaled pressure value at which the curve crosses the scaled distance value of 1 (or, the y-intercept of the curve when the x-axis is defined as log[r']). This value changes with every curve, as tabulated below:

Table 4: c-value constants for the TNO curves

Explosion Level	c-value
1	0.0065
2	0.015
3	0.035
4	0.075
5	0.12
6	0.35

Unfortunately, there is little guidance as to how the severity levels should be chosen, other than that they should be chosen based on the amount of congestion and confinement present. TNO suggests this guidance, based on the work of Kinsella [30]:

Table 5: Suggested severity levels for the TNO Multi Energy Method [30]

Blast strength category	Ignition energy		Obstruction			Parallel plane confinement	Multi-Energy Unconfined	Class
	Low	High	High	Low	No			
	(L)	(H)	(H)	(L)	(N)	(C)	(U)	
1		H	H			C		7-10
2		H	H				U	7-10
3	L		H			C		5-7
4		H		L		C		5-7
5		H		L			U	4-6
6		H			N	C		4-6
7	L		H				U	4-5
8		H			N			4-5
9	L			L		C		3-5
10	L			L			U	2-3
11	L				N	C		1-2
12	L				N		U	1

Now, substituting the expressions for the scaled pressure and distance back into the general equation, we can rearrange to find:

$$= \frac{cP_{atm}[\frac{E}{P_{atm}}]^{1/3}}{r}$$

Which is valid for scaled distances greater than 0.6 and explosion levels less than or equal to 6. This expression can be used to find the overpressure at a unit that is a certain distance away from the center of an explosion and then, using impact modeling, the probability of total structural damage occurring at that point. For more information on impact modeling, see sections 3.4 and 3.5.

3.4 Fire Modeling

Fire is the most frequently reported accidental process safety event for offshore platforms [31] and can have devastating primary and secondary consequences. The primary consequences are the destruction of equipment and harm to personnel by

radiation, but fire can also cause secondary consequences of smoke exposure, blockage of escape routes, and domino effect. In fact, these secondary effects are quite often more damaging than the primary effects. A study by DiMattia, Khan, and Amyotte finds that the probability of human error during the egress phase of escape in gas release and explosion scenarios is significant, especially for those with lower levels of experience aboard a platform [32]. Thus, it is supremely important to design for safety in the case of a fire, not only with emphasis on protecting personnel and processes directly, but also taking account of the secondary effects that may be present, especially with an emphasis on ensuring that escape routes are clearly known and adequately chosen.

Several different types of fire hazard are possible within an offshore environment. Pool fires are possible due to the heavy hydrocarbons that are extracted and processed. Jet fires are a key concern, as they can occur with many different hydrocarbon materials, and can impinge on other process units, causing failure of structural components or piping. Fireballs can occur when a fire impinges on a vessel containing pressure-liquefied gas, causing the boiling of the liquid, rupture of the tank due to overpressure, and flashing of the escaping fuel. Finally, flash fires are also possible in uncongested and unconfined areas of a platform, though the main hazard from this fire is the possibility of ignition of a pool fire, jet fire, or fireball from BLEVE.

The main hazard with fire to be considered in this model is not the direct burning of personnel, but the fact that fire causes the blockage of escape routes, leaving personnel in danger of harm or fatality due to inability to flee the site. To this end, fire modeling will be used to determine optimal layout of sections to facilitate escape.

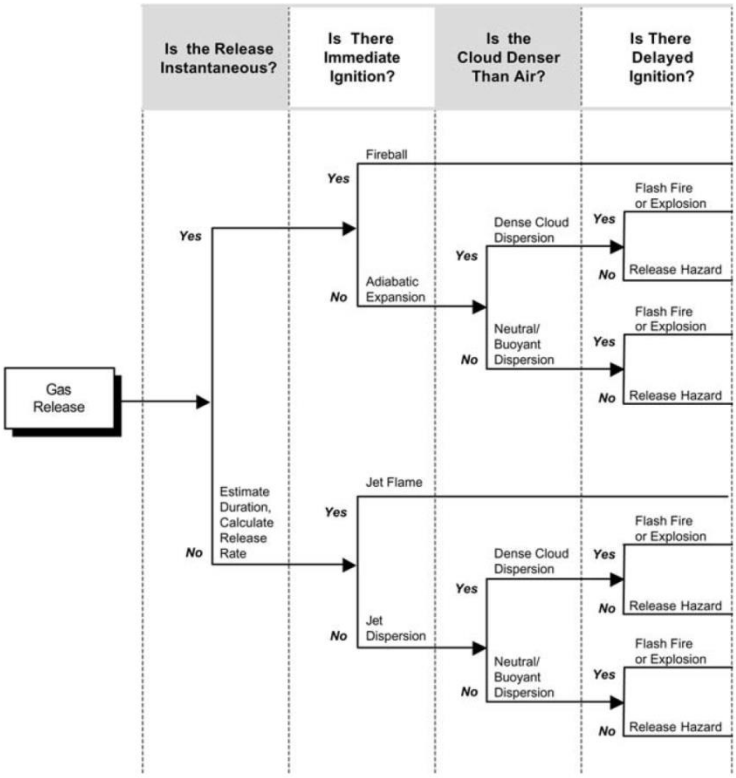

Figure 5: Event tree for fire scenarios in the case of a gas-phase release, from CCPS Guidelines for Fire Protection in Chemical, Petrochemical, and Hydrocarbon Processing Facilities [33]

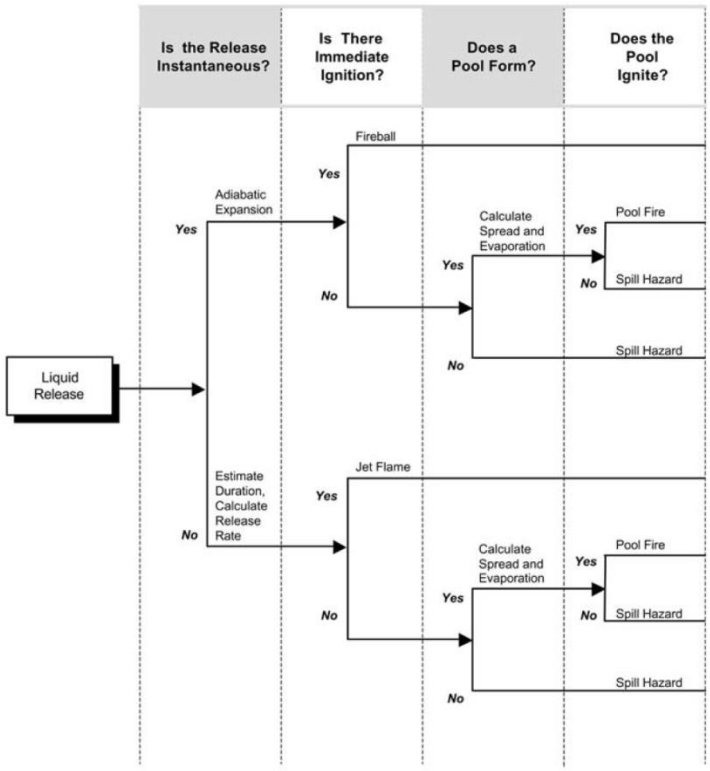

Figure 6: Event tree for fire scenarios in the case of a liquid release, from CCPS Guidelines for Fire Protection in Chemical, Petrochemical, and Hydrocarbon Processing Facilities [33]

Flash fire, pool fire, jet fire, and fireball are all considered in the model. Flash fire modeling is done on the basis of the accumulated cloud that is used for the explosion calculation, but assuming that the local confinement and congestion is not adequate to create a vapor cloud explosion. Thus, the heat flux on a given point is related to the amount of energy in the cloud and the distance from the point of ignition [33], assumed to be the center of the section that the flash fire originates from:

$$I_{s,k} = \frac{E_k}{4\pi r^2}$$

Where E_k is the total amount of energy in the cloud (assumes full combustion), and r is the distance between the ignition and a point of interest. In this case, as in all other cases, because the main hazard from fire is the blockage of escape routes, the points of interest are not just the sections that may be affected by the fire, but also the muster points and intermediate points of interest, as illustrated in the following figure:

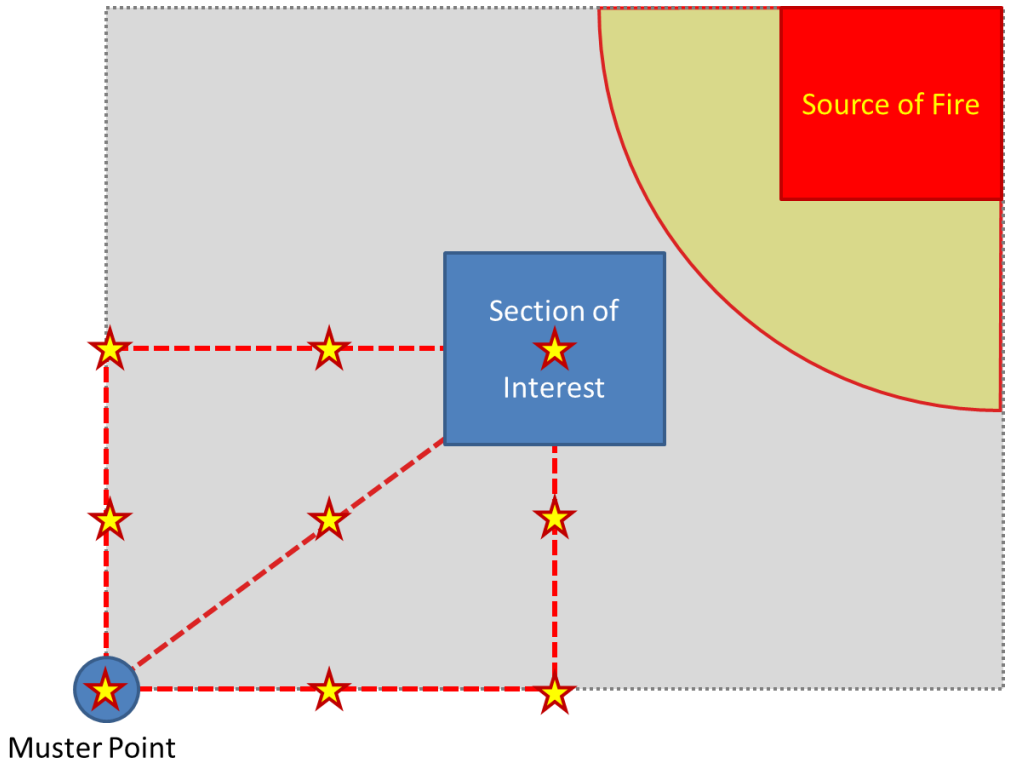

Figure 7: Points of interest in the fire modeling calculation

In this figure, the starred areas are the points at which the heat flux is explicitly calculated for the optimization formulation. There are three different paths that a muster can be reached by in this formulation. The escape can be by a route that moves first in the x-direction, then the y-direction, a route that moves first in the y-direction, then the x-direction, and finally by a direct route. The heat flux from one section on another on

each of the points of interest for each escape method is calculated, and the maximum of those heat fluxes is then used as the value for all escape probability calculations between those two sections. Thus, there are three escape methods, one of which is chosen during the optimization in order to minimize the risk of failure to escape.

Pool fire modeling is done in much the same way as flash fire modeling. The following information must be known or assumed in order to initiate a pool fire model:

- Material released, often hydrocarbon condensate in offshore operations
- Mass released, m, in kilograms based on process conditions
- Mass burning rate, m", in kg/m^2s
- Heat of combustion of the material, ΔH_c, in kJ/kg

From this information, the steady state diameter of the pool can be determined using the simplified pool diameter model:

$$D = \left(\frac{4\dot{m}}{\pi \dot{m}"}\right)^{1/2}$$

And the heat release can be determined using:

$$\dot{Q} = \Delta H_c A \dot{m}"$$

From these expressions, the height of the plume can be found:

$$H = 0.23\dot{Q}^{2/5} - 1.02D$$

The burning time can be found:

$$t_b = \frac{m}{\dot{m}"A}$$

And the heat flux on a point of interest away from the center of the fire can be found:

$$I_{s,k} = \frac{58(10^{-0.00823D})}{4\pi R^2}$$

The burning time is used in this case to scale the amount of heat dosage a point receives from a pool fire, as unlike a flash fire or fireball (which typically have a duration of a few seconds), the duration of a pool fire can be significantly long to cause damage from prolonged exposure. It is taken into account in the probit function (see section 3.6).

For a jet fire, several pieces of information must be known as well. These are:

- Material being released
- Process pressure (P_P) and ambient pressure (P_{amb}) in Pa
- Flammable material density (ρ_P) and ambient density of air (ρ_{amb}) in kg/m^3
- Area of leak (A_h) in m^2
- Isentropic expansion factor, k
- Discharge coefficient, C_D, usually assumed to have a value of 0.85

To determine the mass released from an orifice, the following fluid flow equation is utilized:

$$\dot{m} = C_D \rho_{amb} A_h \sqrt{\left(\frac{2P_P}{\rho_P}\right)\left(\frac{k}{k-1}\right)\left(1 - \left[\frac{P_{amb}}{P_P}\right]^{\frac{k-1}{k}}\right)}$$

The total heat released and heat flux are calculated similarly to the other scenarios:

$$\dot{Q} = m\dot{\Delta}H_C$$

And

$$I_{s,k} = \frac{0.2\dot{Q}}{4\pi R^2}$$

Where the 0.2 is a correction factor to the heat release.

Fireball modeling is based on the Roberts model [34] which gives an empirical correlation of fireball diameter and duration to mass released:

$$D = 5.8M^{\frac{1}{3}}$$

And

$$t = 0.44M^{\frac{1}{3}}$$

Along with a correlation for scaling the heat flux from the surface of the fireball:

$$F_R = 0.27P^{0.32}$$

Where P is the vapor pressure of the flammable material in MPa, and F_R is usually found to be between 0.2 and 0.4. The surface emissive power of a fireball depends on the flammable material. For the probable materials used in this study, a fireball of LPG has a surface emissive power of about 270 kW/m^2 and natural gas has a surface emissive power of 150 kW/m^2.

In the current model, heat flux at points of interest are calculated for all fire scenarios, but only the heat flux with the greatest magnitude on a point of interest is considered in the objective. This is a valid simplification because two fire events are not likely to happen concurrently in the same section, and so there would be no

superposition of the heat fluxes. Therefore, there is no need to consider reinforcing effects of multiple events, and the event with the greatest heat flux is sufficient for a worst-case scenario. This does not imply that only one type of fire event is considered for the whole optimization – one section may have a jet fire as the worst-case event while another may have a flash fire as the worst case event. However, since all fire events scale in the same way, as a function of the inverse-square of the distance between the sections, one section will produce the same worst-case event for all points of interest.

3.5 Ignition Probability Modeling

Ignition probability modeling is based on the work of Moosemiller [35] for fire and explosion frequencies. Default values for ignition probability are often used, such as 0.15 for immediate ignition and 0.3 for delayed ignition, but these values do not capture the variability of ignition probability based on process conditions such as temperature, material, and presence of various types of ignition source. The algorithms for ignition probability modeling used in the model are as follows:

3.5.1 Immediate Ignition

Immediate ignition (prompt ignition) is ignition that occurs early enough in vapor cloud formation that it does not allow an appreciable vapor cloud to form. The probability of this event occurring is based on the process temperature (T), auto-ignition temperature of the material (AIT), pressure of the process material (P), and minimum ignition energy (MIE) in the following manner:

$$P_{imm.ign.} = \left[1 - 5000e^{-9.5\left(\frac{T}{AIT}\right)}\right] + \left[\frac{0.0024P^{\frac{1}{3}}}{MIE^{\frac{2}{3}}}\right]$$

Where the first term is equal to 0 if T/AIT < 0.9 and equal to 1 if T/AIT > 1.2, and the maximum value of the probability of immediate ignition is 1. Values for AIT and MIE are well-documented in literature, and T and P are process parameters.

3.5.2 Delayed Ignition

Delayed ignition occurs when a vapor cloud has accumulated over time before finding a source of ignition. This can result in a flash fire or an explosion if the area is congested. The probability of delayed ignition is based on the flowrate of material (FR), the minimum ignition energy (MIE) of the material, a "source factor" (S), and the time that the material is allowed to accumulate (t) in the following manner:

$$P_{del.ign.} = 1 - \frac{0.7}{[0.6 - 0.85\log(MIE)][7e^{0.642\ln(FR)-4.67}][1-(1-S^2)e^{-(0.015S)t}]}$$

For a denominator greater than 1, and:

$$P_{del.ign.} = 0.3[0.6 - 0.85\log(MIE)]\left[7e^{0.642\ln(FR)-4.67}\right]\left[1-(1-S^2)e^{-(0.015S)t}\right]$$

If the multiplicative factors other than the 0.3 are less than 1.

Where the first term represents ignition probability based on material factors and cannot exceed 3 or be below 0.1, the second term represents ignition probability based on amount of material released and cannot exceed 2, and the final term represents ignition type and response time. The S parameter in this factor is based on the sources of ignition present in the area of the release. This can be replaced with either the fraction of the cloud within a process unit, or generic values based on equipment density from [35].

3.5.3 Delayed Explosion Probability

Given a delayed ignition of a vapor cloud, it is possible that an explosion can occur. The probability is based on the flow rate of flammable material (FR) and modified by a factor for the reactivity of the material (R) as follows:

$$P_{exp} = R * 0.024FR^{0.435}$$

Where R is 0.3 for low reactivity materials (e.g. natural gas), 1 for medium reactivity materials (most materials), and 3 for high reactivity materials (e.g. hydrogen).

3.5.4 Event Frequency

The probabilities for these events can be visualized as an event tree:

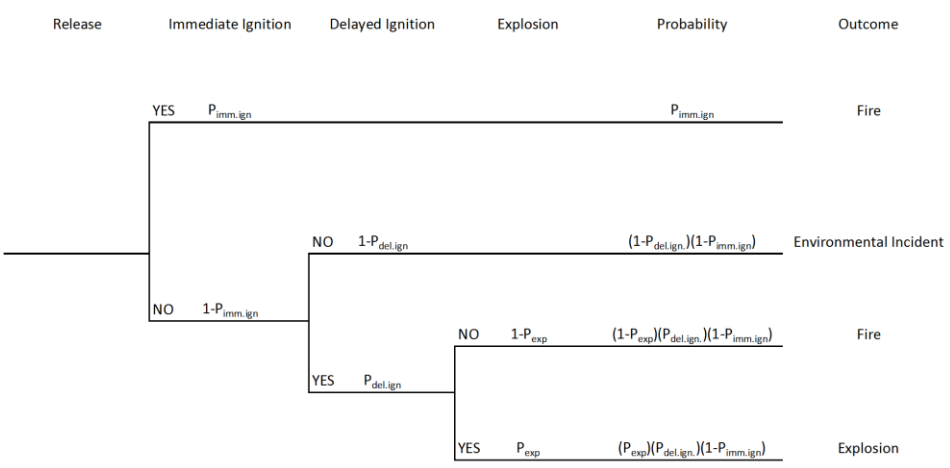

Figure 8: Event tree for fire and explosion probabilities, adapted from [35]

The events that can occur are immediate ignition, delayed ignition, or no ignition and from delayed ignition the cloud can burn as a fire or explode. Each of the associated probabilities is calculated through the process parameters that are input, and then the probabilities illustrated in the event tree for fire, explosion, and environmental incident are calculated. It can be seen that the cumulative probability of an event sums to 1, as is expected. Environmental incidents are not considered in the optimization formulation.

3.6 Impact Modeling

Impact modeling is the determination of the impact of the above-mentioned hazards on the structure of the platform and the personnel on it. Overpressures and radiation levels can be assumed to cause a certain damage at a certain level, but it is important in the optimization formulation to have a mathematical expression that can be used to relate hazards to impact. One widely-used way of measuring impact of a single-exposure event is through the use of experimentally-obtained probit functions [36].

Probit functions are a way of taking a sigmoid dose-response curve and linearizing the response based on the dose. Then, once the proper probit coefficients are determined, the probit value can be found for any dosage and then be converted to a probability of the response occurring. Though dose-response is usually thought of in terms of toxic dosage to humans, the dose could be any single exposure event, such as an explosion overpressure or heat radiation dose, and the response could be the probability of structural failure or shattering of glass.

Probit functions are generally of the form $Y = k_1 + k_2 \ln V$, where Y is the probit value that can be converted to a probability and the k parameters are based on fitting response data to dosage data. V is the variable of interest in determining the response. For vapor cloud explosions, structural damage probability is linked to overpressure using the following probit function:

$$Y = -23.8 + 2.92 \ln P$$

Where the overpressure is measured in pascals. The probability measured in this expression is that of total structural damage, as correlated by Eisenberg [37]. It is more complicated to correlate heat radiation to structural stability, so there are few (if any) probit models that attempt to describe the probability of destruction of a structure in a fire scenario. However, the effect of heat radiation on humans is well-studied. The probit function for the lethality of heat radiation dosage on humans is as follows [31]:

$$Y = -36.38 + 2.56\ln(t_e q_e)$$

Where q is the heat flux value and t is the exposure time. When the Y value is found, the specific equation to convert to a probability of response is:

$$P = 50\left[1 + \frac{Y-5}{|Y-5|}\text{erf}\left(\frac{|Y-5|}{\sqrt{2}}\right)\right]$$

Where erf is the error function. Tabulated data is also available to determine the probability from the Y variable. This formulation can be used in the optimization model to estimate the probability of a fatal incident, which can be minimized in the objective function.

3.7 Case Studies

Two case studies have been formulated to demonstrate the applicability of the model. The first is based on a very well-known offshore process safety event, where the layout is shown to be inadequate, then optimized and improvement is shown. The second is based on an actual layout used in the offshore industry that is not glaringly deficient, but requires that muster points are assigned to the layout. The full optimization is also carried out on this layout and the results are compared with the original.

3.7.1 Case Study: Piper Alpha Layout Deficiency

An initial case study has been prepared to demonstrate the ability of the model to optimize the layout of an offshore platform. This case study has been modeled off of the Piper Alpha incident: a well-known accident that affected the way that process safety is perceived in the offshore industries. The purpose of this case study is to take an actual layout that is known to have significant design flaws which led to a catastrophic loss of life and assets, and apply the prior-defined optimization model to it to evaluate the

improvement in the layout that is obtained, and then turn a critical eye to the advantages and disadvantages of such a model, and find where the model can be improved.

Information for the scenarios and layout of the platform were taken from Drysdale and Sylvester-Evans' case study on the explosion and fire aboard Piper Alpha [38]. Because detailed information about the actual dimensions of the platform and platform modules are not available, the dimensions were estimated from drawings given in this paper. All scenarios that are presented in the paper as contributing to the disaster are assumed to have been credible and foreseeable scenarios that could and should have been taken into account in the design stage of the platform. In addition to the scenarios that contributed to the actual event, several other common-sense scenarios were added to the formulation, as they would likely have been found in a formal risk assessment, and thus would be considered in the design.

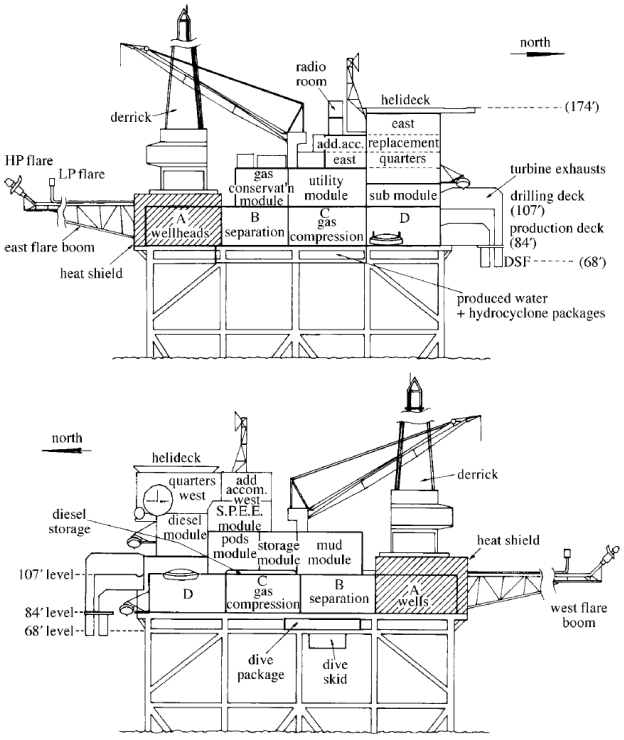

Figure 9: Elevation layout of the Piper Alpha Platform, from Drysdale and Sylvester-Evans [38]

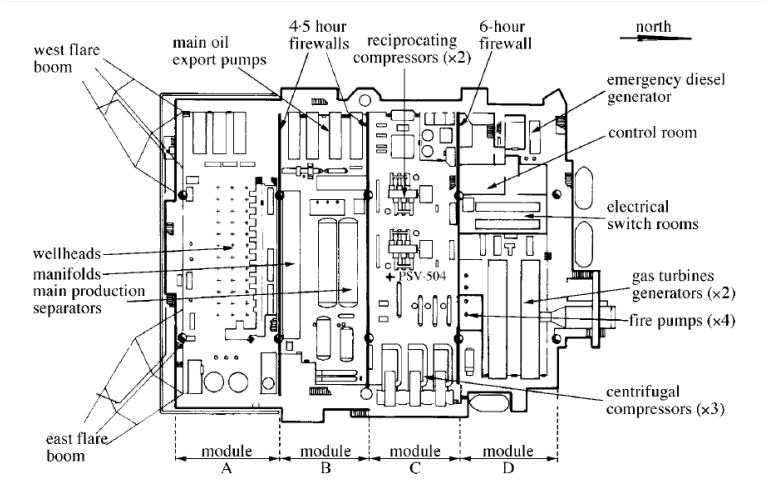

Figure 10: Production deck layout of the Piper Alpha Platform, from Drysdale and Sylvester-Evans [38]

3.7.1.1 Inputs

The following inputs were used in the case study:

Table 6: Input parameters for the optimization formulation – General Properties

Input	Value(s)
Platform Dimensions	184’ x 184’
Sections	Wellhead, Quarters, Shop, Process, Compressors, Control, Storage, Utilities
Floors	Four possible floors
Musters	Four possible musters
Stories	Wellhead: 4 Quarters: 2 All others: 1
Area [ft^2]	Wellhead: 8464 Quarters: 8464 Shop: 8464 Process: 2116 Compressors: 6348 Control: 8464 Storage: 1058 Utilities: 1058
Maximum Aspect Ratio	5
Section Population (Cost)	Wellhead: 5 Quarters: 30 Shop: 10 Process: 1 Compressors: 1 Control: 10 Storage: 1 Utilities: 1

Table 7: Input parameters for the optimization formulation – Vapor Cloud Explosion and Flash Fire

Input	Value(s)
Sections Possible	Wellhead, Compressors, Utilities, Process
Material	Wellhead, Utilities, Process: Natural gas (properties of methane) Compressors: Gas condensate (properties of diesel fuel)
Explosion Severity Level	Wellhead: 6 Compressors: 5 Utilities: 3 Process: 3
Minimum Ignition Energy [mJ]	Natural gas: 0.28 Gas condensate: 0.80
Autoignition Temperature [F]	Natural gas: 1112 Gas condensate: 406
Reactivity Value	Natural gas: 0.3 Gas condensate: 1.0
Heat of Combustion [kJ/kg]	Natural gas: 55700 Gas condensate: 46800
Mass of Gas Cloud [kg]	Wellhead: 45 Compressors, Utilities, Process: 40
Process T [F]	All: 200
Process P [psi]	Wellhead: 500 Compressors, Utilities, Process: 100

Table 8: Input parameters for the optimization formulation – Jet Fire, Pool Fire, Fireball

Input	Value(s)
Sections Possible	Wellhead, Compressors, Utilities, Process
Material	Crude Oil
Heat of Combustion [kJ/kg]	Natural gas: 55700 Crude oil: 42800
Hole Diameter (Jet Fire)	1 inch
Mass Flowrate (Pool Fire)	1 kg/s

3.7.1.2 Results

The optimization formulation was run using DICOPT as the MINLP solver. DICOPT utilized CONOPT as its solver for the NLP subproblem and CPLEX for its MIP subproblem. A simplified MILP problem was solved with CPLEX before solving the layout problem in order to initialize the variables and decrease infeasibility in the initial MINLP problem. The total time to solution was 99.5 seconds on a 2.13 GHz processor with 4 GB RAM. The problem consisted of 3192 individual variables and 8110 individual constraints.

Because of the nonlinearity of the model, it is essential to have a good initial estimate of the values of the variables. In this case study, the initial values were found by solving two optimization sub-problems before solving the main problem. When a sub-problem is solved, the solution information is then passed on to the next optimization as an initial guess where possible. In this way, solution time was cut and infeasibility problems were lessened. The first optimization is an MILP initialization to ensure a feasible layout with respect to non-overlap constraints. All linear constraints are used, and the objective is simply equal to a constant to obtain feasibility. As it would be expected that the optimal muster, more often than not, is the muster point closest to a section, the second optimization is an MINLP optimization to assign sections to the musters closest to them. This is done by setting the objective to minimize the distance

between the midpoints of each section and the respective muster it is assigned to. After this optimization is done, the main problem is initialized.

The results are illustrated in the following figures:

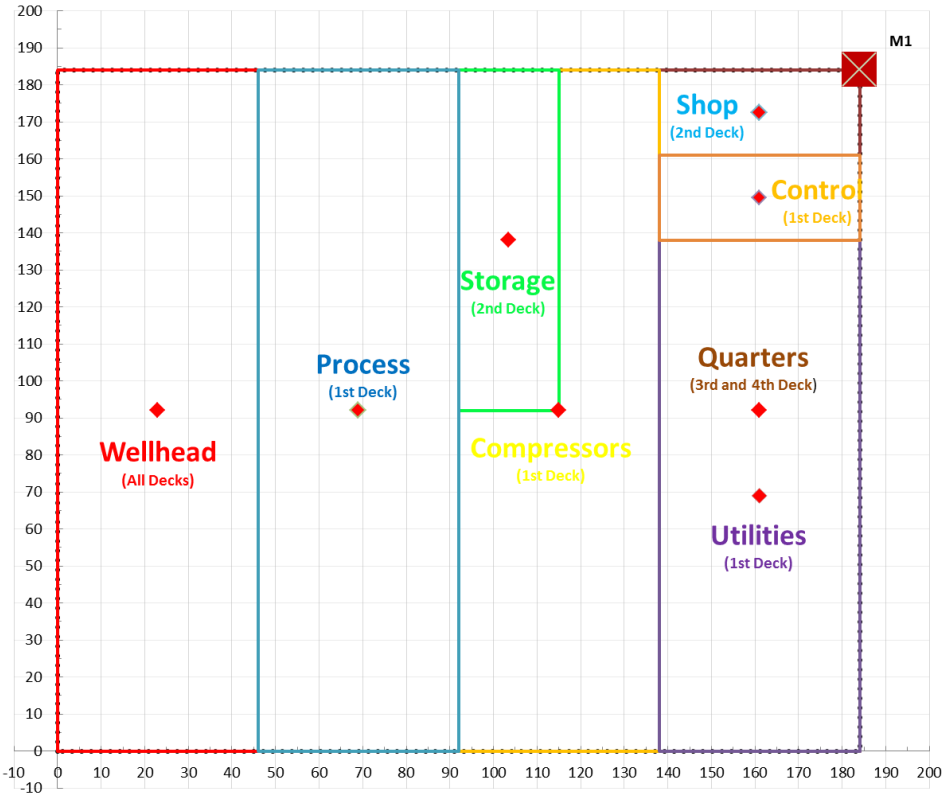

Figure 11: Output footprint of the original Piper Alpha layout

The original footprint of Piper Alpha, as given in the case study by Drysdale and Sylvester-Evans is replicated by fixing the side lengths, x- and y-coordinates, and floor assignment of each of the sections. The scenarios considered are defined in the previous section, and include the events of the disaster, namely the possibility of vapor cloud explosion in the compressor module, and pool fire and fireball in several modules, as well as other credible scenarios that did not occur. Through the use of the optimization

model, though the layout has not been changed, probabilities and an objective value for the original layout can be obtained.

Table 9: Calculated probability of escape failure for original layout

		Fire From				Weighted Cost
		Wellhead	Compressors	Utilities	Process	
Effect on	Wellhead	-	0.367	0.424	0.384	5.875
	Quarters	0.000	0.007	0.163	0.000	5.100
	Compressors	0.000	-	0.659	0.377	1.036
	Storage	0.001	0.086	0.012	0.080	0.179
	Utilities	0.000	0.086	-	0.000	0.086
	Process	0.230	0.394	0.639	-	1.263
	Control	0.002	0.000	0.004	0.000	0.060
	Shop	0.000	0.000	0.000	0.000	0.000
						Sum = 13.599

Table 10: Calculated probability of section destruction for original layout

		Vapor Cloud Explosion From				Weighted Cost
		Wellhead	Compressors	Utilities	Process	
Effect on	Wellhead	-	0.025	0.000	0.039	0.320
	Quarters	0.039	0.090	0.046	0.012	5.610
	Compressors	0.050	-	0.015	0.039	0.104
	Storage	0.050	0.087	0.003	0.030	0.170
	Utilities	0.039	0.079	-	0.011	0.129
	Process	0.054	0.090	0.002	-	0.146
	Control	0.036	0.043	0.004	0.007	0.900
	Shop	0.034	0.024	0.002	0.005	0.650
						Sum = 8.029

It can be seen from the information in the preceding two tables that the original layout performed relatively poorly in the fire scenario, particularly with respect to the quarters and wellhead. Not only was the quarters highly populated on the platform, but it was also the main muster point for the platform and carried the helideck. The probability of escape blockage for the quarters is almost in total due to the utilities, the section that coinhabits the x- and y- coordinates of the quarters, but on a lower floor.

In the case of the explosion scenario, the sum of the probability of destruction is less than that of the fire scenario, but mostly because the calculated probability of a vapor cloud explosion event is much smaller on average than the calculated probability of a fire event (the highest probability of an explosion event was 0.090 for the compressors, as opposed to 0.659 for a fire event). As was expected based on real-life events, the greatest probability of destruction came from the compressors (module C) on the process (module B). This correlates well with actual observation, as the B/C firewall was destroyed during the initial explosion, causing an increase in fire and explosion hazards for the whole platform. This probability value is shared with the quarters, which is an equal distance away from the process and should thus share the same probability based on the explosion calculation. This leads to a high weighted cost for the section, which accounts for about 60% of the explosion cost.

The optimized layout, shown below, fares significantly better in the fire and explosion calculations. Because the same process parameters are used, the probability of a fire or explosion occurrence stays the same, but the probability that a section of interest will be affected is changed by the spacing of the sections and allocation of muster points. In this way, an objective value decrease of 68.7% is obtained (21.628 to 6.778). The weighted cost of the fire scenario has dropped 78.8% (13.599 to 2.885) and the weighted cost of the explosion scenario has dropped 51.5% (8.029 to 3.893). The main factor contributing to the drop in both costs is the fall in the probability of escape blockage and destruction of the most populated sections: the quarters, control room, and shop, which are achieved by the adequate spacing from potential sources of fuel, while allocating logical muster points and escape paths to avoid possible escape blockage. Although the greatest gains are seen in the sections with the highest value, gains are seen almost universally with the exception of several of the lower value sections seeing slight regressions in the explosion scenario.

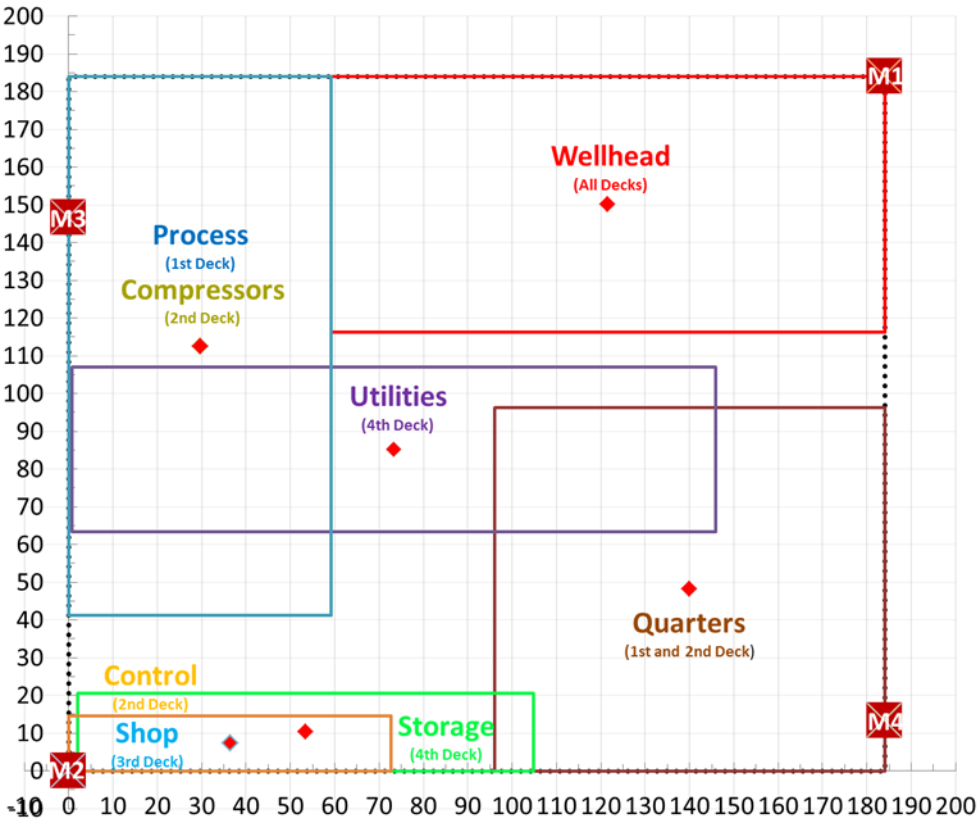

Figure 12: Optimized footprint of the Piper Alpha layout

Table 11: Calculated probability of escape failure for optimized layout

		Fire From				Weighted Cost
		Wellhead	Compressors	Utilities	Process	
Effect on	Wellhead	-	0.118	0.015	0.139	1.360
	Quarters	0.000	0.000	0.000	0.000	0.000
	Compressors	0.000	-	0.044	0.660	0.704
	Storage	0.000	0.024	0.012	0.010	0.046
	Utilities	0.004	0.011	-	0.005	0.020
	Process	0.339	0.394	0.012	-	0.745
	Control	0.000	0.000	0.000	0.000	0.000
	Shop	0.000	0.000	0.001	0.000	0.010
						Sum = 2.885

Table 12: Calculated probability of section destruction for optimized layout

		Vapor Cloud Explosion From				Weighted Cost
		Wellhead	Compressors	Utilities	Process	
Effect on	Wellhead	-	0.020	0.004	0.010	0.170
	Quarters	0.048	0.009	0.005	0.004	1.980
	Compressors	0.048	-	0.015	0.054	0.117
	Storage	0.035	0.017	0.005	0.008	0.065
	Utilities	0.052	0.079	-	0.034	0.165
	Process	0.048	0.133	0.015	-	0.196
	Control	0.032	0.017	0.003	0.008	0.600
	Shop	0.032	0.017	0.003	0.008	0.600
						Sum = 3.893

3.7.1.3 Analysis

In this case study, it can be seen that the objective value is improved, and thus ostensibly the platform should be safer in the case of an event. However, as there are always tradeoffs in offshore layout, it is important to turn a critical eye to what has been found.

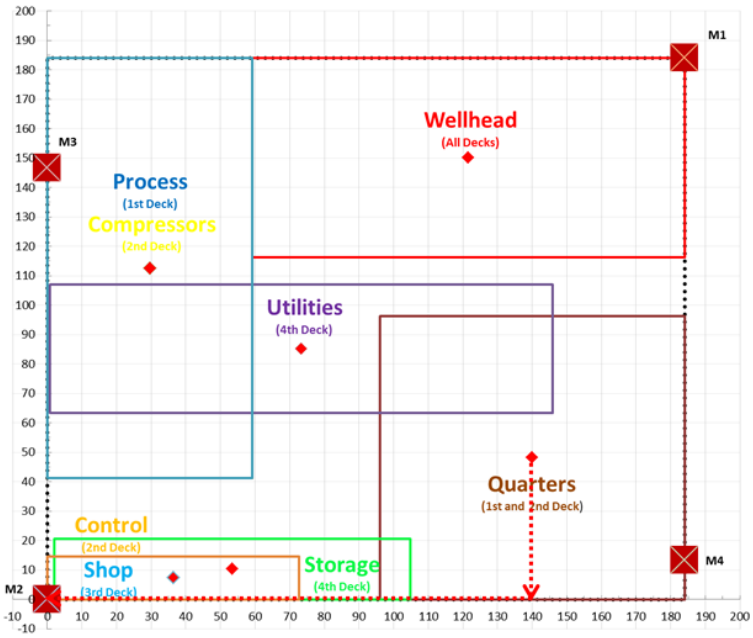

Figure 13: Quarters muster assignment and recommended path

Of interest is the muster allocation for the problem. One consequence of the radiation intensity model is that the muster point assignment for a section may not always seem to be the logical point if the midpoint of a section is the closest point of fire intensity assessment.

Take, as an example, the quarters section, which is allocated to M2 while M4 is much closer with no apparent drawback. Notice, however, that the sources of fire are all closest to the midpoint of the quarters whether M2 or M4 is chosen. Therefore, according to the model, the escape routes are equivalent and neither can be identified as better than the other. The less obvious path is chosen, which according to the model is not strictly incorrect.

A practical concern is whether it is acceptable that certain sections be separated from each other. For all of its failings, the Piper Alpha platform was laid out in a logical manner from a production standpoint. The production modules (wellhead, process, compression) were near each other and the control room and shop were near the production modules. However, this proximity of different modules, though logical in that way, also helped lead to the ultimate demise of the platform due to the 'decapitation' of operations when the control room was destroyed. In the model, sections can easily be fixed near each other if there is a need, but this also limits the options for how the sections can be arranged. There must be a balance between feasibility and freedom.

Of technical concern is the non-linearity of the model. Unfortunately, because of the nature of the explosion and fire probability determination, the model is non-linear and non-convex. Thus, it is not guaranteed that the solution that has been given is globally optimal – only locally optimal. Though the result of the optimized model is significantly better than the original layout, it is not known how close to globally optimal this answer is. This is confirmed by the volatility of the objective value with respect to an initial value of certain variables.

3.7.2 Case Study: Placement and Assignment of Muster Points

An important application of the model is to determine the optimal route of escape and, if necessary, the optimal placement of muster points. This application can still be used even in the case that the layout is already known. In this case, the sections of the platform can simply be fixed and the optimization can be used to vary the muster points in relation to the sections in order to minimize the fire hazard. Though the correct placement of a muster point seems like a trivial matter, it is believed that this is one of the most important considerations in the design of an offshore platform, as a poorly placed or poorly assigned muster can lengthen the amount of time it takes to escape or take an escape path through a hazardous area.

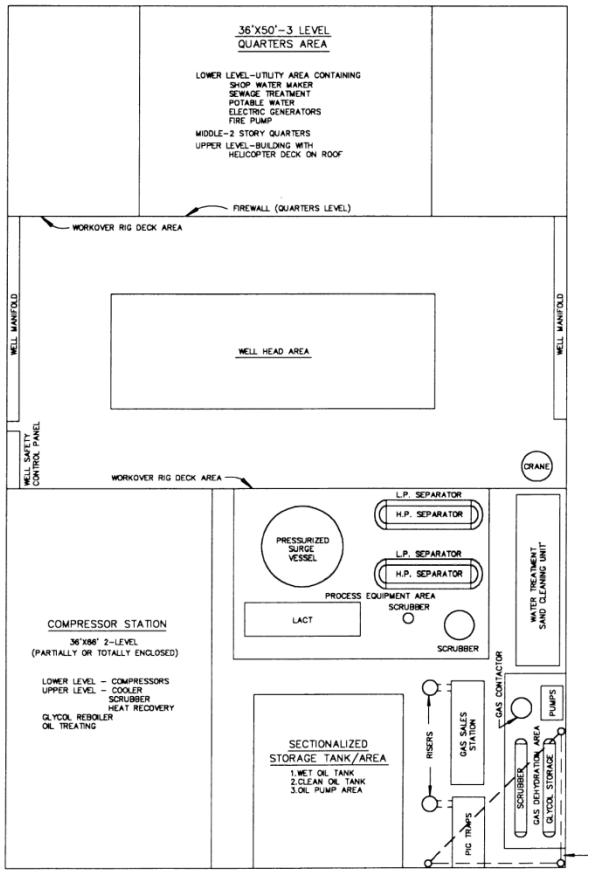

Figure 14: Example layout from API 14J [28]

The preceding layout is an example that has been taken from API Recommended Practice 14J: Recommended Practice for Design and Hazards Analysis for Offshore Production Facilities. This layout is based on a platform that was actually used and exhibits many of the tradeoffs that come with offshore facilities.

Some of the positive and negative points are listed below:

Table 13: Tradeoffs associated with the API 14J layout

Positive Points	Negative Points
Pipeline riser toward the opposite end from the living quarters	Wellhead area immediately adjacent to quarters
Machinery and vessels relatively spaced from the quarters	Wellhead enclosed by quarters and process units restricting escape
Fire pump located near quarters and isolated from process	Process units near compressors
No fired process units	Generator near quarters
	Compressor near treatment area

The following case study aims to illuminate first how the model can be used to assign muster points to sections, and then to compare it to a fully optimized layout created by allowing the sections the be placed on the platform freely.

3.7.2.1 Formulation of the Muster Point Assignment Case Study

In the initial phase of the case study, the above layout is converted into model code, fixing each of the sections to their coordinates and fixing the side lengths to the proper dimensions. Muster points are allowed to vary along the assigned edge, and paths to the muster points are allowed to vary to be subject to the least amount of heat exposure. The process inputs to the muster point assignment formulation are similar to

those of the Piper Alpha case study. The main change is that the control room is not present, and risers and treatment sections are added. The risers contain flammable material that is assumed to be similar in nature to the material in the compressor section (all of the riser process parameters are identical to those of the compressor section). Thus, this is an extra flammability and explosion hazard. The treatment area is not a source of flammable material and only serves to take space with a minimal section cost. Otherwise, the sections that were present in the Piper Alpha case study have the same process inputs as before; the only changes made were in dimensions and layout. The sections are free to go to any muster without constraint – there is no limit on the number of sections assigned to a certain muster point.

The second phase of the case study allows the whole layout to be optimized in order to compare results. In this phase, the process parameters are all identical to the first phase. The areas to be satisfied are equal to the original layout and the maximum aspect ratio allowed is the aspect ratio of the sections in the original layout.

In the study by DiMattia, Khan, and Amyotte, it is noted that the highest probability of human error during the egress phase is when an alternate escape path must be identified because the first is inaccessible [32]. To balance the accessibility of primary and alternate escape routes, as well as to ensure that the alternate is known to a hypothetical person attempting escape, two muster points are now selected, in accordance with the API 14J assertion that there should be at least two escape points for every area. This is accomplished with a simple modification to the muster point assignment constraint:

$$\sum_{m} SectionMuster_{s,m} = 2 \quad \forall s \in S$$

Both escape routes are weighted equally in the optimization. Both phases of this case study use the same initialization method as the Piper Alpha case study.

3.7.2.2 Results

The figure below shows the optimized muster placement for the API layout. Two musters appear in the top corners, one on the right edge of the platform parallel with the midpoint of the quarters and shop, and one on the bottom edge of the deck parallel with the midpoint of the storage section. The total objective value is 19.6. The output information from the optimization is summarized below.

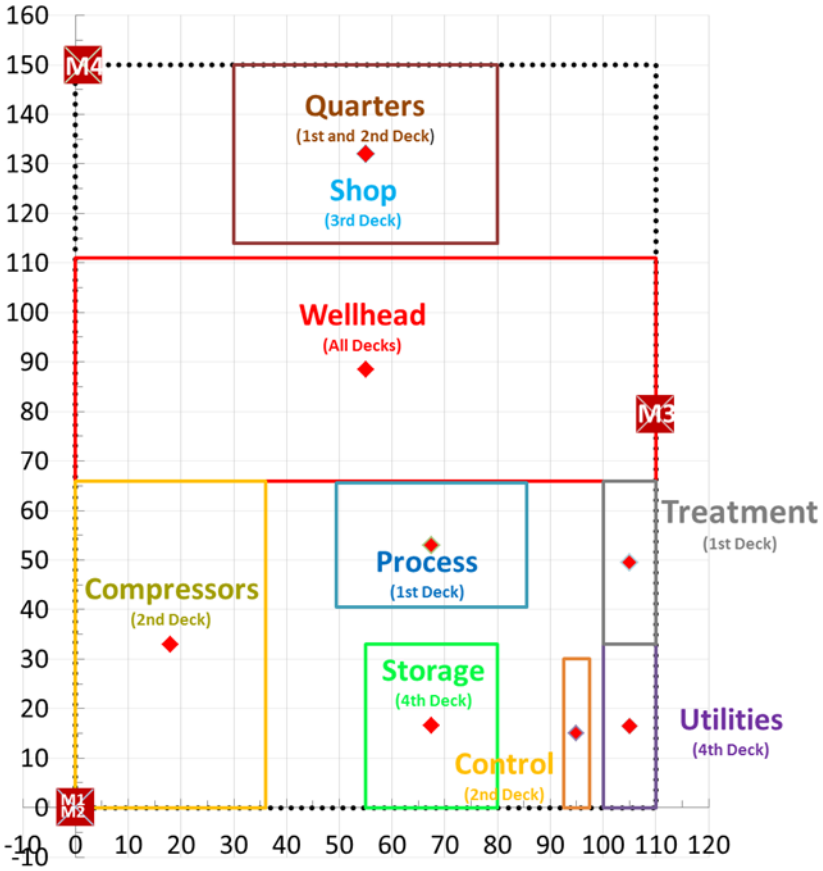

Figure 15: Optimized placement of muster points for a pre-existing layout from API 14J

The figure above shows the optimized muster placement for the API layout. Two musters appear in the bottom left corner, one on the top left corner near the midpoint of

the quarters and shop, and one on the right edge of the deck nearly parallel with the midpoint of the wellhead section. Solution was reached in 280.8 seconds, The problem included 2873 variables and 9648 constraints. The total objective value is 19.607. The output information from the optimization is summarized below.

Table 14: Calculated probability and weighted cost of escape failure for optimized musters, fixed layout

		Fire From					**Weighted Cost**
		Wellhead	Compressors	Utilities	Process	Risers	
Effect on	Wellhead	-	0.367/ 0.000*	0.000/ 0.000	0.104/ 0.104	0.000/ 0.000	2.875
	Quarters	0.056/ 0.056	0.031/ 0.000	0.000/ 0.000	0.000/ 0.000	0.000/ 0.000	4.290
	Compressors	0.000/ 0.008	-	0.000/ 0.000	0.003/ 0.003	0.000/ 0.000	0.014
	Storage	0.000/ 0.000	0.147/ 0.147	0.136/ 0.136	0.162/ 0.162	0.090/ 0.090	0.818
	Utilities	0.000/ 0.014	0.031/ 0.000	-	0.005/ 0.014	0.392/ 0.392	0.848
	Process	0.156/ 0.156	0.000/ 0.228	0.005/ 0.005	-	0.000/ 0.000	0.550
	Risers	0.000/ 0.000	0.042/ 0.042	0.660/ 0.660	0.015/ 0.015	0.000/ 0.000	1.434
	Shop	0.056/ 0.056	0.031/ 0.031	0.000/ 0.000	0.000/ 0.000	0.000/ 0.000	1.740
	Treatment	0.000/ 0.000	0.049/ 0.049	0.276/ 0.276	0.315/ 0.315	0.011/ 0.011	1.302
							Sum = 13.871

*Probability of escape from first allocated muster point/probability of escape from second allocated muster point

Table 15: Calculated probability and weighted cost of section destruction for optimized musters, fixed layout

		Vapor Cloud Explosion From					Weighted Cost
		Wellhead	Compressors	Utilities	Process	Risers	
Effect on	Wellhead	-	0.052	0.003	0.045	0.025	0.625
	Quarters	0.054	0.017	0.000	0.016	0.007	2.820
	Compressors	0.053	-	0.003	0.033	0.029	0.118
	Storage	0.053	0.078	0.028	0.046	0.120	0.325
	Utilities	0.051	0.027	-	0.034	0.133	0.245
	Process	0.054	0.075	0.015	-	0.079	0.223
	Risers	0.051	0.036	0.054	0.038	-	0.179
	Shop	0.054	0.017	0.000	0.016	0.007	0.940
	Treatment	0.053	0.027	0.033	0.045	0.103	0.261
							Sum = 5.736

Table 16: Muster assignment for the API layout

Section	Muster	Path	Muster Point	x-coordinate	y-coordinate
Wellhead	2,4	x-y,direct	M1	0	0
Quarters	2,4	x-y,direct	M2	0	0
Compressors	1,4	direct,direct	M3	110	79.5
Storage	1,2	direct,direct	M4	0	150
Utilities	1,4	y-x,y-x			
Process	3,4	direct,x-y			
Risers	1,2	direct,direct			
Shop	1,2	x-y,x-y			
Treatment	1,2	direct,direct			

The assignment of the muster points is, for the most part, sensical and straightforward. The most costly sections, the quarters and shop, are directed to the nearest muster, and the muster is placed so that it is the shortest possible distance from the quarters on the right side of the platform. Several other sections are assigned to the same muster and follow logical paths to get there, avoiding routes through the sources of fire.

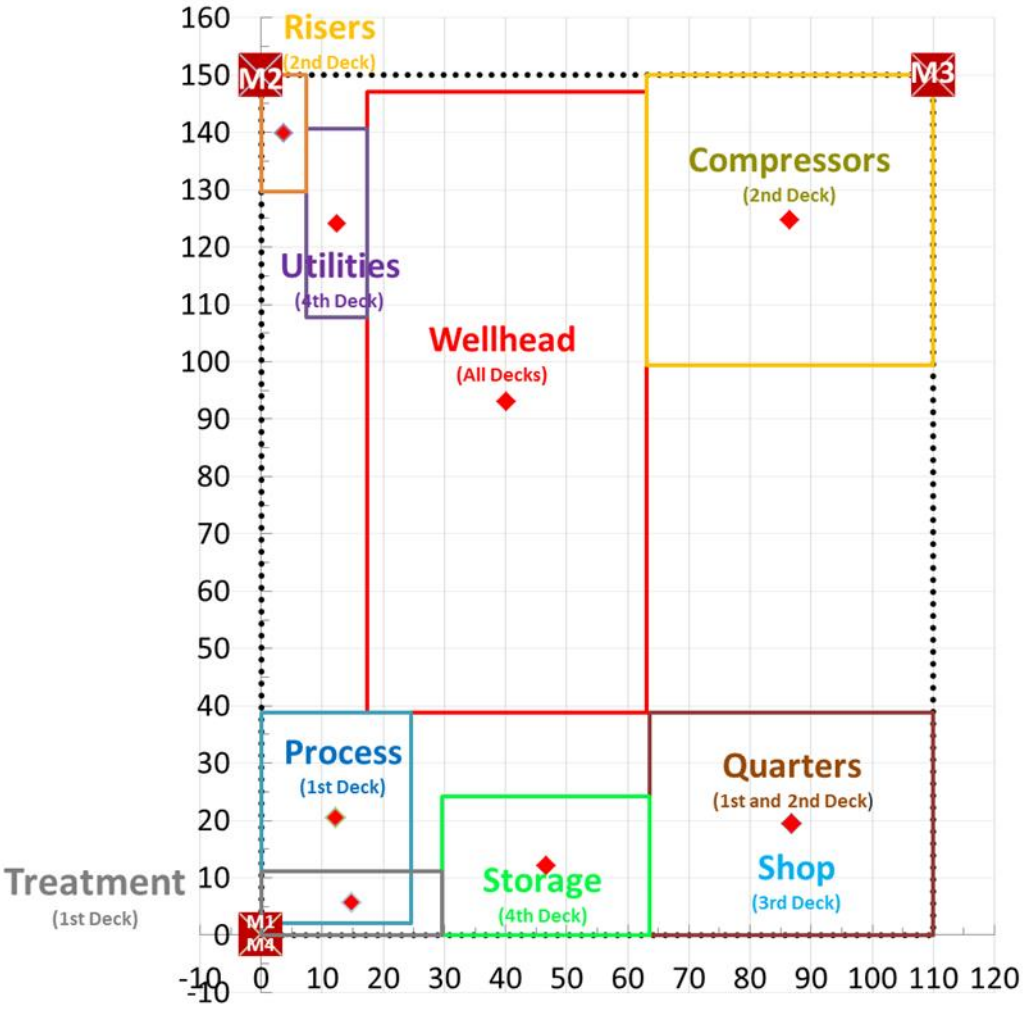

Figure 16: Optimized layout for the API platform

The objective value is decreased by 77.5%, mostly owing to an improvement in the fire scenario. This shows that while allocation of muster points is effective, a full layout decreases the total cost of the layout even further. It does this once again through spacing of possible fire and explosion sources while allocating muster points such that escape is not forced through high-risk areas.

Table 17: Calculated probability and weighted cost of escape failure for optimized musters, optimized layout

		Fire From					Weighted Cost
		Wellhead	Compressors	Utilities	Process	Risers	
Effect on	Wellhead	-	0.000/ 0.000*	0.000/ 0.000	0.000/ 0.000	0.000/ 0.000	0.000
	Quarters	0.002/ 0.000	0.000/ 0.000	0.000/ 0.000	0.000/ 0.000	0.000/ 0.000	0.060
	Compressors	0.000/ 0.000	-	0.000/ 0.000	0.000/ 0.000	0.000/ 0.000	0.000
	Storage	0.000/ 0.000	0.007/ 0.000	0.000/ 0.000	0.000/ 0.000	0.022/ 0.000	0.029
	Utilities	0.000/ 0.000	0.000/ 0.000	-	0.000/ 0.000	0.047/ 0.000	0.047
	Process	0.000/ 0.000	0.000/ 0.000	0.000/ 0.000	-	0.026/ 0.000	0.026
	Risers	0.000/ 0.000	0.000/ 0.000	0.013/ 0.013	0.000/ 0.000	-	0.026
	Shop	0.000/ 0.000	0.000/ 0.000	0.000/ 0.000	0.000/ 0.000	0.000/ 0.000	0.000
	Treatment	0.000/ 0.000	0.000/ 0.000	0.000/ 0.000	0.000/ 0.000	0.000/ 0.000	0.000
Sum = 0.188							

*Probability of escape from first allocated muster point/probability of escape from second allocated muster point

Table 18: Calculated probability and weighted cost of section destruction for optimized musters, optimized layout

		Vapor Cloud Explosion From					Weighted Cost
		Wellhead	Compressors	Utilities	Process	Risers	
Effect on	Wellhead	-	0.070	0.023	0.018	0.054	0.825
	Quarters	0.026	0.017	0.000	0.019	0.004	1.980
	Compressors	0.054	-	0.006	0.004	0.024	0.088
	Storage	0.052	0.011	0.000	0.047	0.005	0.115
	Utilities	0.054	0.042	-	0.008	0.131	0.235
	Process	0.052	0.009	0.002	-	0.008	0.071
	Risers	0.054	0.031	0.051	0.005	-	0.141
	Shop	0.026	0.017	0.000	0.019	0.004	0.660
	Treatment	0.050	0.006	0.000	0.054	0.005	0.115
Sum =4.230							

Table 19: Muster assignment for the optimized API layout

Section	Muster	Path	Muster Point	x-coordinate	y-coordinate
Wellhead	1,4	x-y,direct	M1	0	0
Quarters	1,3	y-x, x-y	M2	0	150
Compressors	3,4	y-x, direct	M3	110	150
Storage	2,3	y-x, y-x	M4	0	0
Utilities	1,2	direct, y-x			
Process	2,4	y-x, x-y			
Risers	2,3	direct, y-x			
Shop	1,3	y-x, x-y			
Treatment	1,4	y-x, y-x			

3.7.2.3 Analysis

As can be seen, the quarters and shop occupy the same area on different floors and are sent to the same set of muster points. Both points are situated on corners of the platform, away from most sources of fire.

The layout itself is predicated on separating the high-value sections, the quarters and shop, from the high hazard sections, particularly the wellhead and compressors. The wellhead is an intermediate in this formulation, as it has a moderate cost but is also a source of hazard. The layout is constrained by the fact that the wellhead and the compressors, two of the largest sections, are also multiple-story objects, thus not allowing other sections to be placed on top of or below them, but this likely isn't a large concern as any section placed directly on top of or below these sections would have a heavy risk of both fire and explosion hazards.

Though it does not explicitly aim to do it, the model does relieve some of the negative points of the original layout. The quarters area is no longer directly adjacent to the wellhead, and escape routes (particularly that of the wellhead) are no longer blocked. However, the treatment area is still relatively close to the compressors and ignition sources are not well spaced from fuel sources. This was not a specific concern of the

model as created, so this is to be expected, but the implicit power of the model to improve the layout concerning most hazards that require trade-offs is encouraging.

Of interest is the fact that the model predicts the same configuration of shop and quarters as the original layout. This makes sense as they are the highest-value sections, the exact same footprint area, and neither is a source of hazard. Thus, they can fit in the same space, they are both valued highly to move away from hazard, and do not affect one another other than for the non-overlap constraints. The optimization model corroborates that this is a good design decision.

Validation for the explosion overpressure scenarios was carried out in FLACS for both the fixed case and the optimized layout case, focusing on impact on the highest-cost sections – the quarters, shop, and wellhead. Full-section vapor clouds of natural gas were put on a geometry approximating the congestion of the platform, and were ignited in the center of each section. Monitor points were placed in the center of the sections of interest to obtain overpressure values against time. The results are summarized below:

Table 20: Comparison of CFD results for overpressure and probit-calculated probability of destruction

	Wellhead		**Compressors**		**Process**	
	Max P [bar]	Destruction Probability	Max P [bar]	Destruction Probability	Max P [bar]	Destruction Probability
Fixed						
Quarters	0.55	1.00	0.11	0.27	0.05	0.00
Shop	0.49	1.00	0.11	0.27	0.05	0.00
Wellhead	0.80	1.00	0.24	0.99	0.11	0.27
Optimized						
Quarters	0.08	0.06	0.04	0.00	0.00	0.00
Shop	0.11	0.27	0.04	0.00	0.00	0.00
Wellhead	0.80	1.00	0.06	0.01	0.01	0.00

As can be seen, the overpressure on the quarters, shop, and wellhead area is drastically reduced with the exception of the effect of an explosion in the wellhead on the wellhead. The destruction probability, calculated by the probit function with the CFD overpressure values, is shown improve in greater proportion than predicted by the optimization, implying greater gains in risk performance than expected.

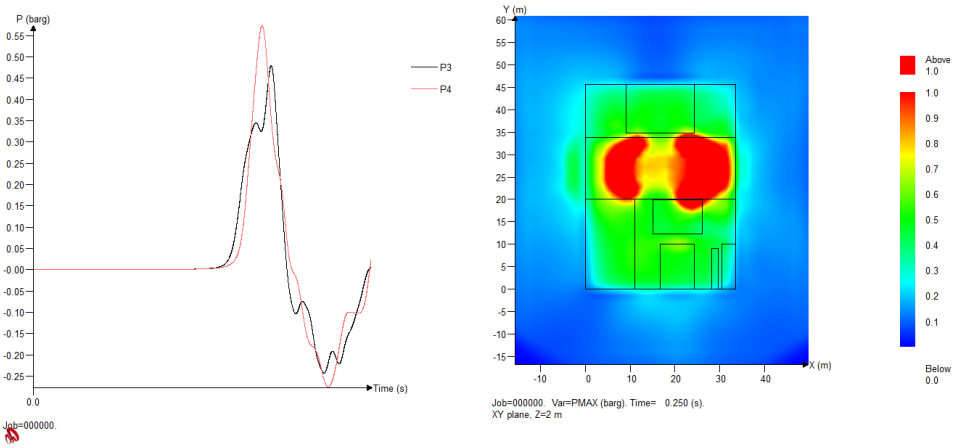

Figure 17: Overpressure profile at monitor points (red: quarters, black: shop) and maximum overpressure for fixed case, wellhead area explosion

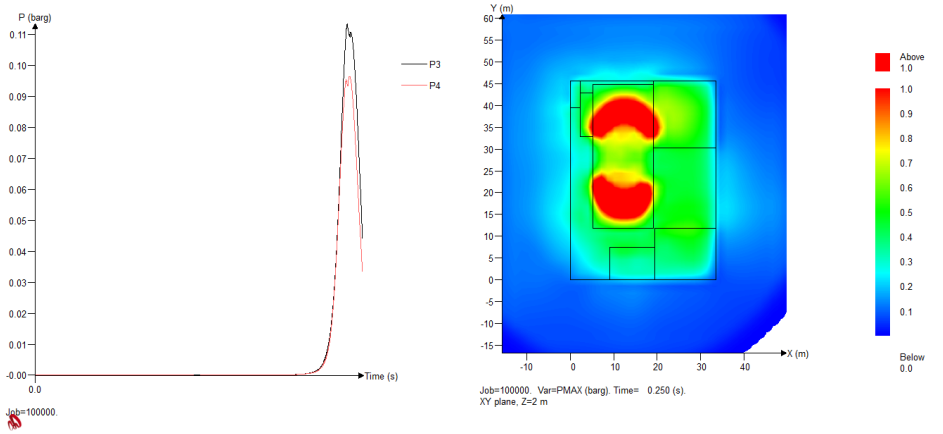

Figure 18: Overpressure profile at monitor points (red: quarters, black: shop) and maximum overpressure for free case, wellhead area explosion

3.8 Base Model Conclusions

An optimization formulation has been created that takes into account many of the main points of interest when laying out offshore platforms. The formulation accounts for the relative lack of space, the possibility of multiple floors, anticipated process conditions in order to predict the interactions between the sections of interest and the personnel that inhabit them. Practical concerns of explosion and fire events are considered in the ways that they would be expected to have the highest impact – infrastructure destruction for explosions and escape route blockage for fires. Sections are placed so as to minimize the human risk in a probabilistic manner, and escape routes and muster points are concurrently optimized.

The formulation has been proven to be a significant improvement over actual layouts, both when initializing the layout with no prior fixing of section locations, and also when using the model to evaluate an existing layout for an improvement in muster points. Other possible uses of the model would include the ability to evaluate current layouts for risk level, ability to site new equipment and sections with respect to minimum risk, and sensitivity analysis of layout risk with respect to changes in platform dimensions, number of floors, process conditions, or monetary considerations.

The formulation will be extended to include improved escape modeling, mitigation techniques such as blast and fire wall allocation, weather conditions for dispersion modeling, and domino effect in the following chapters.

4. AN APPROACH FOR INCORPORATING WEATHER CONDITIONS, TOXIC DISPERSION MODELING, AND MITIGATION SYSTEMS INTO THE OPTIMIZATION MODEL

Whereas the base model accounts for a large portion of the probable events on an offshore platform, it does so in a way that ignores several basic criteria that should be taken into account according to API 14J [28]: It does not account for weather conditions, it does not allow for mitigation systems, and it does not consider toxic dispersion modeling. Nor does it make any attempt at resolving any dispersion modeling considerations.

Each of these omissions can be justified for the base model. The dispersion modeling can be overlooked initially, as the greatest process safety risks posed to a platform are generally considered to be fire and explosion over toxic exposure. Realistic integration of weather conditions cannot be implemented without a satisfactory dispersion model, as a main function of weather conditions, in conjunction with platform geometry, is the effect on dispersion of gases that may result in a fire, explosion, or toxic exposure. Mitigation systems are an important aspect of facility layout, but are not always considered as a key factor during the layout phase – that is to say, while they are ubiquitous and indisputably play a major role in risk-reduction, a human performing a layout evaluation may not consider them in the same detail or with the same weight during the layout as an optimization model may be able to.

Though the omissions can be justified in some ways, it is of paramount importance that they be implemented if the model is to be considered realistic and robust, in addition to satisfying the goals of compliance with best practices and standards. Thus, the objectives of this methodology are as follows:

- Devise a methodology to model effects of dispersion, particularly of toxic material, in the offshore platform environment. Take into account material properties, process conditions, weather conditions, and geometry considerations

in order to realistically estimate concentrations at any given point on the platform, effects on personnel, and cumulative risk to be used in the objective function.

- Weather conditions will be governed by wind speed and direction, which will be used in conjunction with layout considerations that affect air circulation in the platform geometry.
- Incorporate mitigation systems into the model with special emphasis given to blast walls and fire walls, as these are two key mitigations used in the offshore environment.

The improvements will be assimilated into the existing base model and performance will be evaluated by FLACS CFD simulation with respect to fire, explosion, and toxic gas dispersion

4.1 Background Information on Use of Mitigation Systems in an Offshore Environment

Mitigation systems that are commonly encountered in an offshore environment include passive mitigations such as blast and fire walls, active mitigations such as gas detection, structural decisions such as additional cladding on existing structures, and non-structural such as control systems [39]. Optimization of gas detection, a layout problem of a different kind than that studied here, has been examined in the offshore environment for a fixed layout by Legg and Benavides in order to minimize time to detection, maximize number of releases detected, and optimize number of detectors placed [40], as well as incorporate voting strategies and unavailability [41]. However, although detection could be incorporated into the layout phase, it is expected that it would be a less efficient and less accurate use of resources than to lay out the facility and then optimize gas detection. This allows for more accurate estimations of gas cloud concentrations for the placement of detectors.

Blast walls are simply used to segregate areas that have a relatively high probabilities of explosion from areas that are sensitive to the effects of explosion – for example, highly populated areas or areas where explosion could lead to domino effects [42]. They are often constructed of corrugated stainless steel welded to the top and bottom of the floor they occupy, and are rated as acceptable to a certain pressure, though there is no universally utilized manner of determining the rating of a blast wall. They have been studied extensively in academia and industry, primarily for load-response data for different materials and configurations with respect to deflection and deformation of a wall. This information is invaluable when designing a blast wall for an expected impact; however, it is not necessary in the optimization model to design a blast wall, only to explain the effects of a possible explosion on the section that has a wall that is assumed to be properly designed. Thus, the measure of importance in the optimization is how a properly designed wall reacts to an overpressure impact probabilistically, so that the mitigated probability can be taken into account in the objective.

Fire walls mirror blast walls in several ways. They are used to separate areas of possible high-consequence events from sensitive areas that may be compromised and lead to escalation or direct impacts [43]. They are especially useful in lengthening the time available for escape by postponing structural failure or direct human consequences, although they typically only last a finite amount of time under load [44]. Indeed, API 14J [28] recommends that firewalls, as well as blast walls, be considered when quarters areas are in proximity to hydrocarbon-containing areas. Like blast walls, they are often constructed of corrugated stainless steel [45]. As with blast walls, much of the literature focuses on the response of a wall to a heat radiation load. This is very important in the design of firewalls, but is not of interest in the optimization formulation. The key is relating the mere presence of a blast wall to the probability of escape in the case of a fire event.

Human factors and control systems are also important in the mitigation of fire and explosion effects, and although it could be argued that layout affects either of these factors, they are considered outside of the scope of this layout formulation.

4.2 Weather Conditions and Dispersion Modeling Formulation

Dispersion modeling is based upon a probabilistic formulation that penalizes congestion in each direction relative to the section of the release based on the amount of congestion that is present in that direction. The principle behind the modeling is that a jet-type leak can occur in any direction, non-preferentially. The area congestion ratio (ACR) is calculated in each direction for each leak source.

In conjunction with the congestion, the weather conditions, particularly wind direction and magnitude affecting ventilation, can play a large role in the dispersion footprint of a cloud. Higher ventilation allows for more egress of gas from the platform and is an important design criterion in the offshore case. The dispersion expression provided takes into account both of these factors and their interactions in order to describe how gas disperses without a full pre-known layout to work with.

In this chapter, dispersion modeling is used to describe a release of a toxic gas, hydrogen sulfide, based on the layout of the sections to each direction of the release, only on the same floor as the release. This concept is extended in chapter 5 to include dispersion to floors above and below, such as through a grated deck, and the consideration of the dispersion of other materials such as flammable gas, smoke, and combustion products.

4.2.1 Dispersion Modeling using ACM in FLACS

FLACS is a specialized computational fluid dynamics (CFD) software package developed especially to address certain process safety applications[46], key among which is the dispersion of flammable and toxic gas. The governing equations for fluid flow are the Navier-Stokes conservation equations which are solved using the finite volume method on a Cartesian grid. Conservation equations for mass, momentum, enthalpy, and mass fraction of species closed by the ideal gas law are included.

Geometry is written as an obstruction file, which is then converted into an area porosity component in the x-, y-, and z-directions. This is done through the use of the

defined Cartesian grid file to dissect the obstruction into intermediate control volumes, and then averaging the obstructed and unobstructed projection in each direction into a uniform porosity in the control volume. In this way, when the simulation is run the program does not 'see' the geometry, but a generalized version of the geometry that adequately represents the key contributor the physics of the application.

Because of the way that the geometry is converted into a porosity, if the relative level of congestion of an object is known beforehand, then an accurate simulation can be produced even if the detailed geometry is not known [47]. This method, known as the anticipated congestion method (ACM), is very useful in the design-phase of facilities offshore as well as onshore because detailed siting and layout does not necessarily have to be done before a preliminary layout evaluation can be done, as long as the relative blockage can be estimated. However, in this application, the objective is not to evaluate a known layout or even a prospective layout, but to understand how the dispersion pattern of a gas will change as the layout changes, then to relate that to the probability of a toxic incident – a very different problem that can be attacked in a very similar way.

The ACM method has been used with excellent results in practice for blast modelling, but has not been used widely in dispersion modeling. It is contended in this work that the ACM method is equally applicable to dispersion as it is to explosion simulations because both are, with respect to the modeling in FLACS, two applications of the same problem: fluid flow, which is influenced geometrically by the porosity of the object within a grid cell. FLACS does not 'see' a difference between an actual geometry and a simulated geometry given that the pososities are the same for each grid cell. This is not to imply that the approximation is perfect; there is a natural loss in accuracy by a homogeneous approximation of a heterogeneous congestion, and there is no account taken for solid obstructions such as walls. However, because the nature of the problem is that the location of major obstructions is unknown, this is a necessary approximation.

ACM geometries were generated in FLACS for a platform of a fixed 150' x 150' footprint with a height of about 15'. Congestion was simulated for 0.1, 0.3, 0.5, 0.7, and

0.9 congestion ratios using a repeating 1x1x1 m grid of square-faced beams with dimensions calculated to give the correct amount of congestion in each direction.

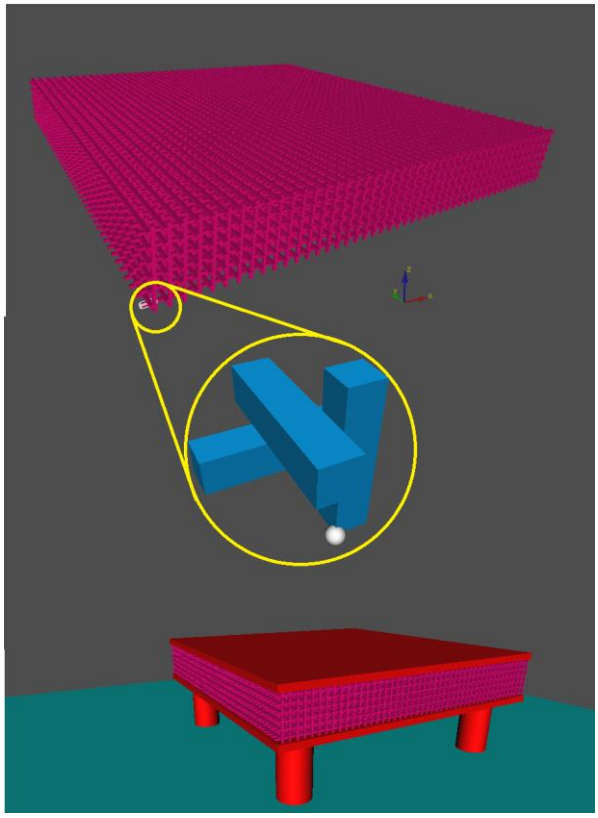

Figure 19: ACM geometry for 0.5 congestion ratio, top: anticipated congestion; middle: one unit cell for ACM; bottom: full ACM geometry

4.2.2 FLACS Simulations and Correlation Modeling

In order to formulate a suitable correlation for the effect of wind on dispersed toxic gas, a set of 720 simulations were run, varying key parameters that are expected to have the greatest effect on gas concentration. These are congestion, flow rate, wind speed, leak direction, and monitor direction. Of interest is the parameter of monitor direction, which is defined as which section of the four sections of the platform the

dispersion of the gas is being recorded for with respect to the leak – positive-x, negative-x, positive-y, or negative-y.

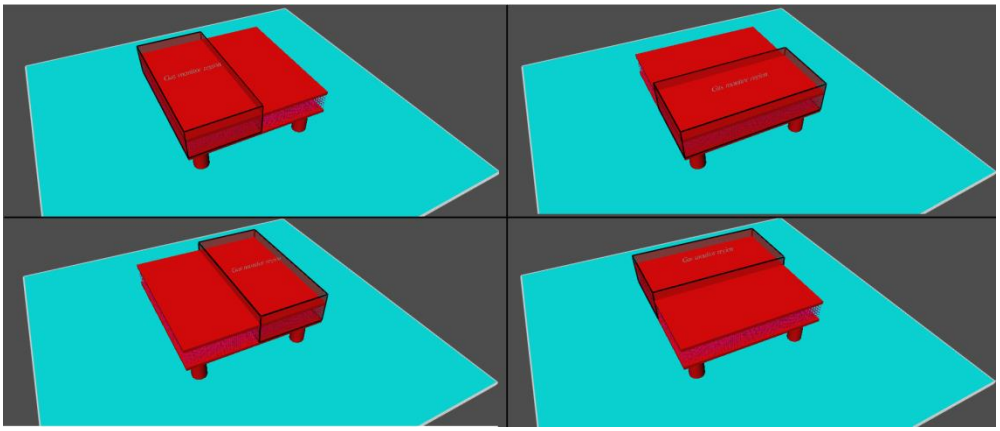

Figure 20: Monitor regions for the correlation modeling simulations: clockwise from top-left - -X-direction, -Y-direction, +Y-direction, +X-direction

This is a convenient formulation for the optimization formulation because the relative cardinal positions of the sections in relation to each other are naturally calculated within the model because of the disjunction formulation of the non-overlap constraints. A correlation can be derived for each of the monitor regions with respect to each of the release directions, which can then be summed over each release direction using the relative congestion level that is calculated during the solution of the optimization formulation in order to find the expected fraction of toxic gas in the region, and from that the probability of toxic effects. More detail is given in section 4.4.3.

A key advantage of the CFD simulation formulation is that, naturally, not all of the gas from a leak in a certain direction will end up in that certain direction unabated. In the hypothetical case of a leak in the negative-x direction, particularly if the wind is in the positive-x direction, some of the gas will end up in each of the four monitor regions – an amount that is expected to gain even more significance if the wind speed is high and

that may possibly be a strong function of the congestion level. Simple dispersion models such as the Pasquill-Gifford [48] dispersion model, though well-suited for applications such as finding worst-case scenarios in an onshore scenario, nonetheless cannot model key phenomena that may cause toxic gas to recirculate behind the leak or lose momentum and disperse further in the transverse direction. Indeed, the Pasquill-Gifford model is unable to calculate a footprint accounting for any wind other than that which occurs directly downwind of the leak. In an offshore environment when there is commonly a prevailing wind direction, the assumption that every release will occur directly downwind, giving unwarranted symmetry between relative placement of sections, is unacceptable. Thus, although the CFD correlation simulation formulation is simplified, it is asserted that the results reflect actual conditions better than other simplified approaches that could are also suitable for implementation in the optimization formulation.

Static parameters used in the simulation are as follows:

Table 21: Static parameters used in the dispersion correlation scenarios

Parameter	Value
Platform Size	150’ x 150’ with 15’ ceiling
Leak Position	75’,75’ (center of platform)
Material	Hydrogen sulfide
Leak Diameter	2 inches
Leak Temperature	50°C
Leak Duration	600 seconds (ensure steady state)
Grid Size within Monitor Domain	1x1x1 meter
Wind Direction	Blowing toward +X

The parameter values varied in the simulation are listed in the table that follows. All combinations were enumerated and correlated.

Table 22: Parameters varied in the dispersion correlation scenarios

Congestion Level	Flow Rate	Wind Speed	Leak Direction	Monitor Direction
0.1	0.1	1	+X	+X
0.3	0.5	3	-X	-X
0.5	1	5	-Y	+Y
0.7	2			-Y
0.9	5			
	10			

All simulations were run using the incompressible release model in order to expedite results. The incompressible model in FLACS simplifies the governing equations for fluid flow by assuming that the solver can neglect compressibility phenomena, thereby reducing the number of equations to be solved and allowing for a longer stable time step with minimal loss in accuracy [49]. The applicability of the incompressible solver depends on the scenario – it is never applicable in an explosion scenario, and high-velocity dispersion simulations may experience a significant loss in accuracy. A Mach number (ratio of release velocity to sound velocity) of less than 0.5 is generally accepted as the upper limit for the incompressible solver. This is not problematic for these simulations, as the maximum Mach number is about 0.2.

The following figures illustrate sample differences in dispersion footprint due to the changes in the aforementioned variable parameters. The scale of the axes is equal in all side-by-side comparisons, and the colors that represent concentrations are constant through all figures. All figures are taken at the time step of the maximum cloud size.

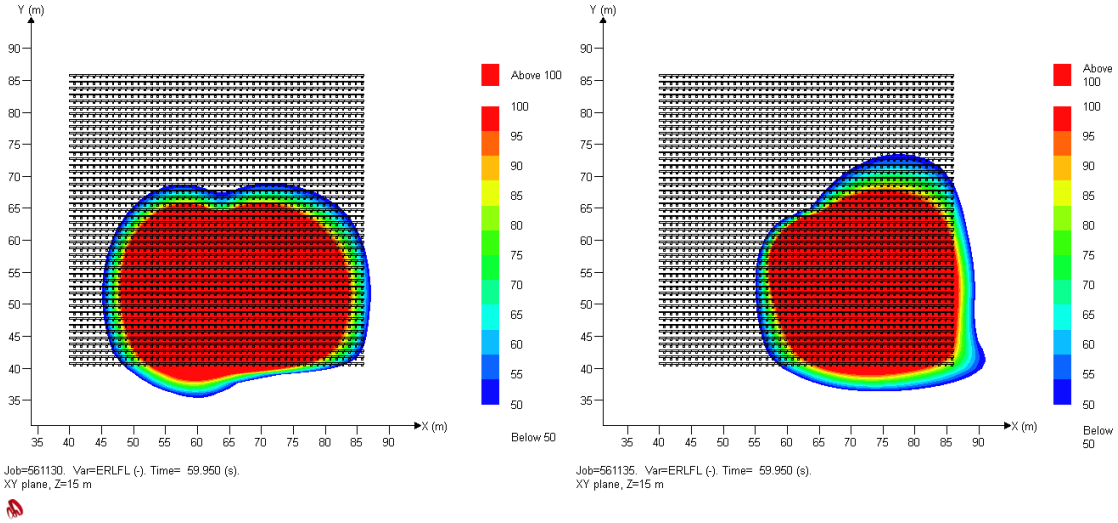

Figure 21: Comparison of congestion ratio 0.5 runs, 10 kg/s releases in the –Y-direction. Left: 1 m/s +X wind; Right: 5 m/s +X wind

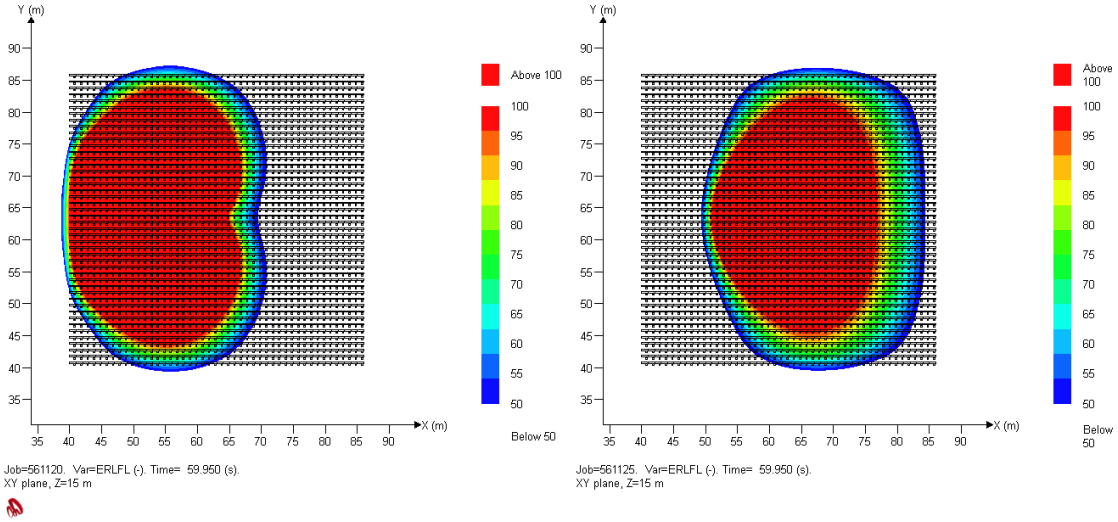

Figure 22: Comparison of congestion ratio 0.5 runs, 10 kg/s releases in the –X-direction. Left: 1 m/s +X wind; Right: 5 m/s +X wind

It is plain in these figures that the wind speed can play a significant role in the dispersion of the gas – Figure 21 shows that the dispersed gas dominates the –X side of the platform with a slight wind against the release, while with a moderate wind against the release, the +X side of the platform is dominated. This result, particularly when the wind direction is opposed to the leak direction, would not be reflected with a simpler method of estimating the footprint of the dispersed cloud. Likewise, the difference in cloud behaviors due to congestion shows that congestion cannot be discounted:

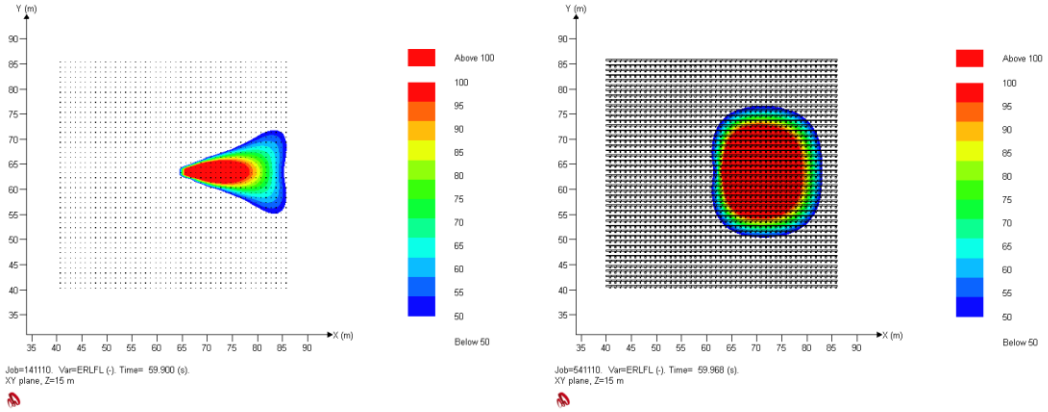

Figure 23: Comparison of 2 kg/s releases in the +X-direction, 1 m/s +X wind: Left: congestion ratio 0.1; Right: congestion ratio 0.5

As can be seen, not only is the footprint of the cloud highly influenced by a change in the congestion ratio, but the amount of gas that is actually trapped within the area of interest is highly variable as well. Note that in the preceding figures, the red region is not a region of equal concentration, but rather a region where the gas concentration is above a certain threshold. It is safe to assume that as one approaches the center of the red region of the cloud, the concentration will be higher than at the outer edge of the red region away from the release point.

Finally, the relation between flowrate and cloud footprint is presented below. As expected, a higher flowrate introduces more gas into the monitor region and in general causes a higher mass fraction in the reason, but the interplay between the higher flowrate and congestion level is of interest, as a higher congestion level will obstruct the escape of the gas while a lower congestion level will allow for the gas to be vented from the platform. This means that as congestion level rises, the relative proportion of the gas that is trapped within the monitor region will rise between the low-flowrate and high-flowrate case.

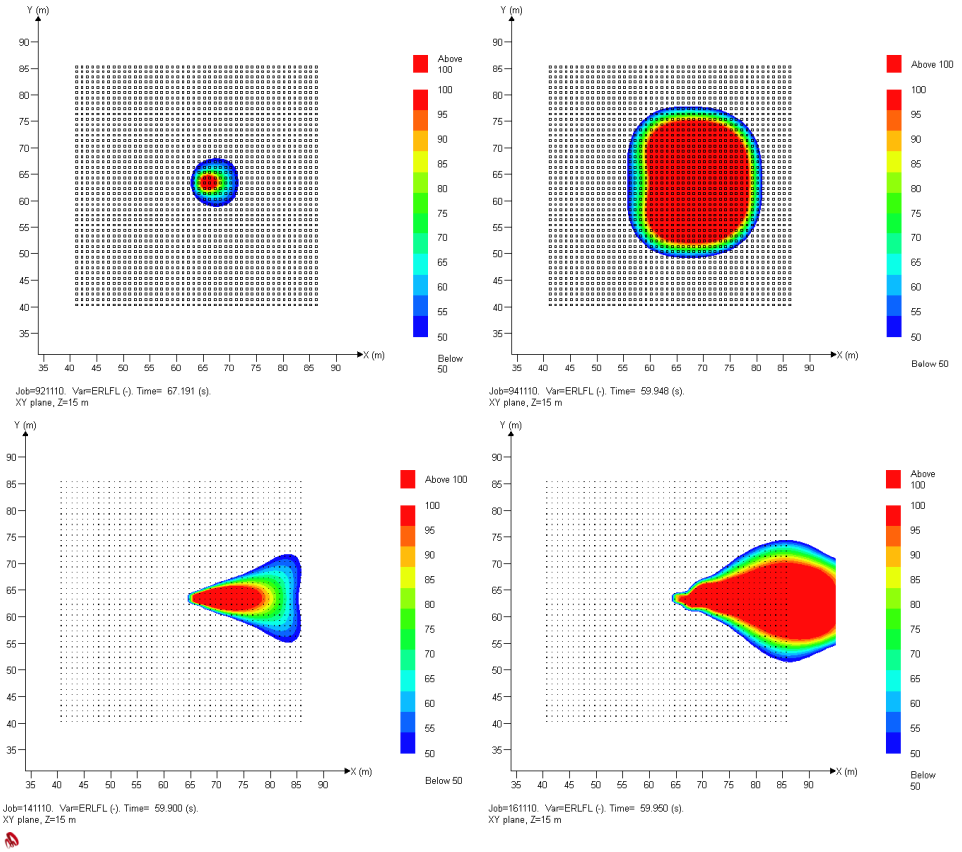

Figure 24: A comparison of flowrates and congestion levels. Top left: 0.5 kg/s flow in 0.5 congestion ratio geometry; Top right: 2 kg/s flow in 0.5 congestion ratio geometry; Bottom left: 2 kg/s flow in 0.1 congestion ratio geometry; Bottom right: 10 kg/s flow in 0.1 congestion ratio geometry

Data from the monitor files was extracted in order to identify trends that could be correlated for use in the optimization model. For each monitor region, total mass of gas and fuel mass were taken at the time of maximum fuel mass. Both are necessary, as the higher congestion ratios have a lower total mass of gas due to the blockage of volume by the congestion. This is used to calculate the maximum mass fraction for the scenario.

Data was fitted linearly by least-squares regression to each of the parameters of interest: release rate, wind speed, and congestion level, for each of the release directions. The linear fit was chosen because it trends with the data relatively well in the cases of wind speed and release rate, and is expected to give a better prediction outside of the bounds of the correlation than a high-level polynomial. Because these parts of the correlation are non-variable parametric in the optimization formulation, a more complex fit would not hinder solution efficiency; this is not true, however, of the congestion regression. Although the linear fit performs relatively well for the congestion level variable, the key consideration here is to have a function that will accurately portray the relation, but will also be expedient for the optimization model. A base linear formulation, if of acceptable predictive power, is ideal.

Correlation was done in a piecewise manner. First, all data was separated by congestion level, release direction, and monitor region. Regression was performed with respect to the independent variable of flow rate and the dependent variable of mass fraction for1 m/s and 5 m/s wind speeds. A y-intercept of zero was assumed, as when there is no flow, there should be no mass fraction of toxic gas. The slope of the correlation was then calculated for each of the congestion levels, and a regression was taken of these slopes with respect to congestion level for both wind speeds. Finally, the difference in slopes between the wind speeds was assumed to follow a linear correlation with a non-zero y-intercept, as when the wind speed is zero, there is still the opportunity for mass accumulation. Thus the form of the correlation is as follows:

$$[(a + Cb) + (c + Wd)] \cdot F = x$$

Where C denotes the congestion ratio (multiplied by 100), W denotes the wind speed (in m/s), and F denotes the flow rate of material (kg/s). The parameters a and c represent the base contribution of the congestion and wind, respectively. They are largely arbitrary individually, but their sum is meaningful as the base coefficient for the flowrate when wind and congestion are both zero. The b and d coefficients represent the scaled contribution that wind and congestion have, respectively, on the congestion and wind contribution to the slope of the flowrate. In other words, congestion and wind within the brackets modifies how the mass fraction linearly depends on flowrate. These modifiers are, in turn, variable with respect to the other. Again, this is assumed to be a linear dependence; b and d are replaced with functions of W and C:

$$[(a + C[e + fW]) + (c + W[g + iC])] \cdot F = x$$

In this equation, e is the base contribution of congestion to the change in mass fraction with the change in flow rate, and g is the analog for wind speed. These values are the limit of the slope as the opposing variable (wind in the case of the e value) approaches zero. The fW term reflects how the wind speed modifies the congestion contribution to the slope of the relation, and iC is the analog with respect to the wind contribution. It can be seen that both components are now intertwined, such that the congestion contribution is a function of the wind and the wind contribution is a function of the congestion. This is physically reasonable because of the negative effect that a rising level of congestion has in allowing wind ventilation, expressed in the i term, and the negative (or positive, largely depending on the relation of wind direction to release direction) effect that a rising level of wind has on the effectiveness of congestion to trap gas, expressed in j.

Rearranging and grouping all C values together, the equation can be put into a more useful form:

$$[(C[e + (f + i)W]) + Wg + a + c] \cdot F = x$$

The derivatives of the function are used to derive the coefficients and constants:

$$\frac{\delta}{\delta C}\frac{\delta}{\delta W}\frac{\delta x}{\delta F} = \frac{\delta}{\delta W}\frac{\delta}{\delta C}\frac{\delta x}{\delta F} = f + i$$

$$\frac{\delta}{\delta W}\frac{\delta x}{\delta F} = (f + i)C + g \quad \rightarrow \quad g = \frac{\delta}{\delta W}\frac{\delta x}{\delta F} - (f + i)C$$

$$\frac{\delta}{\delta C}\frac{\delta x}{\delta F} = (f + i)W + e \quad \rightarrow \quad e = \frac{\delta}{\delta C}\frac{\delta x}{\delta F} - (f + i)W$$

$$\frac{\delta x}{\delta F} = [(C[e + (f + i)W]) + Wg + a + c] \rightarrow a + c = \frac{\delta x}{\delta F} - (C[e + (f + i)W]) + Wg$$

The first equation can be used to find f+i directly. Both third derivatives are theoretically equal, so either can be used. Both methods were used, then compared and verified to be equal. The second equation can be used to find g: the slope values for the second derivative with respect to wind are related as a function of congestion with the prior calculated value of f+i. In order to find the base wind contribution, the congestion level is set at zero, eliminating the f+i term and leaving the value of the second derivative with respect to wind at C = 0. This can be found by correlating an intercept from the values of the second derivatives at each congestion level. Likewise, the third equation can be solved for e in a similar manner, setting W to 0 and correlating the y-intercept of the second derivative with respect to congestion. Finally, a+c, the base change in mass fraction with respect to a change in mass flow, can be found by correlating the slope as C and W approach zero.

Correlated parameters are presented below:

Table 23: Correlation parameters for the dispersion model

Release Direction	Monitor Region	Base Congestion Coefficient (e)	Proportional Wind Coefficient (f+i)	Base Wind Coefficient (g)	Base Flowrate Coefficient (a+c)
+X	+X	9.75E-5	1.25E-6	-2.41E-4	1.12E-3
	-X	2.71E-5	-2.98E-6	5.04E-5	-5.09E-4
	+Y	5.80E-5	-9.22E-7	-8.92E-5	3.23E-4
	-Y	6.46E-5	-9.71E-7	-9.04E-5	2.97E-4
-X	+X	3.63E-5	-9.77E-7	5.99E-4	-8.90E-4
	-X	7.14E-5	-7.59E-6	-3.82E-4	1.29E-3
	+Y	5.68E-5	-6.02E-6	2.90E-4	7.17E-4
	-Y	6.37E-5	-6.17E-6	2.46E-4	7.06E-4
+Y	+X	6.19E-5	3.39E-6	-5.91E-6	5.96E-4
	-X	5.92E-5	-6.30E-6	-1.36E-4	3.22E-4
	+Y	9.18E-5	-3.07E-6	-1.60E-4	1.43E-3
	-Y	3.15E-5	-3.28E-7	1.80E-5	-4.99E-4
-Y	+X	6.19E-5	3.39E-6	-5.91E-6	5.96E-4
	-X	5.92E-5	-6.30E-6	-1.36E-4	3.22E-4
	+Y	3.15E-5	-3.28E-7	1.80E-5	-4.99E-4
	-Y	9.18E-5	-3.07E-6	-1.60E-4	1.43E-3

The base congestion coefficient (e) describes how a change in congestion proportionally changes the mass fraction of dispersed material in the area without respect to wind speed. All are positive numbers, meaning that an increase in congestion increases the mass fraction of material contained, as expected. A higher magnitude implies more effect in the monitor direction.

The proportional wind coefficient (f+i) describes how congestion and wind speed interact to affect the mass fraction. A positive value shows that an increasing wind speed causes a higher mass fraction, as can be seen in the monitor region corresponding with the wind direction in most cases, while a negative value implies that the combined effect of wind and congestion is to push dispersed material out of the monitor region. The

effect of this coefficient lessens with a smaller congestion or wind. Intuitively, this makes sense – considering the positive coefficient in the monitor region in the direction of the wind, a greater wind will push gas in other monitor regions toward the positive wind direction monitor region and the greater congestion will hold the vapor closer to the release so that the wind can more easily move it to the monitor region of interest, which will then be retained more effectively in the positive wind monitor region.

The base wind coefficient (g) describes how the wind effects the dispersion without regard to congestion. This has mixed effects depending on the release direction, where the wind may push dispersed gas off the platform, or lessen its momentum so that it stays on the platform and accumulates.

Finally, the base flowrate coefficient (a+c) simply relates flowrate to dispersed mass fraction in absence of the effects of wind and congestion. This should, theoretically, always be positive; however, the values in the direction opposing the release are each negative. This indicates an imperfection in the correlation that arises at low congestions and wind speeds where the estimated mass fraction will be negative. However, the combination of the low levels of wind speed and congestion imply that the mass fraction would be orders of magnitude smaller in the direction of interest than would be expected to cause any effect, so a negative result can be approximated as zero mass fraction.

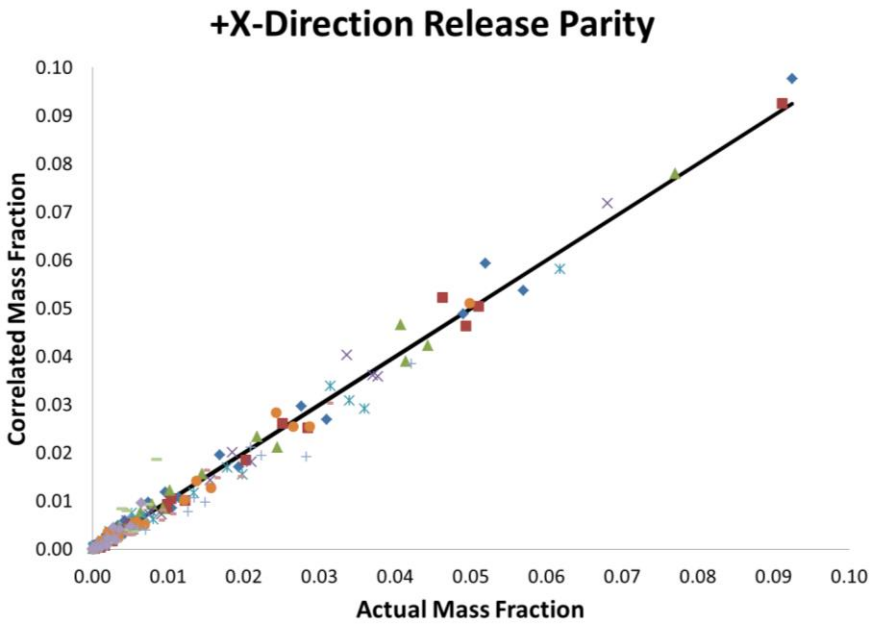

Figure 25: Parity plot for all +X-direction releases. Line denotes equality between correlation and simulation value.

As can be seen in the above figure, the correlation agrees very well with the positive-x direction release data. Data in this plot is not grouped by congestion or wind level, but the data shows a better fit for high congestion scenarios, and is rather more erratic with respect to the lowest congestion scenarios. This is because the initial data for low congestion scenarios is far more erratic and less linear than data from higher congestion scenarios. The divergence is pronounced at congestion ratio 0.1, while congestion ratio 0.3 shows a much smaller degree of divergence, mostly in the underestimation of mass fractions in the monitor regions in the opposite direction of the release. The remaining two parity plots are shown below.

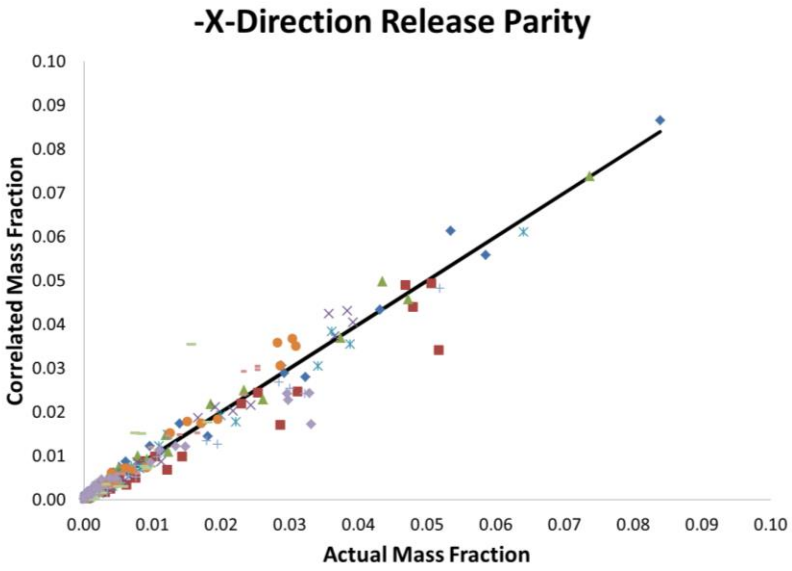

Figure 26: Parity plot for all -X-direction releases. Line denotes equality between correlation and simulation value.

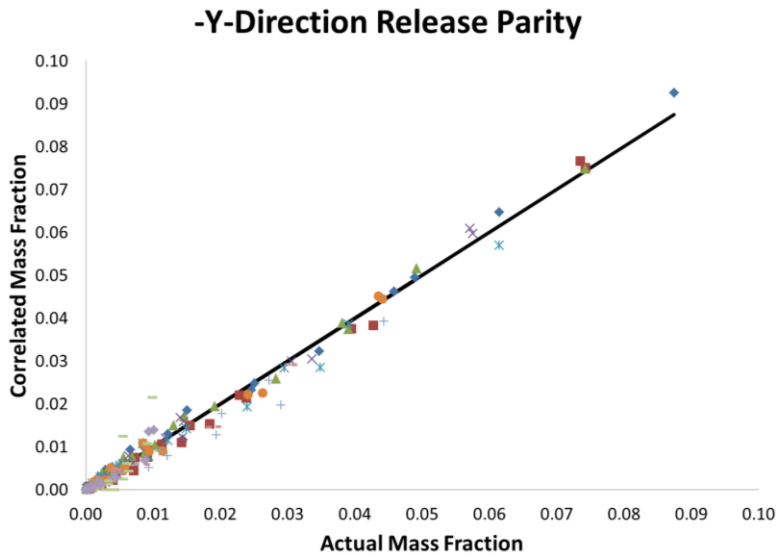

Figure 27: Parity plot for all -Y-direction releases. Line denotes equality between correlation and simulation value.

The positive-y direction releases were not considered, as they have y-axis mirror symmetry with the negative-y direction releases about the center of the platform. Therefore, the y-direction parameters will be flipped and the x-direction parameters will remain the same. This is not true of the positive- and negative-x directions because of the wind effect.

The average relative error for mass fractions in each direction is less than 20% for all congestion ratios greater than 0.1. There is no significant trend in overall accuracy between wind speeds, as they are often within a percentage point of each other and neither is generally higher or lower than the other. However, the accuracy drops slightly at higher wind speeds in the monitor region opposite of the direction of the release. This manifests itself in the form of a general underprediction at low flowrates before converging to the data at high flowrates. As the low flowrates produce lower mass fractions, the higher relative error is caused by a very low absolute error.

The average relative error for mass fractions for a congestion ratio of 0.1 is between 40 and 50%. However, this is misleading because the mass fractions that are found at this congestion level are normally very low, where a large relative error does not imply a large absolute error. As an example, these numbers are highly skewed by an abnormally large relative error in the direction opposite the release where the actual mass fraction is on the order of 10^{-7}-10^{-8} – so small that it would ostensibly add almost no value to the optimization over a zero estimate or over an estimate that is even an order of magnitude higher. In the optimization, it is unlikely that in most cases there will be a congestion level this low due to the relative lack of space on the platform.

To summarize the conclusions in this section, a simple correlation between several parameters was created in order to implement into the layout program, including weather conditions in the form of wind in a set direction. The correlation gives sufficient accuracy in a form that is a linear function of congestion, the only parameter that is variable in the optimization model, but diverges at low congestions, which is not expected to be a large factor. Because the correlation is a linear model of congestion

rather than a more complicated model, it is expected that the performance of the optimization will not suffer unduly.

Because the leaks were centered in the platform, sensitivity analysis was performed to ensure that the concentration of the gas does not change drastically if the position of the leak is changed. A further set of 20 simulations were run, varying the leak position along the x-axis and y-axis to study the effect of leak position on concentration within a monitor region for +x and –x-direction leaks. Leak positions were 10, 25, 75, and 90 percent of the length of the platform along one axis, holding the other at 50 percent, as well as 25%/25% and 75%/75% in the x- and y-axis directions. The leaks were allowed to come to steady state and compared with the concentrations found in the base case.

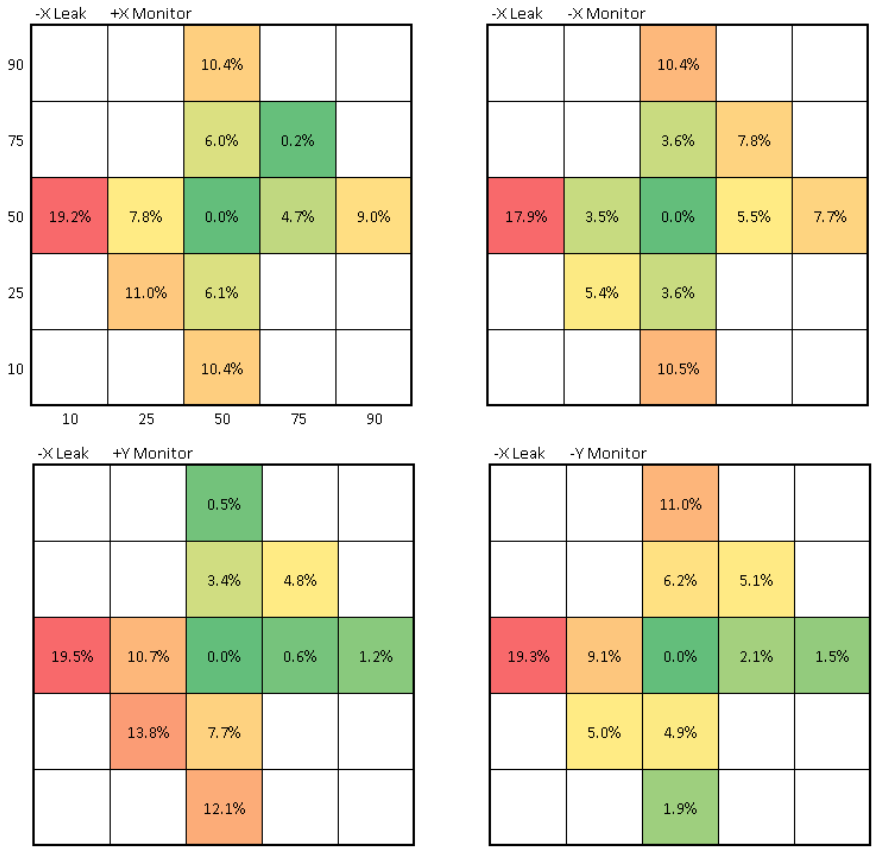

Figure 28: Relative deviation in concentration for various leaks in –x-direction

As seen in the preceding figure, the concentration estimate is generally worst in along the edge of the platform in the direction of the leak and is best closest to the center and skewed toward the side that the monitor region lies in. This effect is mirrored in the +x-direction case not shown above. The greatest deviation is typically within 20% of the base value, but there is no obvious mathematical correlation between accuracy and leak position; there are only the general trends mentioned before. The relatively poor performance near the edge of the platform in the direction of the leak is not expected to highly impact the optimization results, as the closer to the edge of the platform a facility is, the less likely it is that another facility will be between it and the edge of the platform due to non-overlap considerations.

4.2.3 Implementation into the Optimization Model

Implementation of toxic gas dispersion into the optimization model requires the introduction of several new parameters and variables. These are briefly summarized below:

Table 24: Parameters and variables added in the toxic dispersion optimization model

Base Parameters	
$_{R,M}$**te**	Base congestion coefficient for a release in the R-direction in the M-direction monitor region
$_{R,M}$**tfi**	Proportional wind coefficient for a release in the R-direction in the M-direction monitor region
$_{R,M}$**tg**	Base wind coefficient for a release in the R-direction in the M-direction monitor region
$_{R,M}$**tac**	Base flow coefficient for a release in the R-direction in the M-direction monitor region
Base Variables	
$_{M}$**BR$_{s,f}$**	Calculated blockage ratio in the M-direction of section s on floor f
$_{R,M}$**SD$_{s,f}$**	Scaled dispersion mass fraction in monitor region M due to a releasein direction R in section s on floor f with a congestion ratio of $BR_{s,f}$ determined by correlation
P(Toxic)$_{s,k}$	Probability of death in section s due to toxic release in section k

The key component in the new facet of the optimization is the calculation of the congestion ratio in relation to a section. Because the positions of all sections are related to each other through the disjunctive nature of the non-overlap constraints, a convenient framework is inherent in the program. Using the binary non-overlap variables and the pre-defined footprint areas for each of the sections:

$$_{+X}BR_{s,f} = \frac{\sum_k a_{s,k,f} \cdot Area_k}{(Wx - [x_s + \frac{1}{2}Lx]) \cdot Wy}$$

$$_{-X}BR_{s,f} = \frac{\sum_k b_{s,k,f} \cdot Area_k}{(x_s - \frac{1}{2}Lx) \cdot Wy}$$

$$_{+Y}BR_{s,f} = \frac{\sum_k c_{s,k,f} \cdot Area_k}{(Wy - [y_s + \frac{1}{2}Ly]) \cdot Wx}$$

$$_{-Y}BR_{s,f} = \frac{\sum_k d_{s,k,f} \cdot Area_k}{(y_s - \frac{1}{2}Ly) \cdot Wx}$$

These are simply defined as the sum of the footprint areas of the sections in the direction of interest divided by the total area. The factor of half of the area of the considered section is necessary because the area calculation begins at the midpoint of section s, and so the total congested area would include that half of section s.

The dispersion mass fraction from a release in section s in a certain monitor direction M is then calculated straight away as the maximum contribution from directional releases:

$$_{R,M}SD_s = F_s[_MBR_{s,f}(_{R,M}te + _{R,M}tfi \cdot W) + _{R,M}tg \cdot W + _{R,M}tac]$$

There are several different methods for quantifying the toxic effect of hydrogen sulfide, the material that is expected to cause the greatest toxic threat (other than combustion products) in an offshore environment [50]. It can be estimated through the use of a probit function, as radiation effect and overpressure effect can. Such a formulation could be used exactly as previously demonstrated in the prior chapter. The general parameters may vary greatly from source to source. Lees' Loss Prevention in the Process Industries [51] gives the values in the following table for the form P = a+bln(tC^c), where t is the exposure time and C is the concentration in parts per million:

Table 25: Parameters for hydrogen sulfide toxic probit function

Parameter	Value
a	-31.42
b	3.008
c	1.43

The expected toxic effect can also be estimated using the SLOT/SLOD method as explained by the United Kingdom Health and Safety Executive [52], which is based on experimental data which is then extrapolated to give a relation of toxic concentration to the time that 50% mortality would be expected. It takes the form of $C^n t = A$, where C is the concentration [ppm], t is the exposure time [min], A is the dangerous toxic load, and n is a scaling exponent. This form is useful in a time-based formulation, where some function of the total escape time is maximized for the platform.

A value that contributes to the probability of escape in a toxic release is the Immediately Dangerous to Life and Health (IDLH) value. The IDLH is defined by "an atmosphere that poses an immediate threat to life, would cause irreversible adverse health effects, or would impair an individual's ability to escape from a dangerous atmosphere." [53]. Hydrogen sulfide has an IDLH of 100 ppm according to NIOSH [54]. This is a highly conservative number, as the threshold for unconsciousness, cessation of respiration, and death after several minutes is estimated to be 1000-2000 ppm [55], but it does give a well-accepted standardized value to work against. The 100 ppm threshold causes several secondary effects that prevent escape, such as severe eye irritation or disorientation [56]. As such, this value can be implemented in the model to account for low levels of toxic gas causing a secondary effect that impedes escape that can be implemented into the escape probability function that exists for fire radiation.

Ideally, there would be some method of relating exact hydrogen sulfide concentration to the difficulty of escape or the extra time it would take personnel to escape (this concept is explored in Chapter 5 with smoke modeling), but there is not concrete information as to the magnitude of difficulty that a person would have fleeing

an incident with eye irritation or disorientation. As an approximation, it is assumed that a concentration of 100 ppm would begin the onset of effects that prevent escape, escalating linearly to the 2000 ppm threshold of certain (probability 1) failure to escape.

$$P(C_{H2S}) = \begin{cases} 0, & C_{H2S} < 100\ ppm \\ \dfrac{C_{H2S} - 100}{1900}, & 100\ ppm \geq C_{H2S} \geq 2000\ ppm \\ 1, & C_{H2S} > 2000\ ppm \end{cases}$$

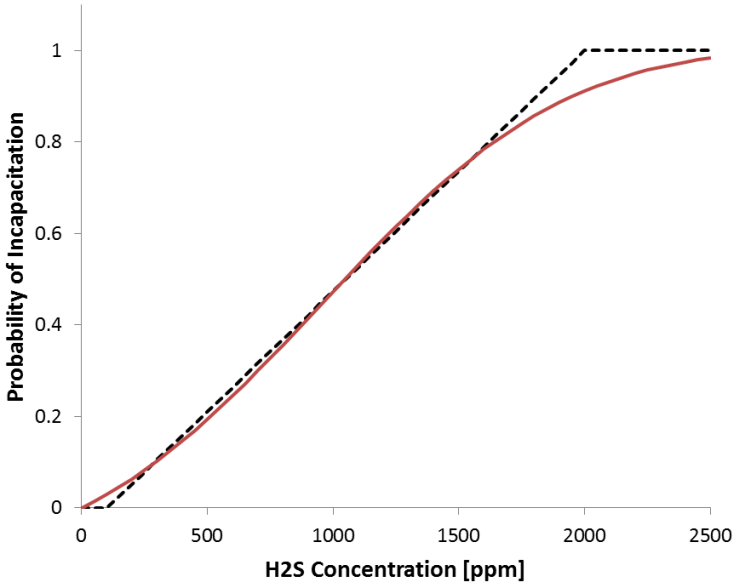

Figure 29: Approximation of the probability of incapacitation due to hydrogen sulfide exposure. Dotted line depicts actual function, solid line depicts approximation to the actual function

However, since the piecewise linear function has practical difficulties, most easily being implemented by two constraints – one which would limit the probability to values greater than zero, and the other a linear function corresponding to the escalation of probability in the preceding function relying on the addition of artificial slack variables (penalized in the objective function) to force the probability value to 1 when

the concentration exceeds 2000 ppm – a logistic formulation to approximate the piecwise function is used. The utilized logistic function is of the form:

$$P = a \cdot [\text{erf}(b \cdot [PPM - c]) + d]$$

Where c is the midpoint of the function , chosen to be 950 ppm, and a, b, and d are parameters that are optimized using a least squares approach to minimize the deviation from the piecewise function. The value for a is 1.13, b is $9.21 \text{x} 10^{-4}$, and d is -0.05. The largest absolute deviation in probability is 0.088 at the 2000 ppm point and the largest percentage deviation, disregarding the first several points where the piecewise function has a low value or a zero value, is 9% at the 2000 ppm point.

If data were to become available for a better approximation to the effects of hydrogen sulfide on egress, a different function could be substituted.

4.3 Mitigation Formulation

Among the most prevalent forms of mitigation on offshore platforms, due to the inability of spacing to mitigate consequences, are fire walls and blast walls [57]. Blast walls are used to protect the structure of the platform from destruction and firewalls are used to protect personnel from fire radiation concerns. Both failure to escape due to fire and section destruction due to explosion were implemented in the initial model described in the last chapter. However, because of the existence of these mitigation measures and the extra flexibility they give in the layout process, the model has been improved to take into account these consequence-reducing possibilities.

4.3.1 Blast Walls

Several practical assumptions are made to ensure ease of implementation without sacrificing utility:

- Blast walls can be implemented on any side of a section.

- More than one blast wall can be allocated to a section, but not to the same side of a section
- Blast walls on a side of a section are assumed to cover all of the floors of that section
- A blast from a section k can only be deflected by a section s blast wall that is in the direction directly facing the blast based on the classification given by the disjunctive constraints. Therefore, if s is in the a-direction (left) of an explosion from k, it must have a b-direction (right) blast wall to deflect the overpressure.
- Redirection of overpressures from the blast wall is negligible – a blast wall has no effect on the overpressure felt by any section but its own.

The following parameters and variables are defined:

Table 26: Parameters and variables introduced in the blast wall formulation

Parameters	
MaxWalls	Maximum number of blast walls that can be allocated
Variables	
${}_{M}W_{s}$	Binary variable denoting a blast wall allocated to the M-direction of s if 1, no wall allocated if 0
${}_{M}BW_{s,k}$	Binary variable denoting that an explosion from section k is affected by an allocated blast wall on section s in the M-direction if 1, not affected if 0
$BW_{s,k}$	Binary variable denoting that a blast from section k is affected by any blast wall if 1, not affected if 0
$MProb_{s,k}$	Mitigated probability of section s destruction due to an explosion in section k

The model is free to allocate a blast wall in any direction. If that direction faces an explosion from another section, it will mitigate that particular explosion. This is expressed in constraint form as follows:

$$ {}_{M}BW_{s,k} \leq \left(1 - \frac{1}{Stories_s + 1}\right) \cdot \left(\sum_{f} \frac{M_{s,k,f}}{Stories_s} + {}_{M}W_s\right) $$

Where $M_{s,k,f}$ denotes the disjunction binary variable defining to which direction of section s section k lies. The inequality is necessary because ${}_{M}BW_{s,k}$ must be binary and the result of the right hand side will not necessarily be zero or one. The first term on the right hand side is always less than one. This implies that if ${}_{M}W_s$ is zero, the second term must be less than or equal to one and the whole right hand side will always be less than one. This forces ${}_{M}BW_{s,k}$ to zero. However, if ${}_{M}W_s$ is equal to one and there is at least one floor that s and k both occupy with k in the M-direction of s, the right hand side will always be greater than or equal to one and ${}_{M}BW_{s,k}$ may be either zero or one, but is not forced to one. The optimization will naturally force this number to one if allowed as long as the objective to minimize explosion effects is included in the objective and as long as there is a blast effect from k on s. If s and k do not cohabitate any floor, or if k is not in the M-direction of s, the ΣM_{skf} term will be zero and the right hand side will always be less than one. Thus, if a blast wall is allocated in this direction, it has no effect on the blast from k, and the sum of the ${}_{M}BW_{s,k}$ components is either one or zero.

The effect of the explosion overpressure is directly modified by the binary variable $BW_{s,k}$, defined as:

$$ BW_{s,k} = \sum_{M} {}_{M}BW_{s,k} $$

And that effect is implemented by modifying the calculated probability in the following way:

$$MProb_{s,k} = DestProb_{s,k} \cdot (1 - BW_{s,k})$$

4.3.2 Fire Walls

Fire walls are also extensively used in the offshore environment. The formulation for firewalls is largely the same as the formulation for blast walls, except that it modifies the probability of failure to escape based on the heat radiation on the section of interest and does not affect the probability of failure to escape based on the escape route or muster point. The calculation of the three components of failure to escape – section effects, route effects, and muster effects, have been split from each other as explained in section 4.6.1.1. This formulation assumes that the wall can withstand any level of radiation it faces.

4.4 Case Studies

Two case studies are presented hereafter to demonstrate the vast effect that the assumptions of toxic effects and mitigation effects can have when considered during the layout phase. The first assumes mitigation is available and a low but non-negligible level of toxic gas being released in conjunction with the original fire and blast hazards. The second case study assumes the same features of the first, but with a much higher toxic concentration scenario. Recall that blast wall incorporation is usually thought of as an add-on to the layout, where layout considerations are set before adding walls, while the formulation considers this not as an add-on, but in conjunction with the layout.

The first part of each case study looks at an existing layout and optimizes walls and escape routes as the sections are fixed. The cumulative effect of multiple walls on calculated risk is studied. The second part of the case study assumes that sections are allowed to vary in placement and dimension across the platform. It is shown that comparably lower risk can be achieved with less use of resources simply by optimizing the layout using the formulation outlined in this chapter. Validation of results for explosion and dispersion is carried out in FLACS.

4.4.1 Muster Point Case Study Revisited

This case study is superficially equivalent to the second case study of chapter three, this time including the toxic and mitigation formulations in order to illuminate how these considerations change the overall layout, with the mitigations being considered in tandem with the layout as well as after the layout as an 'add-on' consideration. Performance is compared quantitatively as well as qualitatively and conclusions are drawn.

4.4.1.1 Other Modifications to the Model

Because of the increasing complexity of the model, it is necessary to make several changes in order to ensure efficient solution and tractability. The first simplification was to condense hazard constraints (explosion effect, fire effect, and toxic effect) to apply only to those sections that have a cost. In this way, the high-value areas can be emphasized for risk reduction, and the low value areas can be held simply to the base constraints. The high-value sections in this case study are the quarters, with section cost 30, the shop, with section cost 10, and the wellhead, with section cost 5. The rest of the sections are set to a cost of zero, and the hazardous effect on them is ignored. The effect of this change is to reduce solution time per major iteration from a scale of tens of minutes to tens of seconds. It also allows stochastic initial point sampling to become time-feasible. The stochastic method used is explained later.

Redundant constraints are deleted in the escape model. This is accomplished through the use of a decision parameter that decides which fire scenario will cause the greatest effect, and then feeds this to the fire modeling constraints. This is possible because all fire models follow the same general form of reaction energy scaled by squared distance from the fire. Thus, the reaction energies, which are fully parametric, can be compared and the energy with the highest magnitude can be chosen for a section, relieving the need for four sets of constraints for four fire scenarios. In addition, fire effect on the affected section is considered separately, as is the fire effect on the affected

muster point, and each of the aforementioned five escape probability values are given equal weight in the overall escape probability:

$$EscapeProbability_{s,k} = \frac{1}{5}\left(EProbSection_{s,k} + \sum_{m} SectionMuster_{s,k,m} \cdot EProbMuster_{s,k,m} + \sum_{m} SectionMuster_{s,k,m} \cdot EProbEscape_{s,k,m} \right)$$

Finally, because of the high non-linearity and non-convexity of the model, the global minimum risk is not guaranteed. Because of this, there may exist many local minima that can be expected to be greater than the global minimum [58]. Indeed, it is often necessary in this case to give a suitable initial guess for variables [59] that, depending on the difficulty of the problem, may have to begin relatively close to the global optimum , as the solution may come to rest in a local (non-global) optimum, or, in the case of the utilized solver DICOPT, the MIP master problem may cut off the global optimum, leaving only non-global local optima [60], though the global optimum may still be found as convexity of the objective and certain constraints are only sufficient conditions and not necessary conditions to find the global optimum.

In order to find solutions closer to the global optimum, a stochastic method of sampling initial values is proposed. Methods that involve a stochastic sampling of points are often the most efficient method for finding a global minimum of a non-convex objective function [61]. In conjunction with the simplifications made to the model in this section, a stochastic method of sampling initial points becomes a feasible method of identifying optimal solutions – if not global then at least closer to global than one isolated guess. Accordingly, the model has been modified to sample 100 sets of initial midpoints, each set comprised of a random choice of midpoints over a uniform

distribution of points within the platform area. From these initial points, the solver is allowed to find the local optimum corresponding to the initial guess. The relevant data, if the objective value is superior to the current best objective value, is then stored as the properties of the current best optimum solution, and the solver runs anew with the next initial guess. No layout information from the prior solution is carried over from run to run, though some information about feasibility that can be used to expedite the next solution is. At the end of the sequence of runs, the best sampled solution is recorded as the optimal solution, if not global then sufficiently close to be acceptable.

4.4.1.2 Case Study Specifications

The simulations were run on a personal computer with a 3.4 GHz processor and 8 GB RAM. The problem contains 3510 variables, of which 2158 are non-linear and 939 are binary or integer, and 3177 constraints. The GAMS software was used, with the DICOPT MINLP solver using CONOPT for the NLP subproblem and CPLEX for the MIP subproblem. The simulations take an average of 30-45 minutes to complete using a stochastic approach where initial guesses for midpoints are randomly sampled between iterations in an attempt to break free of local optima and find the global optimum. Because the model is non-linear and non-convex, the input guess plays a large role in the final answer for the layout, and may lead to objectives that are much greater than the global optimum. In this formulation, the initial guess is randomly sampled and the model is allowed to solve. If the solution is better than the current best, the new solution becomes the current best and the model is run again.

The following parameters are used in the revisited muster point case study:

Table 27: Parameters used in the revisited case study

Input	Value(s)
Platform Dimensions	110’ x 150’, 2 floors
Sections	Wellhead, Quarters, Shop, Process, Compressors, Risers, Storage, Utilities
Stories	Wellhead: 2, Compressors: 2, Risers: 2
Area [ft^2], per floor	Wellhead: 4950, Quarters: 1800, Compressors: 2376, Storage: 825, Utilities: 330, Process: 900, Risers: 150, Shop: 1800
Maximum Aspect Ratios	Wellhead: 2.5, Quarters: 1.4, Compressors: 1.9, Storage: 1.4, Utilities: 3.3, Process: 1.5, Risers: 6.0, Shop: 1.4
Section Cost	Quarters: 30, Shop: 10, Wellhead: 5
Release Sections	Wellhead, Compressors, Utilities, Process
VCE Material	Natural Gas (properties of methane)
Jet Fire Release	Natural Gas, release through 1 inch hole
Pool Fire Release	Crude Oil, at 1 kg/s
Explosion Severity Level	Wellhead: 6 Compressors: 5 Utilities: 3 Process: 3
Mass of Gas Cloud [kg]	Wellhead: 45 Compressors, Utilities, Process: 40
Process T [F]	All: 200
Process P [psi]	Wellhead: 500 Compressors, Utilities, Process: 100

All physical properties and assumptions are kept from the original case study, with the only exceptions being the amount of mass in the stoichiometric gas cloud, and the fact that the jet fire mass flow is assumed to contain 10% hydrogen sulfide for the toxic dispersion portion. Wind speed was assumed to be 5 m/s in the positive-x direction.

Two versions of the case study are run: one with a low hydrogen sulfide release concentration to illustrate the effects of the mitigation formulation and one with a high hydrogen sulfide release concentration to illustrate the effect of toxic dispersion in conjunction with the mitigation formulation.

In both studies, 5% of the volume of the section was assumed to be filled with flammable gas in order to find the amount of energy available for an explosion. The mass of the cloud was rounded to the nearest 5 with a minimum of 15 kg. This gives the wellhead 50 kg, the compressor area 40 kg, and the process, risers, and utilities 15 kg each. The platform dimension is 110’ by 150’.

4.4.1.3 Objective Function

The objective function for this model is simply to minimize the summed risk over each scenario for each section of interest. The escape probability is introduced in section 4.6.1.1, the destruction probability is the same as in the prior chapter, and the toxic probability is the sum of the probabilities from each possible release direction divided by the number of possible release directions, in this case four:

$$ToxicProbability_{s,k} = \frac{\sum_M \sum_f \sum_R M_{s,k,f} \cdot {}_R TProb_{s,k}}{4}$$

And the overall objective to minimize is:

$$Prob = \sum_{s} SectionCost_s \cdot \sum_{k} \left(DestProbability_{s,k} + EscapeProbability_{s,k} + ToxicProbability_{s,k} \right)$$

So that each outcome is equally weighted against one another, but each section is weighted differently based on the expected population.

4.4.1.4 Results – Low H2S Concentration

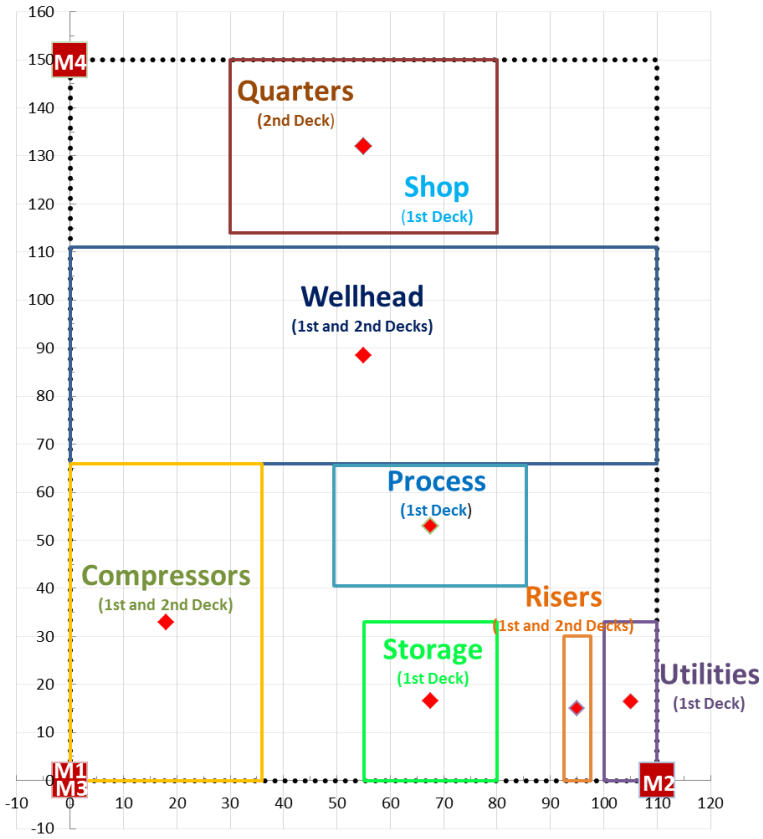

Figure 30: Base layout for muster point case study

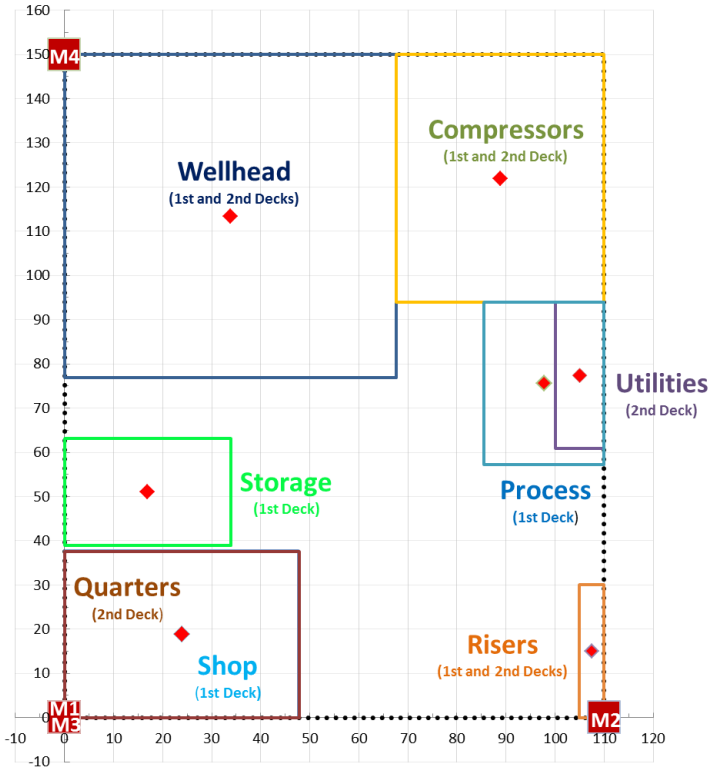

Figure 31: Optimal layout, no walls, two muster points

The fixed layout in Figure 32 was run to determine the level of risk associated with the layout when escape routes are optimized with no walls, and one to five walls. Because the fixed layout cannot be rearranged, the risk is static other than the reductions that can be made due to escape routes and allocation of walls for mitigation.

The layout was then allowed to move freely to minimize fire, blast, and toxic risk. Scenarios were run for walls that only mitigate blast as well as walls that mitigate fire and blast. A sample optimized layout for one blast wall is shown in Figure 3. A summary of the results follows in Table 28.

It can be seen that by simply allowing the layout to be manipulated, even when mitigation is not incorporated, the risk of the layout can be reduced by about 43%, mostly owing to improved fire scenario performance. By adding walls, the performance

can be marginally improved further until the opportunity for mitigation no longer exists, at which point walls are still allocated but no longer serve any purpose. This can be seen in Figure 31, where walls after the second in the case of blast walls or the third in the case of combined walls no longer improve safety performance greatly. Note that the toxic risk in this case is relatively low. This implies that layout is driven by fire and blast risks rather than minimization of toxic risk, since the risk is already almost negligible.

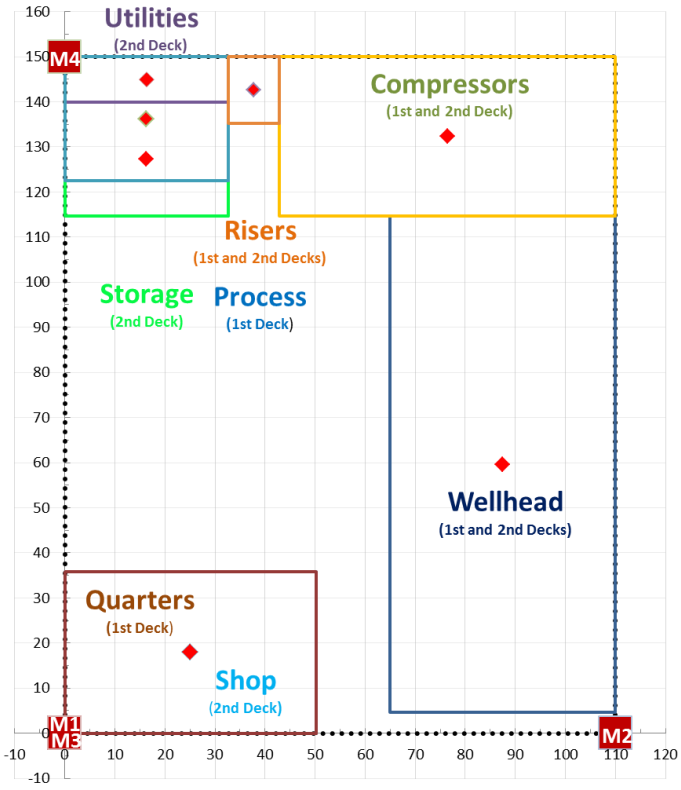

Figure 32: 1-wall optimized layout, two muster points

Table 28: Combined risk for different layout configurations

	Fixed Layout – 0 Walls	Free Layout – 0 Walls	Free Layout – 1 Blast Wall	Free Layout – 1 Blast/Fire Wall
Toxic Effect	0.68	0.66	0.59	0.72
Fire Effect	82.87	44.08	38.73	27.77
Blast Effect	7.68	7.08	1.86	1.81
Total	91.23	51.82	41.18	30.30

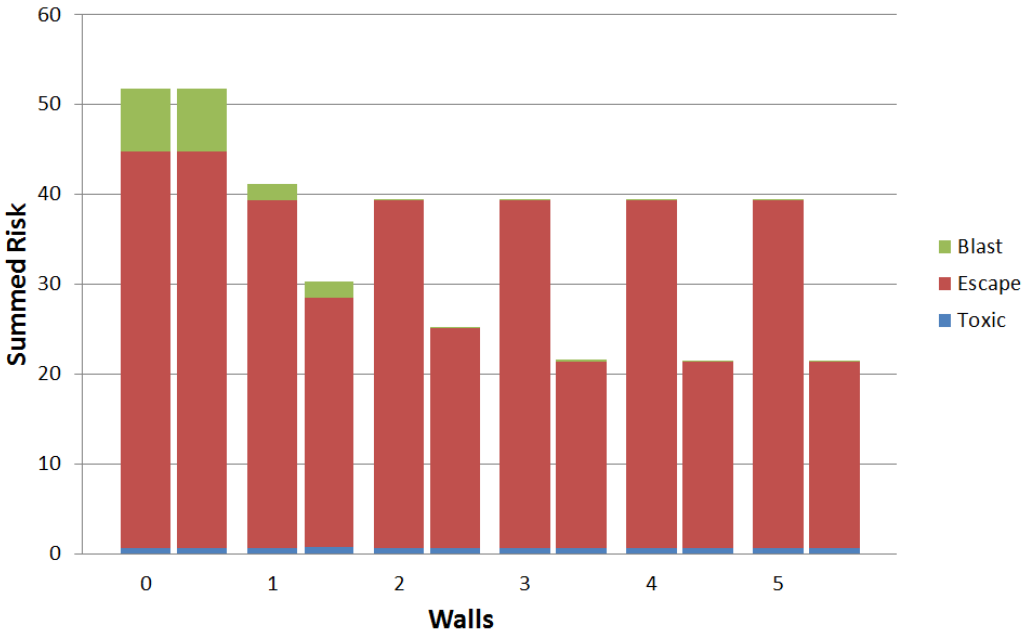

Figure 33: Difference in risk reduction between blast walls and blast/fire walls

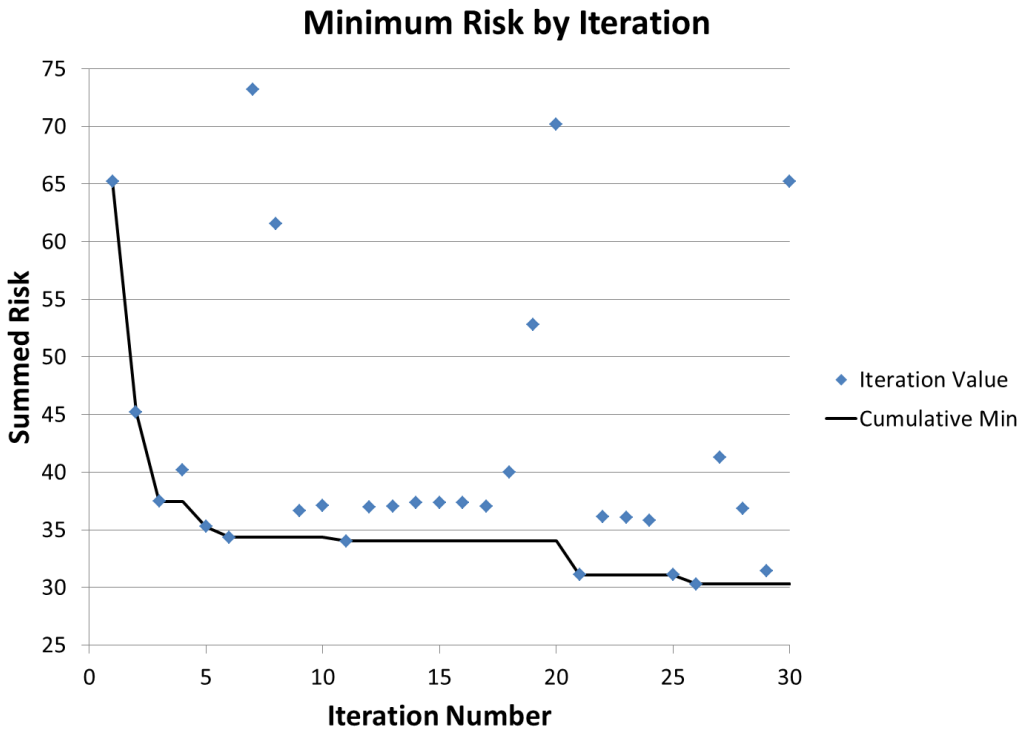

Figure 34: Evolution of the cumulative global minimum by iteration number, free layout, one wall

Also of interest is the performance of the midpoint sampling in the optimization. Figure 36 shows the evolution of the cumulative minimum by iteration for an example scenario, which shows that there is an initial vast improvement in objective value that dwindles after several iterations. The objective value improves by about 45% in the first three iterations, and then by about 14% over the next 27. While there is great variation in the local minima in this case, they tend to cluster around a case where the solution is about 15% higher than the final minimum, owing normally to a slightly heightened risk of failure to escape due to a change in allocation of muster points, whereas the highest local minima are typically due to a large divergence in layout from the minimal risk layout. This is to say that the highest values are pure layout problems, while the lower sub-optimal values are typically muster point allocation problems. Similar results are found in other cases.

4.4.1.5 Results – High H2S Concentration

Hydrogen sulfide may be present in natural gas at concentrations of up to or exceeding 50% v/v [62]. This case study assumes that there is 50% hydrogen sulfide in a postulated natural gas leak. Toxic considerations become more highly weighted, and the layouts change as a result. Of interest is the assertion that mitigation walls may normally be considered as an 'add-on' [63] after the layout has been done, rather than directly in conjunction with the layout planning. In order to test for possible risk reduction by considering the walls in conjunction with the layout, the initial layout without walls has been performed, and sections are then fixed in those places for the model to allocate walls as it finds to be optimal.

Figures 37 and 38 show the optimal layouts in the high H_2S case for the free layout case and the mitigation add-on case. The outcome is vastly different, and the free case is found to be about 15% better in risk reduction, mostly owing to the improvement in toxic performance, where risk is reduced by 60% over the add-on layout. This can be attributed to the use of the non-mitigated layout, which seeks to minimize the much greater fire risk at the cost of raising the toxic risk, whereas the free layout is able to take into account the risk reduction that can be gained by spacing sections differently to reduce congestion while using mitigation to reduce the risk of blast and fire scenarios. It is indeed beneficial to consider the mitigation during the layout phase.

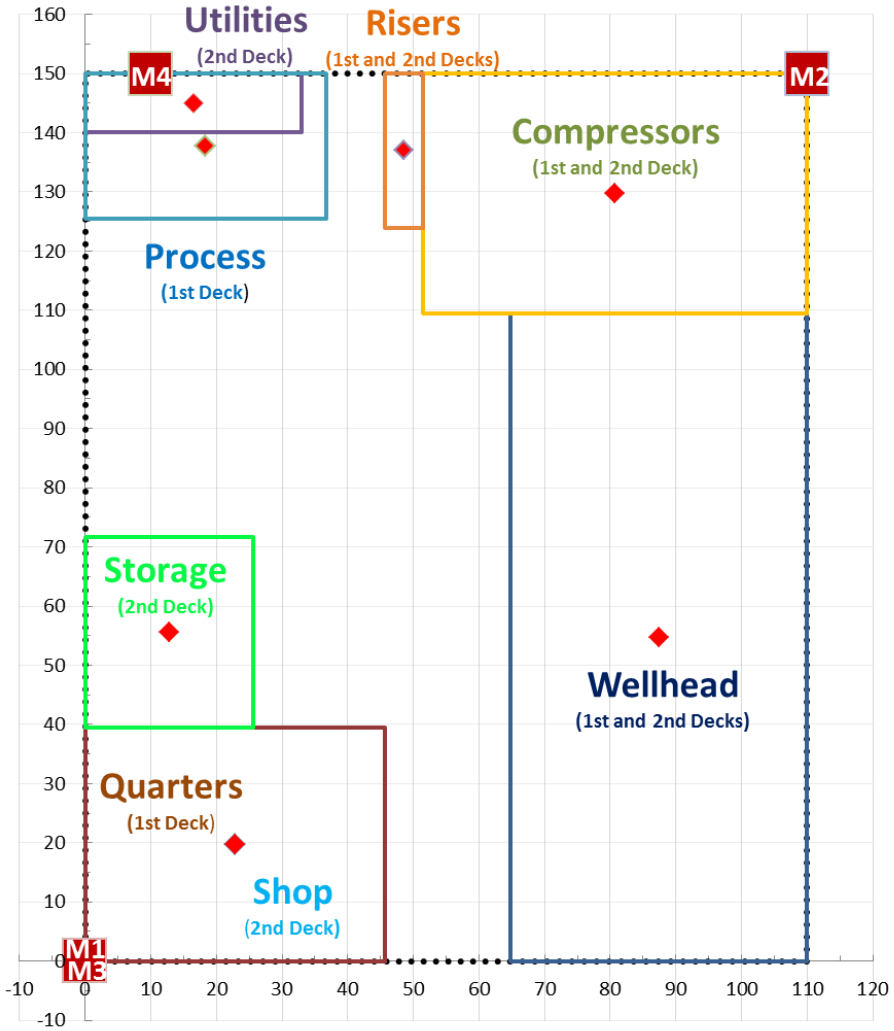

Figure 35: One blast/fire wall, free layout, wall considered during optimization

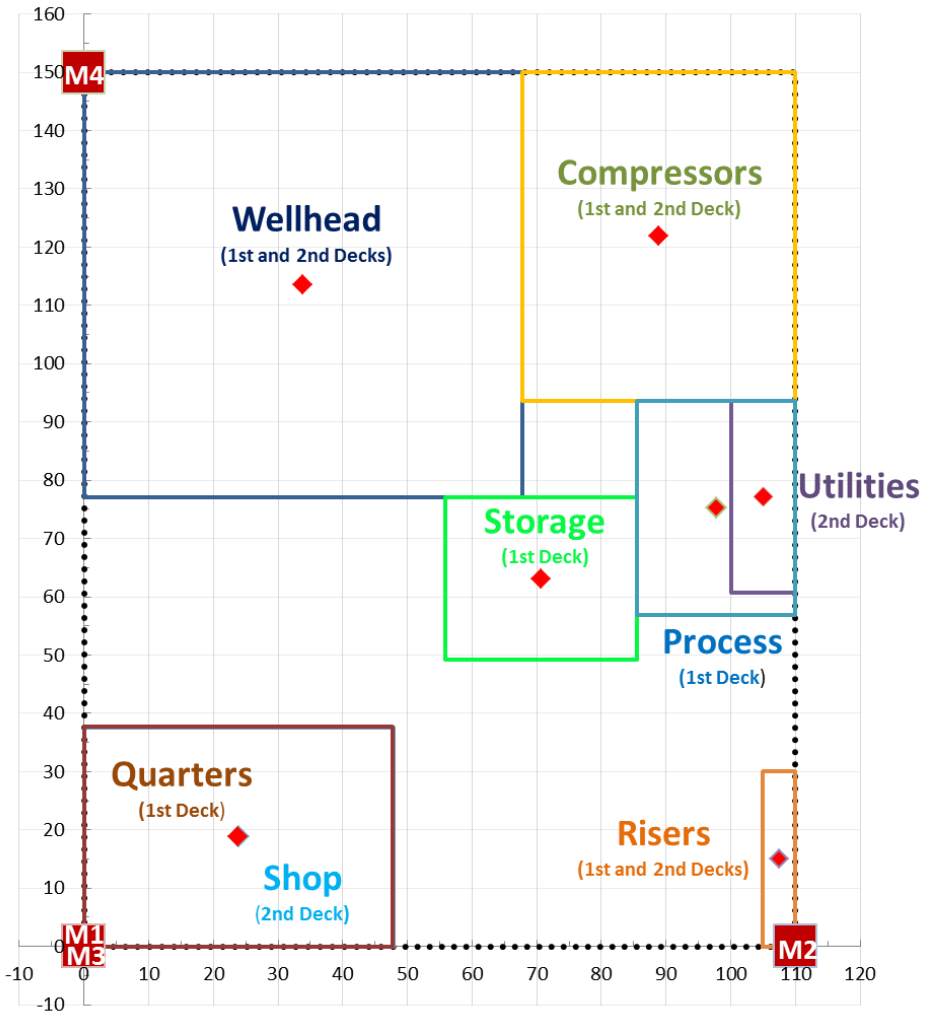

Figure 36: One blast/fire wall, wall considered as an add-on to optimization

Figure 39 presents risk information for each layout type and number of walls. As expected, either optimized layout outperforms the original layout, which suffers from a widely greater fire risk and a significantly larger toxic risk that cannot be mitigated, as toxic risk is governed by the layout of the platform and cannot be lowered without rearrangement. The original layout cannot take advantage of fire wall risk reduction as readily as the optimized layouts, leading to a lower marginal gain in risk performance per wall allocated and causing the relative performance of the fixed layout to fall from

about 1.8 times the risk of the optimized zero wall case to 2.8 times the risk of the optimized three wall case.

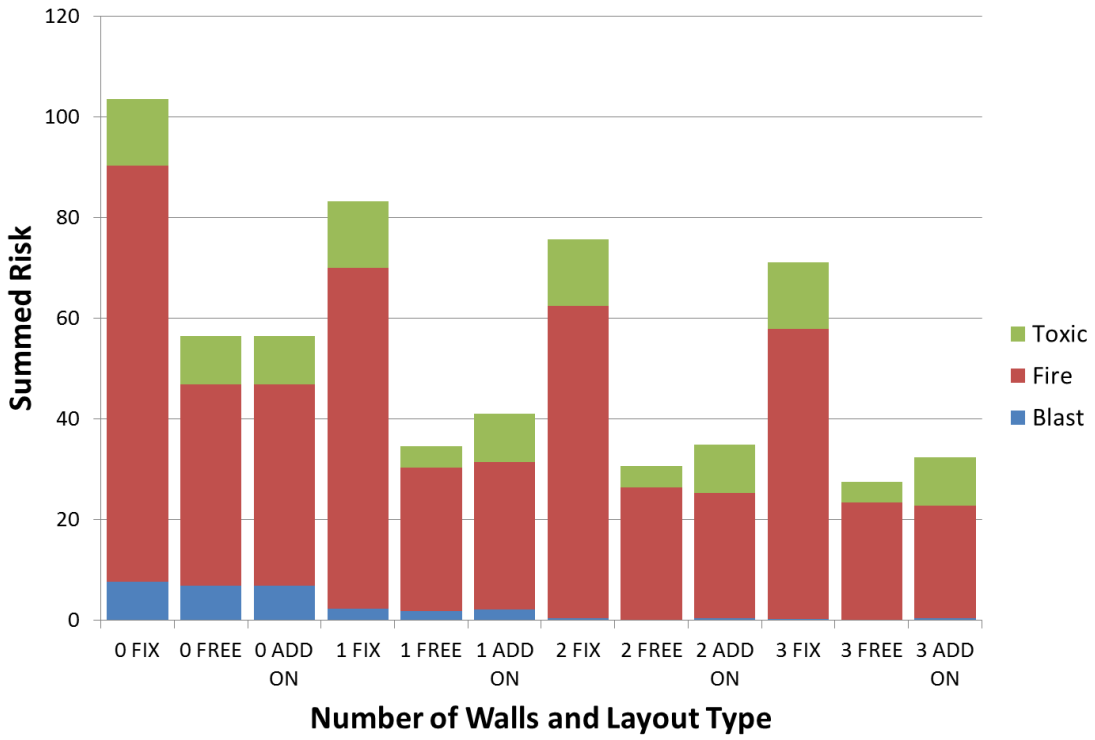

Figure 37: Layout Risk Comparison for High H_2S Concentration Scenario

4.4.1.6 CFD Validation

CFD validation using FLACS has been carried out in the high hydrogen sulfide case in order to verify that the model gives improved safety performance in practice. The difference in blast performance between the fixed no-wall case and the free no-wall case is almost negligible because of the high overpressures caused by the increase in mass in the gas clouds, but the optimization of the layout allows for a greater chance of escape. The CFD simulation corroborates this, showing that the overpressure felt by the shop and quarters are almost identical, both above the value needed for a 100% chance of destruction according to probit value. The wellhead overpressure is decreased from 0.25

bar to 0.15 bar, corresponding to a 15% decrease in destruction probability, which matches well with the optimization model value.

Table 29: Maximum toxic concentration at monitor points for the fixed and one-wall free layouts

	Wellhead		**Compressors**		**Process**	
	Max C [ppm]	Change	Max C [ppm]	Change	Max C [ppm]	Change
Fixed						
Quarters	20000	-	10000	-	50000	-
Shop	20000	-	10000	-	50000	-
Wellhead	90000	-	10000	-	110000	-
Optimized						
Quarters	Negl.	-100%	Negl.	-100%	Negl.	-100%
Shop	Negl.	-100%	Negl.	-100%	9000	-82%
Wellhead	50000	-44.4%	5000	-50%	30000	-72.7%

The toxic concentrations at each of the monitor points of the key sections is reduced by over 40% and the toxic concentrations at several points is negligible, not rising appreciably due in large part to wind effects blowing the toxic gas away from the monitor point in the section. In most cases the toxic gas did intrude within the boundary of the section, but did not hit the center of the section where the monitor point was located; thus the toxic gas would have an effect on the section from a practical standpoint, but the concentration would be greatly decreased from the fixed case. An example of this is shown in the figures that follow.

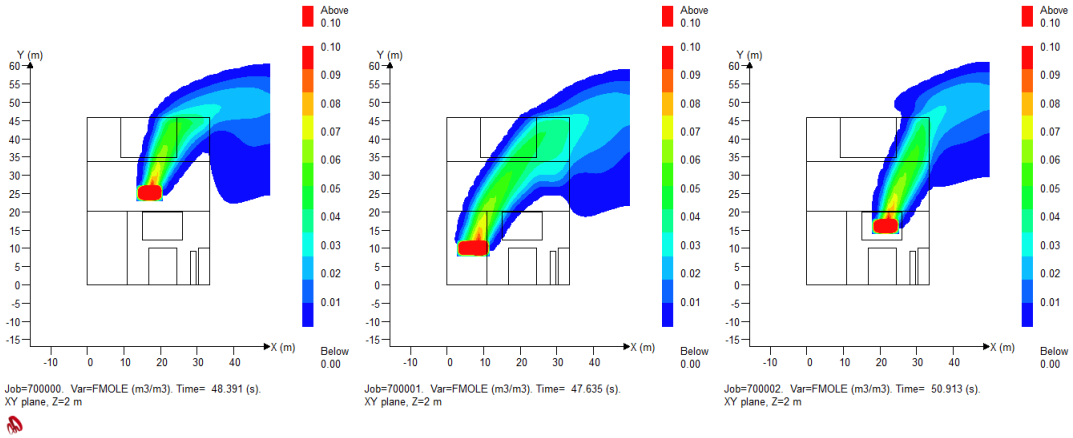

Figure 38: Fixed layout toxic footprints by mole fraction. Quarters and shop located at the top of the platform

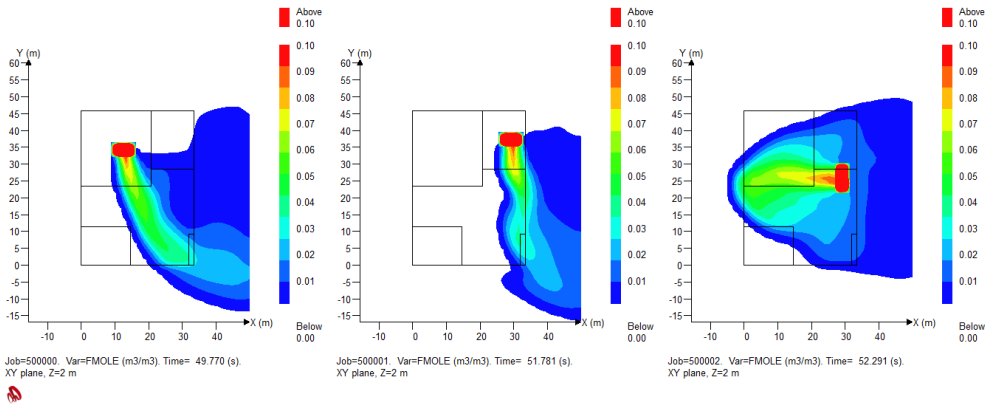

Figure 39: Free layout toxic footprints by mole fraction. Quarters and shop located on bottom left of platform

4.5 Conclusions

A model has been constructed that is able to optimize platform layout for three scenarios: blast, fire, and toxic dispersion. Toxic dispersion is approximated using a

correlation based on the flow rate of material, wind conditions, and amount of congestion in the direction of the release. Information for the dispersion correlation was gathered using a set of simulations in FLACS using an artificial congestion method, as the prior layout is not known. Mitigation is also considered as a binary choice of allocation of blast and fire walls. A blast wall can be allocated to any section on any side of the section and completely blocks any risk due to overpressure or radiation, but can only benefit the section if the blast or fire comes from the side that the wall is built on.

The results show that the risk can be greatly reduced over a fixed layout in either case and with all numbers and any method of mitigation. It further shows that considering walls as an add-on rather than as a part of the layout process may limit the effectiveness of the wall and cause the marginal risk improvement per wall to fall drastically when comparable or better results could be realized by consideration of mitigation in conjunction with an optimization. CFD studies confirm the superiority of the optimized layout to the fixed layout.

5. A FORMULATION TO ACCOUNT FOR DOMINO EFFECT AND OTHER SECONDARY EFFECTS IN OFFSHORE PLATFORM LAYOUT OPTIMIZATION

5.1 Domino Effects

Many definitions for domino effect have been proposed. Among the earliest definitions, Lees, in the 1980 first edition of his encyclopedia Loss Prevention in the Process Industries, defined domino effect as "a factor to take account of the hazard that can occur if leakage of a hazardous material can lead to the escalation of the incident, e.g. a small leak which catches fire and damages by flame impingement a larger pipe or vessel with subsequent spillage of a large inventory of hazardous material" [64]. More recently, more specific definitions are used such as that of Cozzani [65], which stipulates three main components, which are now widely accepted as integral to the definition [66]:

- Primary event occurring in one area
- Propagation of event effects to another area where secondary events occur
- Escalation, where the effect of the secondary effect is usually more severe than that of the first event

These events are not infrequent. A recent study by Abdolhamidzadeh et al [67] identified 224 instances of domino effect culminating in fire or an explosion since 1917, with 67 of these events occurring since the year 2000 and 139 events since 1980. Though it is debatable whether the increase in frequency of domino effect incidents indicates a lack of understanding of and design for its effects rather than an increase in incident reporting and improvement in incident analysis, it is not debatable that domino effect is an important consideration in facility design, and that one of the best ways to design for domino effect is a proper layout.

Several domino effects will be explored in this chapter. Dispersion of flammable gas to a remote ignition point in another section leading to directionally-influenced

blasts, smoke propagation due to a fire event and its effect on probability of escape, and the expanded effect of layout on dispersion patterns, both for toxic and explosion scenarios, are implemented. Other improvements such as blast wall failure and fire modeling improvements are also incorporated.

5.2 Pool Fire Modeling Improvement

In the previous chapters, pool fire has been taken into account, but only as a point source of radiation based on the floor in which the release occurs. In actuality, this is only a passable estimation of the heat radiation from a pool fire. Indeed, the flame from a pool fire may be substantial and can cause damage to equipment above the flame due to radiation and direct impingement [51], but would not necessarily be expected to damage equipment below the fire. The fire is also not necessarily expected to have a significant diminishing of radiation or temperature near the top of the flame as compared to the middle or base; rather it is found that the maximum temperature at the top of the flame may even exceed that of the bottom of the flame and fluxes are quite comparable [68], indicating that the upward radiation of the flame cannot be discounted.

Furthermore, tilt of the flame can play a role in the radiation that is received at a certain point above the base of the flame [31]. This tilt is a function of wind speed and can be estimated by the following equation:

$$\theta = \cos^{-1}\left(\frac{1}{\sqrt{u^*}}\right)$$

where

$$u^* = \frac{u}{(g\dot{m}"D/\rho)^{1/3}}$$

Barbrauskas [69], argues in his pool fire model that due to the approximation of treating the flame as a cylinder, refined methods of approximating flux are not

necessarily justified, instead opting for a simple expression based on the heat of combustion, mass burning rate, diameter of the pool, distance from the pool, and an experimental correction factor:

$$q = \frac{\chi_r \Delta H_C \dot{m}''}{16(\frac{r}{D})^2}$$

This equation is meant for a target on the ground a certain distance away from the pool fire. However, since there are multiple stories to offshore platforms and the aim is to be able to estimate effect on each floor, it is useful to make a modification to the equation. Because the surface emissive power over the surface of the flame is fairly constant, the diameter can be approximated at each point of interest, in this case each floor, and the heat flux as a function of distance from that component of the flame can be used. This is also useful in incorporating the tilt of the flame into the formulation, where the midpoint of the flame will be different for each point of interest due to the effect of wind.

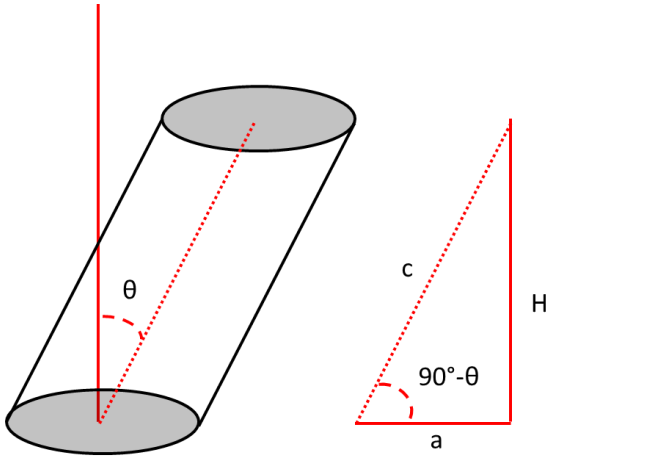

Figure 40: Cylindrical pool fire model, degree of tilt, and center point position modifier expressions

Using this formulation, and assuming that the wind direction is positive-x, the modified center point can be found as:

$$x'_s = x_s + \frac{FloorSpacing * (Floor_k - Floor_s)}{\tan(90° - \theta)}$$

Which can be used in the radiation calculation for a pool fire from section s affecting section k on a floor equal to or higher than s.

5.3 Upward and Downward Dispersion

Grated decks are often installed in offshore facilities in order to aid ventilation in the case of a possible flammable release [70]. This is useful, as it may allow gas to escape the congested and confined spaces of the platform or allow it to disperse to below its flammability limit, but it also presents the possibility of a large flammable release having more opportunities to find an ignition source, a large toxic release affecting more of the platform area, or a pool fire affecting higher floors instead of impinging on a ceiling. Indeed, this is yet another trade-off that is associated with decisions made offshore.

In order to obtain a more accurate picture of the effect of more generalized dispersion on toxic and blast effects, and their effects on the layout of an offshore platform, upward and downward dispersion have been incorporated into the model.

It is necessary for the model to discern where sections lie on the platform in relation to each other. Up to this point, the relationship between sections was defined by the non-overlap constraints (defining whether a section is left, right, above, or below another section), and the floor constraint, which simply defines whether two sections occupy the same floor. This information is now extended to define whether a section is ‘up’ from or ‘down’ from another section with respect to a certain floor.

The following constraints are added in order to define a certain section, s, on floor f, which is above floor l, is ‘up’ from section k that is on floor l:

$$up^*_{s,k,f,l} \leq 2 - F_{s,k,f} - F_{s,k,l} \qquad \forall l = f$$

$$up^*_{s,k,f,l} \geq V_{s,f} + V_{k,l} \qquad \forall l < f$$

$$up^*_{s,k,f,l} \leq 1 - V_{s,f} + V_{k,l} \qquad \forall l < f$$

$$up^*_{s,k,f,l} \leq 1 + V_{s,f} - V_{k,l} \qquad \forall l < f$$

$$up^*_{s,k,f,l} \leq V_{s,f} \qquad \forall l < f$$

$$up^*_{s,k,f,l} = 0 \qquad \forall l > f$$

$$up_{s,k,f} \geq up^*_{s,k,f,l} \qquad \forall l < f$$

$$up_{s,k,f} \leq \sum_l up^*_{s,k,f,l} \qquad \forall l < f$$

Where $up^*_{s,k,f,l}$ defines whether section s on floor f is above section k on floor l, and $up_{s,k,f}$ defines in general whether s is above k regardless of the floor of k. Further constraints include defining the opposite binary – $down_{s,k,f}$:

$$up^*_{s,k,f,l} = down^*_{k,s,l,f} \qquad \forall l < f$$

$$down_{s,k,f} \geq down^*_{s,k,f,l} \qquad \forall l > f$$

$$up_{s,k,f} \leq \sum_l up^*_{s,k,f,l} \qquad \forall l > f$$

In order to accommodate dispersion in all directions, the FLACS simulation introduced in Chapter 4 was rerun for the same set of parameters, but with three floors, and a leak in the center of the second floor. Monitor regions were added for the whole of the first and third floors while keeping the configuration of the monitor regions on the second deck. Two additional release sides also were given – an upward release and a downward release. The parameters for the concentration expression, calculated in the same way as in Chapter 4, are given in the table that follows.

Table 30: Correlation parameters for the generalized dispersion case

Release Direction	Monitor Region	Base Congestion Coefficient (e)	Proportional Wind Coefficient (f+i)	Base Wind Coefficient (g)	Base Flowrate Coefficient (a+c)
+X	+X	2.645E-5	2.710E-6	-9.706E-5	8.148E-4
	-X	7.933E-6	-1.093E-6	1.529E-5	-1.285E-4
	+Y	1.588E-5	8.181E-7	-3.875E-5	3.718E-4
	-Y	1.893E-5	6.976E-7	-4.020E-5	3.141E-4
	+Z	3.496E-5	-2.831E-6	-8.311E-5	2.758E-4
-X	+X	1.009E-05	1.572E-06	1.793E-04	-1.355E-04
	-X	2.258E-05	-2.535E-06	-4.375E-05	1.090E-03
	+Y	1.531E-05	-4.742E-07	7.398E-05	5.104E-04
	-Y	1.820E-05	-4.906E-07	6.324E-05	4.371E-04
	+Z	2.544E-05	-2.172E-06	-1.721E-04	1.176E-03
+Y	+X	1.704E-05	2.920E-06	-1.393E-05	6.020E-04
	-X	1.694E-05	-1.736E-06	-5.058E-05	1.821E-04
	+Y	2.493E-05	1.328E-07	-6.727E-06	-8.248E-05
	-Y	1.529E-06	9.632E-07	-5.719E-05	8.694E-04
	+Z	3.348E-05	-3.009E-06	-9.819E-05	4.732E-04
-Y	+X	1.704E-05	2.920E-06	-1.393E-05	6.020E-04
	-X	1.694E-05	-1.736E-06	-5.058E-05	1.821E-04
	+Y	1.529E-06	9.632E-07	-5.719E-05	8.694E-04
	-Y	2.493E-05	1.328E-07	-6.727E-06	-8.248E-05
	+Z	3.348E-05	-3.009E-06	-9.819E-05	4.732E-04

5.4 Explosion Domino Effect

Domino effect of explosion effects is based on the simple principle that the gas dispersed from one section can be ignited and cause overpressure in another section that is a viable source of ignition. A key weakness in the TNO method when compared to the more sophisticated CFD method is that, while it accounts for congestion by scaling the perceived overpressure, it cannot account for directional effects [71], instead assuming that the overpressure is equal in all directions regardless of the size and shape of the cloud and the directional variation in congestion surrounding the ignition point. Even the

position of the ignition point in relation to the cloud has a profound effect on the overpressure footprint [72], where an end-ignition causes run-up effects leading to a high overpressure in the direction of the dispersed cloud and relatively little overpressure in the non-dispersed direction. This effect can be seen in the FLACS simulation below:

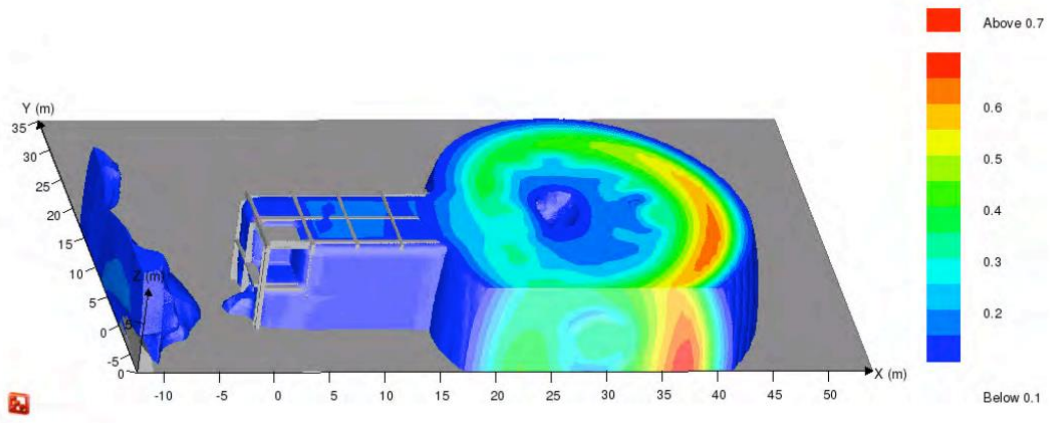

Figure 41: Run-up effect of a non-symmetrical gas cloud ignition, from Hansen et al. [72] Ignition point on the –X side of the module

The directional effects of vapor cloud explosions, though they cannot be fully captured by a relatively simple model like the TNO method used in this optimization formulation, do show properties that can be exploited by the model. If it is assumed that the dispersed cloud ignites relatively quickly after entering the section, the overpressure can be assumed to propagate almost exclusively in the direction that the gas was dispersed from. Because the position of each section in relation to the other is defined by the non-overlap constraints, the overpressure effects can be filtered to only affect those sections that are in the direction of the expected blast propagation. Using the methodology already presented in this and the previous chapter, the concentration of

flammable gas within its flammable limits in a monitor region in direction M which section s occupies due to a release in direction R from section k is:

$$_{R,M}Conc_{s,k,f} \geq [(_{M}C \cdot [_{R,M}a + {}_{R,M}bW] + {}_{R,M}cW + {}_{R,M}d) \cdot F_k] \cdot {}_{M}x_{s,k,f}$$

Where ${}_{M}x_{s,k,f}$ is the directional non-overlap constraint that corresponds to section s laying within monitor region M and the concentration is measured in mass units [kg/kg].

This concentration in the monitor region of interest is assumed to be constant throughout the monitor region. To estimate the amount of energy available for the vapor cloud explosion, the mass in the flammable cloud must be ascertained. As an estimation, the full volume of the section is assumed to be filled with flammable gas at the monitor region's concentration, and all of the gas contributes to the explosion:

$$_{R,M}E_{s,k,f} = {}_{R,M}Conc_{s,k,f} \cdot Area_s \cdot FloorHeight \cdot \rho_{gas} \cdot \Delta H_C$$

The calculated energy is then used in the standard overpressure calculation to calculate the effect of an explosion in section s on any section j that lies in the opposite direction of the dispersion:

$$_{R,M}P_{j,s,f} = \frac{c_s P_{atm}[\frac{_{R,M}E_{s,k,f}}{P_{atm}}]^{1/3}}{r} \cdot {}_{-M}x_{j,s,f}$$

And the standard probit function for structural destruction can be used, where the overpressure is measured in Pa:

$${}_{R,M}Y_{s,k,f} = -23.8 + 2.92\ln {}_{R,M}P_{s,k,f}$$

Which, if the binary terms are extracted leads to:

$$ {}_{R,M}Y_{s,k,f} = -23.8 + 2.92 \cdot \left(\ln\left[{}_{R,M}c'_{s,k,f}\right] + \ln\left[{}_{-M}x_{j,s,f} + \varepsilon\right] + \ln\left[{}_{M}x_{s,k,f} + \varepsilon\right]\right) $$

Where ${}_{R,M}c'_{s,k,f}$ is:

$$ \frac{c_s P_{atm}\left[\frac{\left[\left({}_{M}C \cdot \left[{}_{R,M}a + {}_{R,M}bW\right] + {}_{R,M}cW + {}_{R,M}d\right) \cdot F_k\right] \cdot Area_s \cdot FloorHeight \cdot \rho_{gas} \cdot \Delta H_C}{P_{atm}}\right]^{1/3}}{r} $$

The expression of the probit function is useful because it eliminates multiples of binaries, leaving just summation. The natural logarithm terms for the binary variables are augmented by adding a very small number to the binary so that there is no numerical error if the binary is equal to zero, which has the effect of making the probit function highly negative if either condition is not true, and forcing the probability to zero; if the binary is true, the term approaches zero and does not affect the probit calculation. This can also be exploited to set a lower limit on the concentration needed for an explosion event.

$$ {}_{R,M}Conc_{s,k} \leq (1 - {}_{R,M}S_{s,k,f}) \cdot LFL $$

${}_{R,M}S_{s,k}$ is a binary that has a value of one if the LFL is exceeded and is left free if it is not. The minimization of the objective will force all free S terms to zero. This term is added to the probit expression in the same way as the other binaries, leaving:

$$ {}_{R,M}Y_{s,k} = -23.8 + 2.92 \cdot \left(\ln[c'] + \ln\left[{}_{-M}x_{j,s,f} + \varepsilon\right] + \ln\left[{}_{M}x_{s,k,f} + \varepsilon\right] + \ln\left[{}_{R,M}S_{s,k,f} + \varepsilon\right]\right) $$

This value can be plugged into the original probit-to-probability equation to find the base probability that a dispersion in section k causing an explosion in section s will cause the structural destruction of section j.

The values for the flammable mass correlation are tabulated in the following table:

Table 31: Flammable mass correlated parameter values

Release Direction	Monitor Region	Base Congestion Coefficient (e)	Proportional Wind Coefficient (f+i)	Base Wind Coefficient (g)	Base Flowrate Coefficient (a+c)
+X	+X	-1.889E-06	2.084E-06	-8.263E-05	7.505E-04
	-X	5.583E-08	-1.117E-08	3.350E-07	-1.675E-06
	+Y	-5.207E-07	1.065E-06	-3.992E-05	4.176E-04
	-Y	-7.064E-07	9.681E-07	-4.119E-05	3.273E-04
	+Z	1.317E-05	-6.974E-07	-8.155E-05	2.477E-04
-X	+X	-1.544E-06	2.448E-06	-5.088E-05	2.617E-05
	-X	-3.108E-06	-6.063E-07	-2.540E-05	8.484E-04
	+Y	-1.679E-06	1.088E-06	-4.427E-05	4.883E-04
	-Y	-2.085E-06	7.357E-07	-3.035E-05	3.791E-04
	+Z	1.190E-05	-8.669E-07	-1.085E-04	3.677E-04
+Y	+X	-3.474E-06	2.385E-06	-6.662E-05	5.644E-04
	-X	4.386E-07	1.100E-07	-4.452E-05	2.442E-04
	+Y	-3.283E-06	1.082E-07	-3.320E-06	-7.143E-06
	-Y	-4.487E-06	2.370E-06	-1.081E-04	8.196E-04
	+Z	1.316E-05	-7.593E-07	-9.037E-05	2.647E-04
-Y	+X	-3.474E-06	2.385E-06	-6.662E-05	5.644E-04
	-X	4.386E-07	1.100E-07	-4.452E-05	2.442E-04
	+Y	-4.487E-06	2.370E-06	-1.081E-04	8.196E-04
	-Y	-3.283E-06	1.082E-07	-3.320E-06	-7.143E-06
	+Z	1.316E-05	-7.593E-07	-9.037E-05	2.647E-04

5.5 Smoke Modeling

Smoke is a key concern in the design of offshore platforms due to its physiological effects and reduction of visibility [73], and must be taken into account in escape considerations. Indeed, smoke was a key factor in most of the deaths aboard the

Piper Alpha and hindered escape aboard the Deepwater Horizon [7]. Unfortunately, as with the dispersion of other materials in the offshore environment, there are many properties that have an effect on how smoke disperses including weather conditions, congestion, size of the fire, propagation of the fire, material burning, among others. Thus, it can be difficult to predict how escape will be affected.

Nevertheless, the effect of loss of visibility may be more important in success of escape than the radiative effect on humans and must be accounted for. The effects of smoke can be broken into three groups: obscuration of sight, either due to interruption of light or scattering of light, pain from heat, and toxic effects of combustion materials, primarily carbon monoxide and carbon dioxide [74]. In this formulation, effects from obscuration of sight and toxic effects are considered.

Obscuration of sight is related to the optical density of smoke in the area which is naturally related to the concentration and composition of smoke, but also, according to Jin, physiological and psychological effects such as eye irritation and panic [75]. These factors, especially the psychological, may vary greatly from person to person based on gender, physical factors, and personality. Thus, psychological factors are not taken into account in this study; only the obscuration of sight and effects that can be verified physically and quantitatively will be used.

The visibility through the smoke must be quantified. Applicable information has been tabulated experimentally by Mulholland [76] as a function of mass concentration for different hydrocarbons for a visible wavelength. Jin [75], suggests that visibility and extinction coefficient, C_S, can be related by the expression $C_S \cdot V = 2$ [m] for the visibility of floors, walls, stairways and doors for non-irritant smoke in indoor conditions. He further suggests that a visibility of 13 m for those unfamiliar with an area and 4 m for those that are familiar with an area are tenability limits for reliable escape. However, in another publication [77], he suggests a linear correlation between extinction coefficient and escape speed, where below a certain value of extinction coefficient the maximum speed is constant, and below a lower threshold value the area is for practical

purposes considered ‘dark’ where escaping personnel were forced to feel along walls for their way or turn back. This relation can be expressed as:

$$v_{esc} = \begin{cases} 1.2 - 1.8C_S, & C_S < 0.5 \\ 0.3, & C_S \geq 0.5 \end{cases}$$

Where v_{esc} is measured in m/s. The threshold for the minimum escape speed is a visibility of about 2 m, which translates to a smoke concentration of approximately 4000 ppm, which varies based on the burning material.

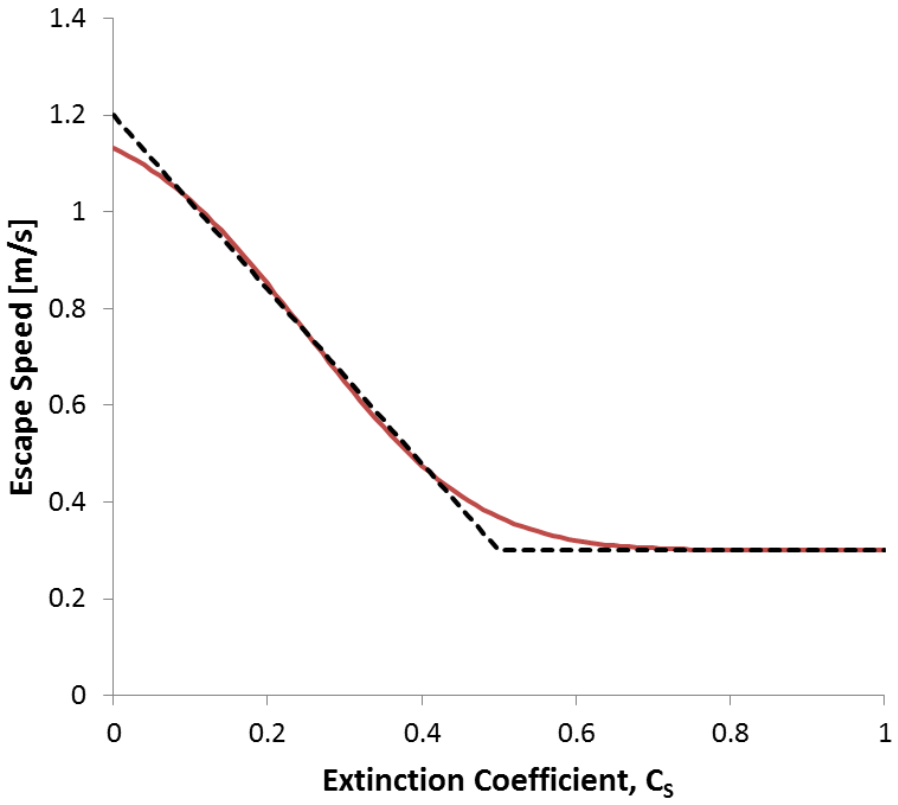

Figure 42: Approximation to escape speed as a function of extinction coefficient. Dotted line represents actual function, solid line represents approximation

As in Chapter 4, a logistic approximation is used, in this case of the form:

$$v_{esc} = a \cdot [\text{erf}(b \cdot [PPM - c])] + d$$

Is used to alleviate the difficulties of the piecewise function. The c parameter is taken to be 0.25, as the midpoint of the linear part of the function, the a and d parameters are chosen to make the initial and endpoint match the piecewise function, and b is optimized based on a least-squares approach to minimize the deviation between the approximation and the actual function. The a value is -0.9, the b value is 4.05, and the d value is 1.2. The maximum absolute difference is 0.07 m/s which occurs at the 0.5 extinction coefficient value, and the maximum percentage difference occurs at the same point at about 23%. Nevertheless, since the absolute differences are small and the original function is rather simplified in the first place, the accuracy of the approximation should be sufficient for this application.

This relation can be used to estimate the time to escape which can in turn be used either as a parameter for minimization in its own objective, or as the time scaling factor for toxic and fire effect in the probit function:

$$t_{esc} = \frac{r_{esc}}{v_{esc}} = \frac{|x_s - mx_s| + |y_s - my_s|}{a \cdot [\text{erf}(b \cdot [PPM - c])] + d}$$

The evolution of smoke products in comparison to other combustion products must be quantified in order to find the concentration and thus the escape velocity and time in a fire event. Smoke generation is a complicated phenomenon that depends highly on the chemical structure, with simple hydrocarbons such as methane and ethane producing less smoke and aromatic compounds producing relatively high levels of smoke, and moderately on fire size and level of ventilation, with underventilation causing higher smoke output due to incomplete burning [78]. Tabulated data on smoke and carbon monoxide generation from the experimental burning of alkanes, alkenes, alkynes, arenes, aliphatics, and aromatics is available from the work of Tewarson [79],

and can be used to estimate the evolution of smoke as well as two of the most common and impactful toxics in an offshore fire scenario: carbon monoxide and carbon dioxide.

Assuming that smoke is comprised of elemental carbon and that the sole reactants in a fire scenario are fuel and oxygen and the sole products are carbon dioxide, water, carbon monoxide, and smoke, the reaction stoichiometry is as follows:

$$u(C_aH_bO_c) + v(O_2) \rightarrow w(H_2O) + x(CO) + y(CO_2) + z(C)$$

Where all coefficients are molar and the fuel is defined (a and b are known). It is clear from atom balances that:

$$au = x + y + z$$
$$bu = 2w$$
$$cu + 2v = w + x + 2y$$

There are three equations and six unknowns, which can be resolved by using the yield of carbon monoxide and smoke, both on a mass per mass basis, from Tewarson:

$$x = \frac{\alpha M_{fuel} u}{M_{CO}} = \frac{\alpha M_{fuel} u}{28}$$
$$z = \frac{\beta M_{fuel} u}{M_C} = \frac{\beta M_{fuel} u}{12}$$

Implying:

$$y = au - \frac{\alpha M_{fuel} u}{M_{CO}} - \frac{\beta M_{fuel} u}{M_C}$$

And the yield of carbon dioxide is:

$$\gamma = y\left(\frac{M_{CO2}}{M_{fuel}}\right)$$

Table 32: Experimental smoke and carbon monoxide evolution properties for typical compounds found offshore, with calculated carbon dioxide evolution. Adapted from Tewarson [79]

Material	M_{fuel} [g/mol]	CO yield α [g/g]	Smoke yield β [g/g]	CO_2 evolution y [mol/mol]	CO_2 yield γ [g/g]
Ethane	30	0.005	0.013	1.962	2.878
n-Octane	114	0.010	0.038	7.598	2.933
Cyclohexane	84	0.019	0.061	5.516	2.889
Xylene	106	0.065	0.177	6.190	2.570

These numbers assume a stoichiometric amount of oxygen.

Toxic effects of these combustion products also exist, the most dangerous of which relate to asphyxia and loss of consciousness. Carbon monoxide poisoning can cause incapacitation through the buildup of carboxyhemoglobin in the blood. For short doses of high concentration carbon monoxide, Purser [80] suggests that the Stewart equation based on concentration of carbon monoxide and breathing rate can be used to find the time to incapacitation:

$$t_{inc,CO} = \frac{\%_{COHb}}{(3.317 \times 10^{-5}) \cdot {C_{CO}}^{1.037} \cdot RMV}$$

Where the concentration of carbon monoxide is expressed in parts per million and RMV is the amount of air that is breathed by a person per minute, assumed to be 50 L/min for a person under high stress. At this level of exertion, incapacitation occurs at a 30% dose.

Carbon dioxide can also cause asphyxiation and is generated in far higher proportions than either carbon monoxide or smoke. The time to incapacitation suggested by Purser is:

$$t_{inc,CO2} = \exp(6.1623 - 0.5189 \cdot \%_{CO2})$$

These concentration times are important because the doses of carbon monoxide and carbon dioxide that cause rapid death are generally quite high, but the possibility of unconsciousness, which in the case of a catastrophic event has a high probability of leading to death, is much lower and more likely to occur in a fire scenario.

Concentration, like other dispersion, is a function of release rate, congestion, and wind speed and direction. This release rate is modeled as a diffuse leak in FLACS with properties of combustion products of fire. This assumption is made because it is assumed that the smoke particles will follow the dispersion of the combustion products and will be dispersed in roughly equal concentrations.

Table 33: Properties for combustion dispersion simulation

Property	Value	Reasoning
Fuel	Natural gas: 90% Methane 10% Ethane	Most likely combustion reactant
Products	Natural gas toxic and smoke combustion products: 0.005 g/g CO 1.962 g/g CO_2 0.013 g/g smoke particulates	Amounts based on calculation in equations above
Temperature	1000˚C	Possible flame temperature
Dispersion	Diffuse	Combustion products best modeled as a buoyant release without jet momentum

The dispersion coefficients ascertained from this simulation setup are as follows:

Table 34: Correlation parameters for the smoke diffuse dispersion case

Release Direction	Monitor Region	Base Congestion Coefficient (e)	Proportional Wind Coefficient (f+i)	Base Wind Coefficient (g)	Base Flowrate Coefficient (a+c)
Diffuse	+X	1.861E-06	4.963E-06	1.038E-04	-1.100E-04
	-X	2.016E-06	1.329E-06	-1.198E-05	1.626E-05
	+Y	1.500E-06	2.983E-06	4.782E-05	-3.088E-05
	-Y	3.211E-06	2.908E-06	4.378E-05	-6.113E-05
	+Z	4.690E-05	-5.034E-06	-1.198E-04	6.831E-04

5.6 Further Improvements to the Model

Blast walls can be modeled as having a certain failure pressure, above which the structure will fail in the same way as if the wall was not there. To model this, a failure pressure for the blast wall is assumed and the probability of destruction of the section is shifted based on this failure pressure such that the probability of destruction at the yield pressure of the wall is 1% and grows at the normal probit-predicted rate from that point, which occurs at a nominal overpressure of 8660 Pa (1.26 psi). A modification to the pressure is proposed for this:

$$P_{s,k(mitigated)} \geq P_{s,k(nom)} - (P_{rated} - P_{1\%\,dest}) \cdot BW_{s,k}$$

Where the nominal value of the overpressure is calculated as in the prior formulations, the rated value of the wall is a parametric input, the 1% destruction pressure is 1.26 psi, and $BW_{s,k}$ denotes the existence of a blast wall on section s that mitigates a blast from k. The mitigated pressure expression must be greater than or equal to rather than equal to because the pressure value must be strictly positive and the right-hand side can be negative. If the right-hand side is negative, the left-hand side will be forced upward to

zero and will not be forced higher due to the minimization of the objective. The explicit calculation of the destruction probability then reverts back to the original probability formulation, unmodified by the blast wall binary.

A background congestion is also added to the formulation. This is used to simulate the congestion that is not related to specific sections, but nevertheless exists in the platform due to extraneous equipment, pipes, and other objects. Also included is a characteristic congestion for each section, taking into account that some may add less to the congestion than others. The new formulation for blockage ratio in a direction is a linear interpolation expressed as follows:

$$_{+X}BR_{s,f} = \frac{\sum_k a_{s,k,f} \cdot Area_k \cdot CC_k}{(Wx - [x_s + \frac{1}{2}Lx]) \cdot Wy} + \left[1 - \frac{\sum_k a_{s,k,f} \cdot Area_k}{(Wx - [x_s + \frac{1}{2}Lx]) \cdot Wy}\right] \cdot CC_B$$

$$_{-X}BR_{s,f} = \frac{\sum_k b_{s,k,f} \cdot Area_k \cdot CC_k}{(x_s - \frac{1}{2}Lx) \cdot Wy} + \left[1 - \frac{\sum_k b_{s,k,f} \cdot Area_k}{(x_s - \frac{1}{2}Lx) \cdot Wy}\right] \cdot CC_B$$

$$_{+Y}BR_{s,f} = \frac{\sum_k c_{s,k,f} \cdot Area_k}{(Wy - [y_s + \frac{1}{2}Ly]) \cdot Wx} + \left[1 - \frac{\sum_k c_{s,k,f} \cdot Area_k}{(Wy - [y_s + \frac{1}{2}Ly]) \cdot Wx}\right] \cdot CC_B$$

$$_{-Y}BR_{s,f} = \frac{\sum_k d_{s,k,f} \cdot Area_k}{(y_s - \frac{1}{2}Ly) \cdot Wx} + \left[1 - \frac{\sum_k d_{s,k,f} \cdot Area_k}{(y_s - \frac{1}{2}Ly) \cdot Wx}\right] \cdot CC_B$$

5.7 Case Studies

Two case studies are presented to demonstrate the applicability of the formulation. The first case study is the standard muster point case study which is presented as a common thread between all three iterations of the model for comparison. The second case study is the application of the completed model to a Floating

Production Storage Offloading (FPSO) unit, showing that the model can be applied to other offshore-related facilities that show similar characteristics to a normal offshore platform. Both case studies use the same formulation; the only changes made are parametric and not constraint-based, objective-based, or variable-based: the size of the facility, the sections that are included, and the operating conditions and properties (area and number of stories, for example) of those sections are modified.

5.7.1 Objective Function and Components

The base objective function for the model is unchanged from the previous formulation:

$$Prob = \sum_{s} SectionCost_s \cdot \sum_{k} \left(DestProbability_{s,k} + EscapeProbability_{s,k} + ToxicProbability_{s,k} \right)$$

However, the escape probability is modified to include the possibility of incapacitation due to carbon dioxide and carbon monoxide poisoning while trying to escape. Furthermore, the exposure time to fire and toxic hazards is now based on the smoke-scaled time to escape rather than on an assumption of exposure time. Destruction probability is based on the greater of risk from a base vapor cloud explosion within section k affecting section s or a dispersed cloud from section j igniting in section k and affecting section s. As before, the section cost is used as a scaling factor and is based on the average number of personnel that are expected to be in a section. The input parameters for the operating conditions were changed slightly so as to give a more balanced base probability to each of the risk components.

5.7.2 Muster Point Case Study

Five different cases were studied in this iteration: Fixed sections, free sections, walls that could fail under a low pressure, high toxic concentrations, and a flipped platform where the x and y-dimensions were exchanged. The lowered failure pressure for walls may estimate a worst-case scenario where a wall fails at a much lower pressure than expected and allow for design around this case. For the purposes of this study, the lowered failure pressure is 5 psi, while the nominal failure pressure is 15 psi. The nominal toxic scenario for combustion products assumes the normal combustion of natural gas, while the high toxic concentration scenario multiplies the amount of carbon monoxide and carbon dioxide by 5. In this case study, the shop is considered an additional source of ignition and the storage area is considered an additional source of fuel.

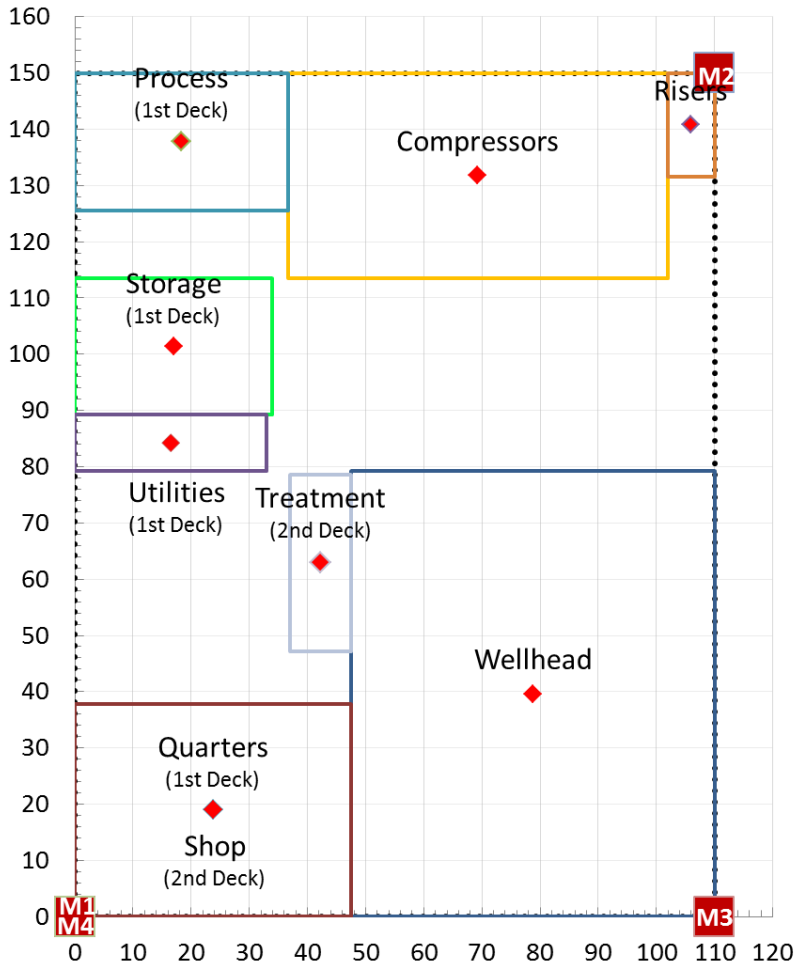

Figure 43: 0 Wall Base Case

The simulation consists of 9,225 variables, of which 1,863 are discrete, and 10,315 constraints. The average time to solution was about 3 hours, using the stochastic method outlined in Chapter 4. The model was solved in DICOPT using CONOPT as the NLP solver and CPLEX as the MIP solver.

As expected, the optimization reduces the risk in any of the cases against the fixed case by between 20 and 40%. An interesting result of the optimization, and not wholly unexpected, is that the muster points tend to be closer to the costliest sections in order to expedite escape, as the smoke concentration in the air lowers escape velocity, often to the minimum value of 0.3 m/s, and the toxic and radiation effects depend on the

time to escape more heavily than in previous formulations. Because of this, escape risk cannot be lowered as readily as in the previous formulations – for most scenarios, the risk reduction in escape by adding a wall is no longer realized after the first, wheras in the previous formulation the majority of risk reduction was a product of the wall allowing for a better escape layout.

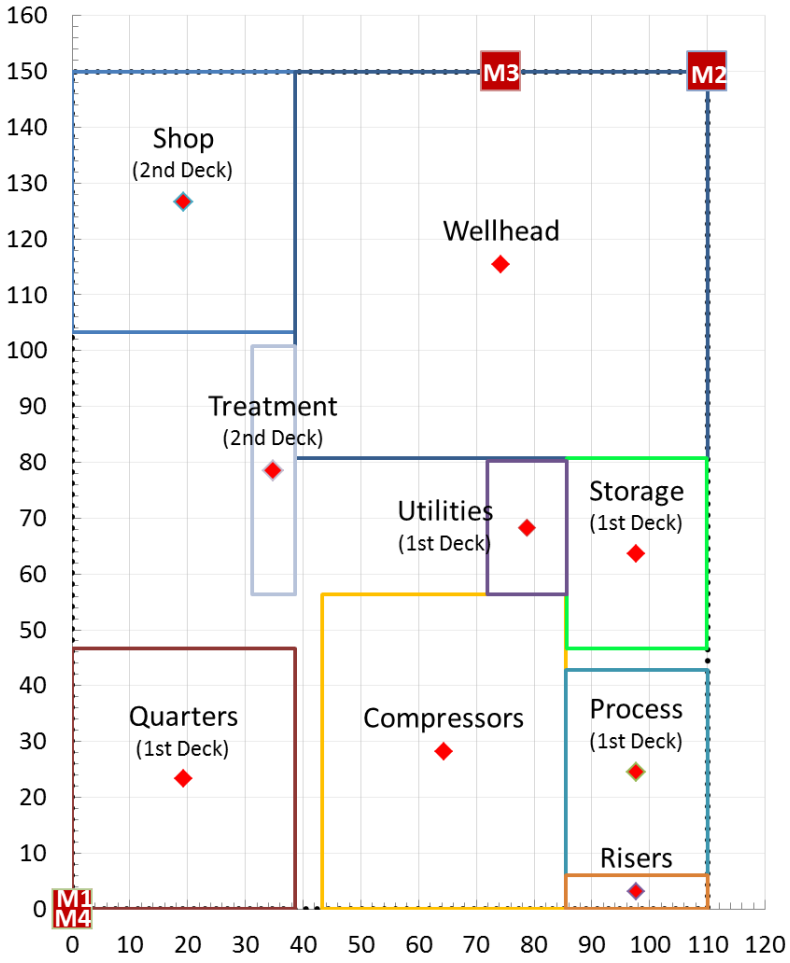

Figure 44: 1 wall free – blast wall failure 5 psi

As an example of the model's decision-making, consider the 0-wall free case and the 1-wall free case with a wall that fails at low blast pressure. The two cases are nearly

symmetrical, reflected in the x-axis which would be equivalent in the model, as only the wind (which is in the +x-direction) causes directional effects. As the wall is added to the quarters in the +x-direction, the section is moved to where the wall can absorb the most possible damage with three sources of overpressure to the side. It still sees a small amount of destruction probability due to the close proximity of the compressors, but it moves away from the stronger overpressures of the wellhead area. In the same way, the shop stays nearer the wellhead despite the higher overpressure in order to avoid the multiple sources that it cannot withstand without a wall.

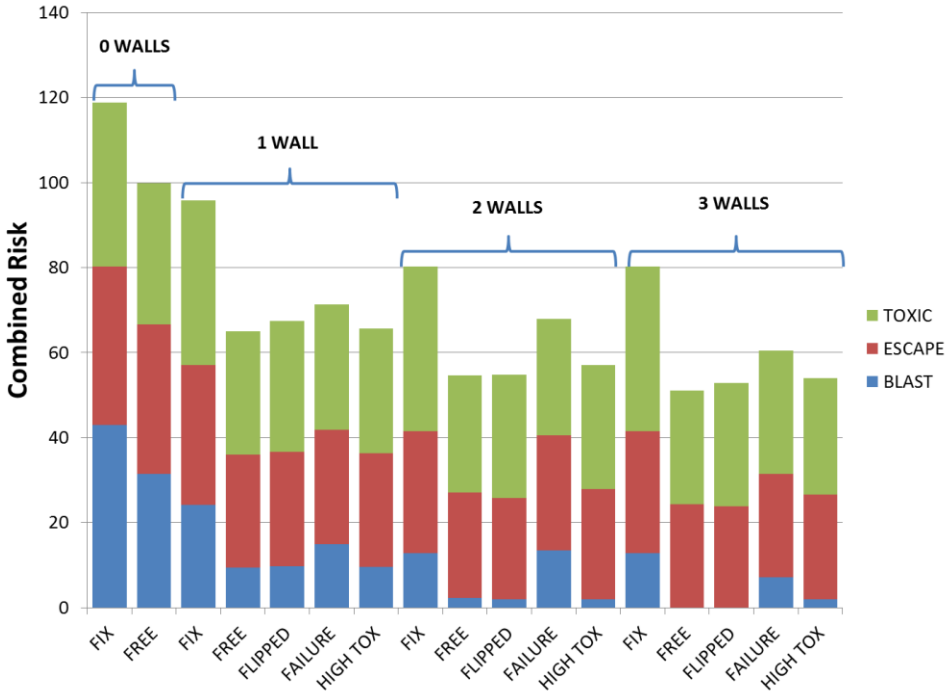

Figure 45: Comparison of risk for the cases

CFD validation on the overpressure effects of the wall failure case and the smoke propagation properties between the fixed and free layouts was performed in FLACS. The

one-wall failure case places a wall on the quarters, which moves to the bottom corner near the compressors and away from the wellhead.

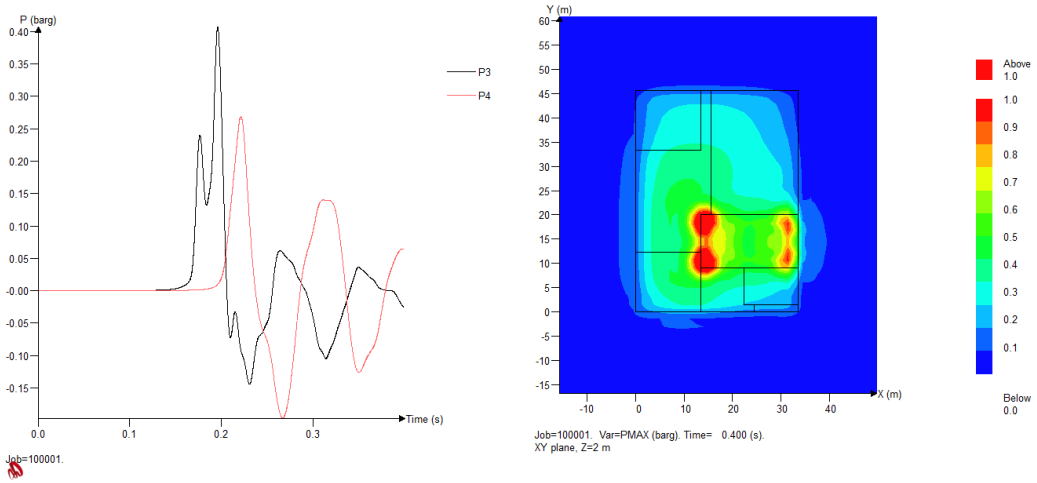

Figure 46: Overpressure profile for one-wall failure case, 5 psi, explosion from compressors

The overpressure on the quarters from the compressors is relatively high, but most of the damage is assumed to be deflected by the wall, which lowers the probability of destruction from 1 to about 0.26. Importantly, the movement of the quarters forces the escape cost down because it is farther away from the wellhead and it lessens the effect of smoke and toxic effects. Meanwhile, the shop stays close to the wellhead, protecting it from the compressors, but heightening the probability of failure to escape.

As in the previous chapter, wind effects tend to keep the toxic gas and smoke away from the high-value areas. This lowers the probability of failure to escape and the probability of death by toxic inhalation. In particular, smoke effects are also mitigated by siting high-value sections on the ground floor rather than on the second floor. Buoyancy effects prove to raise the concentration of smoke on the second floor by a factor of about 5 compared to the ground floor.

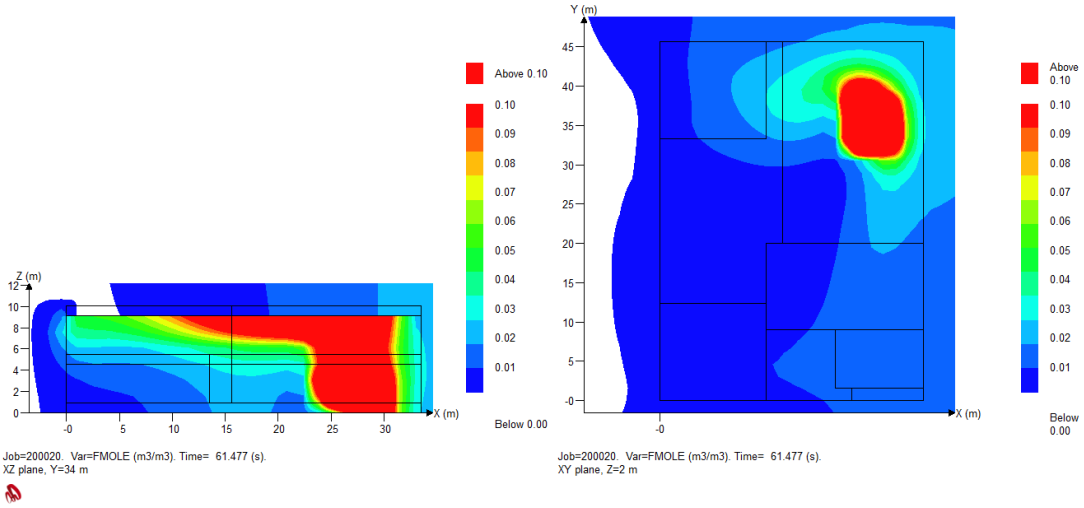

Figure 47: Smoke evolution from the wellhead. Upward directional effects are seen in the left figure while lateral wind effects are seen in the right.

5.7.3 FPSO Case Study

In order to demonstrate the applicability of the model to other offshore facilities, as well as to demonstrate that in constrained cases the model shows good agreement with human layouts, a more novel application of an FPSO has been studied. FPSO are widely utilized outside of the Gulf of Mexico, with 156 operating worldwide and 6 active in North America as of August 2012 according to Wood Group Mustang [81]. Like fixed platforms, they are a relatively small space with a large amount of congestion, though they are normally larger and have a higher aspect ratio than fixed platforms since they are boat-shaped for transportation, so the layout considerations are relatively similar [82]. General information about size and personnel distribution have been taken from the aforementioned survey by Wood Group Mustang, and a sample layout has been taken from Bechtel [83].

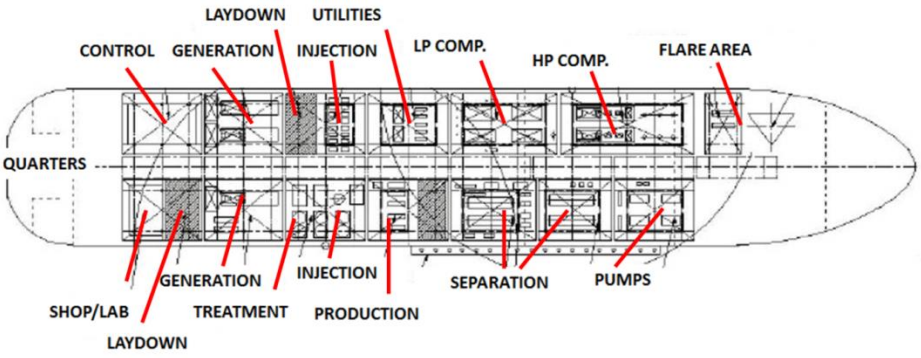

Figure 48: Sample layout for an FPSO [83]

This layout has been simplified to ten sections, of which there are six sources of fuel, six sources of ignition, and four sources of people (section cost). Information pertaining to the simulation is presented in the table that follows:

Table 35: FPSO optimization information

Section	Fuel	Ignition	Cost	Area [ft^2]
Control	NO	NO	40	10000
Generation	YES	YES	0	20000
Utilities	YES	YES	0	10000
Compression	YES	YES	0	20000
Flare	NO	YES	0	5000
Pumps	YES	NO	0	10000
Separations	YES	NO	0	20000
Production	YES	YES	10	10000
Shop/Lab	NO	YES	30	10000
Quarters	NO	NO	60	20000
FPSO Area	1000'x200' = 200000 sq. ft.			

Properties for the sections are comparable to the prior case studies, natural gas is the main flammability hazard and crude oil pool fires are considered. No walls are considered, but toxic effects due to a high concentration of hydrogen sulfide as well as carbon monoxide and carbon dioxide are possible. The following layouts show the original product and the optimized product.

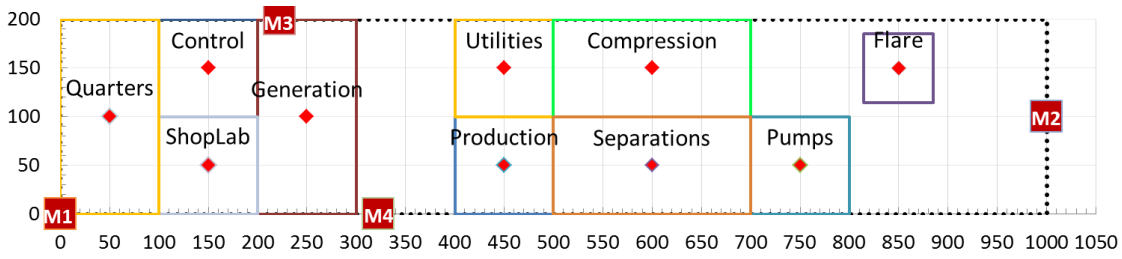

Figure 49: Original layout for FPSO, optimized musters

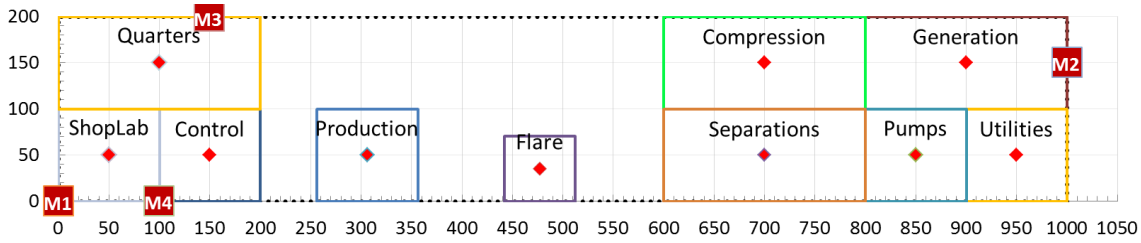

Figure 50: Optimized layout for FPSO

The optimized layout is found to be about 10% better in performance compared to the original layout, but the most striking feature is that with the exception of the production and flare, the layouts are largely similar. The difference in the position of the production module is most likely due to the fact that it is assigned a section cost that splits it away from the other sources of fuel and ignition, which contributes to a portion of the risk reduction. The other main component of the risk reduction is the movement of

the generation module from closer to the costly sections to the other side of the FPSO. The flare in the optimized formulation moves to the center of the FPSO, which, as a source of ignition, would seem to be a strange choice, but the dispersed amount of flammable is not high enough to have a great impact on the sections with a cost. Further, the directional explosion effect of a dispersed cloud would dictate that the flare, as a source of ignition but not fuel, would only be able to propagate an explosion in the direction of a dispersed cloud, and since all sources of fuel other than the production are to the opposite side of all key sections, this layout makes sense from the optimization standpoint. The production, being a key section and a source of fuel is more difficult to prognosticate, but stays on the opposite side of the sources of fuel in order to protect it from the dispersed explosion, while its own dispersed cloud will cause an effect on other key sections. The cost of this event does not, however, outweigh the cost of the effect on the production section. Muster points are allocated to be close to the sections they serve.

As is an underlying theme of these optimizations, the human layouts balance both cost and practicality in flow – the FPSO that is not optimized makes sense from a flow perspective, whereas the optimized layout may not pose much of a challenge from a piping perspective, but does not flow as linearly.

In a way, the question of layout on large FPSOs more approximates the onshore layout problem because there is ample space to separate sections where personnel may be present from the sources of fuel and ignition, but still retains the offshore problem of escape and high congestion ratios. It is expected that human layouts of FPSO facilities would be relatively close to what is predicted by the model because of the extra spacing available.

5.8 Conclusions

An optimization model that takes into account domino effect from dispersed flammable gas causing an explosion in another section, wind effects on pool fires, smoke effects on time to escape, combustion products' toxicity, and failing blast walls has been formulated. The explosion domino effect component uses the dispersion formulation

proposed in Chapter 4 and extends it to flammable gases and determination whether the gas would be within its flammability limit. The explosions include directional effects that are often present in dispersed cloud explosions.

Smoke modeling is also carried out using the formulation found in Chapter 4 and is used to determine the speed at which personnel are able to escape from a fire event. The time to escape becomes an important variable as it affects the time of exposure to radiation and toxic gas, which is taken into account in the probability of failure to escape. It is seen that the muster points are modified such that they are now much closer to the sections that have high cost, sometimes at the expense of the escape routes being closer to sources of fire.

The model is applied to two cases showing its application to the standard platform as well as to an FPSO. The standard platform gives greatly different results than the fixed actual layout with great gains in risk performance over a span of many cases, while the FPSO case gives a marginal increase in risk performance and a very similar layout to the actual layout. This leads to the conclusion that though the model is applicable to larger facilities, the formulation may lead to it being less useful since there is readily available spacing between the sources of fuel and ignition and the sections that are expected to have personnel.

6. CONCLUSIONS

Several optimization models of varying degrees of complexity have been proposed for the layout of offshore platforms. The models take risk of the greatest expected hazards – explosion, fire, and toxic release – into account. In the base case, explosions are assumed to be caused by a fixed amount of flammable gas finding ignition in the section of origination. This explosion can cause the destruction of other sections, some of which may be populated, based on the expected overpressure. The expected overpressure is based on a modification to the standard TNO multi-energy method that allows for the explosion overpressure to be simply calculated as a function of material reactivity, obstruction, and amount of material.

Fire modeling in the base case is based on a release of flammables that does not meet the criteria for an explosion. The main outcome of a fire is obstruction of escape paths due to radiant flux, which is a function of the material released, amount released, and the distance from the release to the point of interest, which includes the section itself, the muster point, and intermediate points on the escape route. Escape route choice is variable based on which route minimizes the probability of failure to escape.

Toxic modeling is based upon the notion that dispersion concentration is a strong function of release rate, weather conditions, and congestion in the direction of the release. Indeed, it is found that the congestion in the direction of the release is far more important than the congestion in any other direction and can be taken as the sole consideration in congestion's effect on dispersion. A correlation is proposed for the relation of these three factors of interest to the concentration of toxic gas given a leak of a certain flow rate in an environment with a certain wind speed and a certain congestion level in the direction of the release. This, along with known toxic effect criteria, can be used to estimate the effect of a toxic release on a section laying a certain direction from the release.

Great improvements in safety performance can be realized through the simple optimization of layout, both as measured against the optimization criteria and through

CFD validation. CFD validation was carried out in FLACS and was found to agree with the results of the optimization with respect to all major components – blast, toxic dispersion, and smoke dispersion – that can be measured by the tool.

Mitigation of the blast and fire is done with the incorporation of blast and fire wall modeling, consisting in the base case of an impervious wall that cannot fail no matter the load it bears. The optimization strategy can allocate blast and fire walls as part of the initial optimization or as an add-on for safety considerations, as is most often done in offshore facility design presently. As expected, the marginal benefit of blast walls goes down with each further wall allocated, and considering walls in conjunction with the original layout gives better risk reduction than considering them as an add-on.

Finally, advanced fire modeling is explored, and smoke modeling and directional effects of dispersion and explosion are taken into account through the aforementioned generalized dispersion correlation. Because of the small spaces that platforms occupy, it is important to take each of these effects into account for a more accurate model. Propagation of smoke is perhaps the most hazardous event that can occur in a catastrophic event offshore. To incorporate this effect into the escape model, a correlation is used to estimate the time that escape will take and use this as the time scaling for the probability of failure to escape due to heat radiative flux. This is comparable to surveys that are currently done in offshore risk modeling where the expected time to escape is estimated, and it is attempted to maximize this value. Toxic effects of the smoke are also added into the model, with incapacitation due to inhalation of carbon monoxide and carbon dioxide assumed to cause failure to escape. The time to incapacitation can be calculated as a function of the concentration of either combustion product and can be measured against the average time to escape as a function of smoke concentration and distance from the escape point.

The direction and speed of wind can have a profound effect on the heat radiated onto a point from the fire at different elevations, as well as on the dispersion of smoke from a fire and flammable dispersion. The center-point of the fire is modified for each of the floors based on the wind conditions and fire properties, which makes it safer, with

respect to fire radiation, for sections to be placed upwind of a possible fire scenario. However, dispersion to explosion domino effect is more difficult to prognosticate because being upwind of a dispersion means that there will often be a higher concentration of flammable gas downwind, where an explosion will propagate back toward the upwind direction. In this way, an optimization model is incredibly useful to take into account the many trade-offs and difficult-to-quantify effects of the change of layout.

The main objective of this research was to create an optimization formulation for the layout of an offshore platform with respect to minimization of combined risk, taking into account the following considerations:

- Account for the lack of space on an offshore platform as it relates to the added risk from catastrophic events and balance trade-offs that occur due to this lack of space
- Create a multi-floor model that resolves the differences in risk from catastrophic events at different points in space with different elevations
- Quantify effects of added congestion and confinement on explosions, fire, and dispersion
- Facilitate escape through optimal placement of sections and muster points associated with the sections to minimize the effects of heat radiation and smoke effects from fire
- Incorporate domino effect, where flammable gas may disperse to another section and be ignited, and account for directional effects of the ensuing blast
- Ensure that the optimization models solve in a reasonable amount of time, and create the model in such a way that efficiency is maximized
- Take into account relevant existing guidance in the field of offshore layout and design as useful
- Verify the findings using advanced risk analysis models such as CFD

These objectives have all been accomplished and verified through CFD validation. The models all solve in an acceptable amount of time, and could be used in practice for the layout of an offshore platform based on a relatively small amount of information that could realistically be known before the design phase. It is shown that the model is a positive step into an area that has sparsely been considered, contributing a framework for the integrated consideration of several key risk factors in the offshore realm that, as yet, have been unexplored from the numerical optimization viewpoint.

Nevertheless, there are still improvements that could be made to the model. These improvements and other opportunities for future research, both directly related to this work and other research directions are presented in the next chapter.

7. FUTURE WORK

Though a detailed and practical model has been presented for the optimal layout of offshore platforms facing fire, toxic, and blast scenarios, there are still opportunities for improvement of the model and other avenues for research in the future. These include extensions of the basic model proposed in this research, refocus of the objective of the model, and integration of other process safety topics such as human error and reliability into the facility layout problem. Several of these opportunities are presented in this chapter.

7.1 Further Analysis of Mitigation

The extent of the current mitigation formulation is explicit consideration of fire walls and blast walls, and implicit consideration of the mitigating effects of spacing and relative placement of sections. However, there are more mitigations used in offshore environments than just these.

Deluge is commonly used on offshore platforms, especially with regards to well testing [84], but more generally as a mitigation in any flammable release scenario [9]. However, the use of deluge is not as simple as activation at the first sign of a flammable gas release – according to Spouge there is a tradeoff between the lowered probability of eventual ignition due to the deluge and lowered overpressure in the case of an explosion, balanced against the increase in probability of an immediate ignition of the cloud due to sparking of static or shorting of electrical equipment. Furthermore, the effect of deluge on initial overpressures may be a positive one, with higher overpressures realized due to increased turbulence and mixing effects [85]. Reliability is also a concern, with probability of failure on demand generally accepted as about 1% and up to 50% on older platforms considering human error [86]. There exists a great research opportunity for the optimization of common deluge parameters such as flowrate, outlet spacing and layout, activation criteria, and reliability and human error concerns for better mitigation of overpressure, minimization of the turbulent effects of deluge, coverage of possible

hazards, and greater reliability. Research may be guided by the 4 BFETS Phase II large-scale experimental tests, which measured the effect of deluge on explosion overpressures [87], continuing work of research institutions and corporations such as GexCon AS, and optimization formulations such as the research put forth in this dissertation and others such as the gas-detection work by Benavides [88].

7.2 Emphasis on Domino Effects

Just as explosions can cause firewalls to fail, which can, in turn, cause heightened dispersion or flame impingement among other consequences, many other types of domino effect are possible on an offshore platform. The proposed model considers domino effect in that a dispersion from one section may ignite in another section and cause an overpressure in the opposite direction of the dispersion. Further improvements to be considered in an offshore optimization may include the following components:

- Effect of blast walls and fire walls on ventilation rates and flammable/toxic gas dispersion patterns
- Blasts or fire leading to the loss of functionality of the platform through a decapitation mechanism or inability to access critical controls
- Possibility of an explosion causing loss of containment of hydrocarbons and a secondary event
- Fire impingement (particularly jet fire and pool fire) on piping and structural integrity
- Projectiles from explosions

These considerations are of high importance due to the close spacing of the offshore environment, which yields a greater probability of domino effects [66].

7.3 Improvement of Escape Modeling

A foundation for escape modeling as a part of the optimization has been laid with this research, but there are areas for improvement. Primarily, the number of intermediate points of interest in the escape route could be expanded. A lack of resolution in points where the radiant flux is calculated may lead to poor decisions being made as to path, where an escape path may lead personnel directly by a source of fire that is not captured adequately. More intermediate points can be added, but the model will become ever more complex as these constraints and variables are added. For each iteration of addition of intermediate points, the number of constraints will be

$$FS[4 + \sum_{n=1}^{N} 5(2^{n-1})]$$

where F is the number of fire scenarios considered, S is the number of sections in the formulation, and N is the number of iterations of additions to intermediate points (the first iteration is number 1 and is simply the four vertices of the rectangle and a single intermediate point on all edges and in the middle. If three fires are considered and eight sections are used, the number of constraints increases from 96 to 216 to 456 to 936 when increased from simply the vertices of the rectangle to a formulation with 5 intermediate points.

Other methods of determining escape adequacy can also be explored. For example, a framework for adequate time to escape has been created as part of the smoke modeling formulation of this work. Time allowed for escape can be found as a function of fire intensity and placement, as a human can only withstand the radiation for a finite amount of time and firewalls have finite periods of survival, toxic and escape effects of smoke, and toxic effects of the dispersion of gases such as hydrogen sulfide. The time to escape can be minimized or the time allowed for escape can be maximized if the effect of these factors on time can be quantified.

7.4 Improvement Based on Ventilation Rates, Weather Conditions, and Solid Obstructions

A formulation to incorporate wind speed and direction is proposed in this research. Ventilation and obstruction are considered as part of the congestion level. However, the effect of ventilation blockage by solid obstructions and dispersion effects of interior configuration is not specifically studied. Though this is an application that CFD is best suited to, it could have a large effect on the optimal layout of equipment and modules. This could be extended to the layout of the equipment within a section before the layout of the sections so as to facilitate the flow of air through the platform and to help the dispersed flammable or toxic exit the area.

7.5 Further Applications of a Layout Model

Offshore platforms are not necessarily as idealized as is modeled in this research, though it would not be a stretch to model more unique or novel configurations, such as a production platform with an accommodation platform connected to it. In this case, it may be an interesting study to consider the distance between the platforms and the configuration in order to minimize the effect of an event on the production platform and maximize the probability of escape of the personnel on with platform.

An obvious extension of this model, which was purposely avoided during this research, is to balance the cost considerations of the platform such as pumping cost, marginal cost of increasing size, number of floors, or number of separate platforms (in the case of having a separate accommodations platform). This was not explored in this research for several reasons, the first being that the focus and objective of the research was to decrease safety risk without concern to cost considerations insomuch as the layout remained practical. Further, the incorporation of monetary costs requires either a monetary value put on the loss of personnel or a utility function relating the two values, each of which is difficult to define and may vary drastically from scenario to scenario based on many factors. Finally, cost considerations are often used in facility layout models to balance safety factors because the hazards can, for the most part, be mitigated

by separation of the asset from the hazard. In this formulation, because the distance is necessarily finite, this balance is not necessary (though it may not be undesirable).

REFERENCES

[1] J. A. Baker, G. Erwin, S. Priest, P. V. Tebo, I. Rosenthal, F. L. Bowman, D. Hendershot, N. Leveson, L. D. Wilson, S. Gorton, and D. A. Wiegmann, "The Report of the BP U.S. Refineries Independent Safety Review Panel," 2007.

[2] United States Chemical Safety Board, "Investigation Report - Refinery Explosion and Fire - BP, Texas City, Texas," 2005.

[3] American Petroleum Institute, "Management of Hazards Associated with Location of Process Plant Portable Buildings," vol. API RP 753, ed, 2007.

[4] R. E. Sanders, "Designs that lacked inherent safety: case histories," *Journal of Hazardous Materials,* vol. 104, pp. 149-161, 2003.

[5] E. Dole and G. F. Scannell, "Phillips 66 Company Houston Chemical Complex Explosion and Fire: A Report to the President," Occupational Safety and Health Administration1990.

[6] M. E. Paté-Cornell, "Learning from the Piper Alpha Accident: A Postmortem Analysis of Technical and Organizational Factors," *Risk Analysis,* vol. 13, pp. 215-232, 1993.

[7] J. E. Skogdalen, J. Khorsandi, and J. E. Vinnem, "Evacuation, escape, and rescue experiences from offshore accidents including the Deepwater Horizon," *Journal of Loss Prevention in the Process Industries,* vol. 25, pp. 148-158, 2012.

[8] S. Chakrabarti, "Handbook of Offshore Engineering, Volumes 1-2," ed: Elsevier, 2005.

[9] J. Spouge, *Guide to Quantitative Risk Assessment for Offshore Installations*: Energy Institute, 1999.

[10] M. A. El-Reedy, *Offshore Structures - Design, Construction, and Maintenance*: Elsevier, 2012.

[11] C. F. Conway, *The Petroleum Industry: A Nontechnical Guide*: PennWell, 1999.

[12] T. C. Koopmans and M. Beckmann, "Assignment Problems and the Location of Economic Activities," *Econometrica,* vol. 25, pp. 53-76, 1957.

[13] F. D. Penteado and A. R. Ciric, "An MINLP Approach for Safe Process Plant Layout," *Industrial and Engineering Chemistry Research,* vol. 35, pp. 1354-1361, 1996.

[14] L. G. Papageorgiou and G. E. Rotstein, "Continuous-Domain Mathematical Models for Optimal Process Plant Layout," *Industrial & Engineering Chemistry Research,* vol. 37, pp. 3631-3639, 1998/09/01 1998.

[15] M. C. Georgiadis, G. Schilling, G. E. Rotstein, and S. Macchietto, "A general programming approach for process plant layout," *Computers and Chemical Engineering,* vol. 23, pp. 823-840, 1999.

[16] D. I. Patsiatzis and L. G. Papageorgiou, "Optimal multi-floor process plant layout," *Computers and Chemical Engineering,* vol. 26, pp. 575-583, 2002.

[17] K. Park, J. Koo, D. Shin, C. Lee, and E. Yoon, "Optimal multi-floor plant layout with consideration of safety distance based on mathematical programming and modified consequence analysis," *Korean Journal of Chemical Engineering,* vol. 28, pp. 1009-1018, 2011.

[18] N. K. Ku, J. H. Hwang, J. C. Lee, M. I. Roh, and K. Y. Lee, "Optimal module layout for a generic offshore LNG liquefaction process of LNG-FPSO," *Ships and Offshore Structures,* vol. 9, pp. 311-332, 2013.

[19] S. Jung, D. Ng, C. Diaz-Ovalle, R. Vazquez-Roman, and M. S. Mannan, "New Approach To Optimizing the Facility Siting and Layout for Fire and Explosion Scenarios," *Industrial & Engineering Chemistry Research,* vol. 50, pp. 3928-3937, 2011/04/06 2011.

[20] S. Jung, D. Ng, J. Lee, R. Vazquez-Roman, and M. S. Mannan, "An approach for risk reduction (methodology) based upon optimizing the facility layout and siting in toxic gas release scenarios," *Journal of Loss Prevention in the Process Industries,* vol. 23, pp. 139-148, 2010.

[21] S. Jung, D. Ng, C. D. Laird, and M. S. Mannan, "A New Approach for Facility Siting using Mapping Risks on a Plant Grid Area and Optimization," *Journal of Loss Prevention in the Process Industries,* vol. 23, pp. 824-830, 2010.

[22] R. Vazquez-Roman, J. H. Lee, S. Jung, and M. S. Mannan, "Designing plant layouts with toxic releases based on wind statistics," presented at the IASTED: International Conference on Modelling and Simulation, Quebec, Canada, 2008.

[23] I. E. Grossman and S. Lee, "Generalized Convex Disjunctive Programming: Nolinear Convex Hull Relaxation," *Computational Optimization and Applications,* vol. 26, pp. 83-100, 2003.

[24] M. C. Georgiadis and S. Macchietto, "Layout of Process Plants: A Novel Approach," *Computers and Chemical Engineering,* vol. 21, pp. S337-S342, 1997.

[25] C. Diaz-Ovalle, R. Vazquez-Roman, and M. S. Mannan, "An approach to solve the facility layout problem based on the worst-case scenario," *Journal of Loss Prevention in the Process Industries,* vol. 23, pp. 385-392, 2010.

[26] N. K. Ku, J. C. Lee, J. H. Hwang, M. I. Roh, and K. Y. Lee, "Multi-floor layout for the liquefaction process systems of LNG FPSO using the Optimization Technique," *J Soc Naval Architects Korea,* vol. 49, pp. 68-78, 2012.

[27] American Petroleum Institute, "Recommended Practice for Development of a Safety and Environmental Management Program for Offshore Operations and Facilities," vol. RP 75, ed: API, 2004.

[28] American Petroleum Institute, "Recommended Practice for Design and Hazards Analysis for Offshore Production Facilities," vol. 14J, ed, 2001.

[29] TNO, "Methods for the Calculation of Physical Effects due to Releases of Hazardous Materials (Liquids and Gases)," vol. PGS2, ed, 2005.

[30] K. G. Kinsella, "A rapid assessment methodology for the prediction of vapour cloud explosion overpressure," presented at the International Conference and Exhibition on Safety, Health, and Loss Prevention in the Oil, Chemical, and Process Industries, Singapore, 1993.

[31] R. Pula, F. I. Khan, B. Veitch, and P. R. Amyotte, "Revised fire consequence models for offshore quantitative risk assessment," *Journal of Loss Prevention in the Process Industries,* vol. 18, pp. 443-454, 2005.

[32] D. G. DiMattia, F. I. Khan, and P. R. Amyotte, "Determination of human error probabilities for offshore platform musters," *Journal of Loss Prevention in the Process Industries,* vol. 18, pp. 488-501, 2005.

[33] *Guidelines for Fire Protection in Chemical, Petrochemical, and Hydrocarbon Processing Facilities*: CCPS, 2003.

[34] A. F. Roberts, "Thermal Radiation Hazards from Large Pool Fires and Fireballs," *Fire Safety Journal,* vol. 4, pp. 197-212, 1982.

[35] M. Moosemiller, "Development of algorithms for predicting ignition probabilities and explosion frequencies," *Journal of Loss Prevention in the Process Industries,* vol. 24, pp. 259-265, 2011.

[36] D. A. Crowl and J. F. Louvar, *Chemical Process Safety: Fundamentals with Applications,* 3rd ed. Boston, MA: Prentice Hall, 2011.

[37] N. Eisenberg, C. Lynch, and R. Breeding, "Vulnerability model: A simulation system for assessing damage resulting from marine spills, Final report," NTIS Report AD-A015-245, 1975.

[38] D. D. Drysdale and R. Sylvester-Evans, "The explosion and fire on the Piper Alpha platform, 6 July 1988. A case study," *Philosophical Transactions of the Royal Society of London. Series A: Mathematical, Physical and Engineering Sciences,* vol. 356, pp. 2929-2951, December 15, 1998 1998.

[39] R. M. M. Ali and L. A. Louca, "Performance based design of blast resistant offshore topsides, Part I: Philosophy," *Journal of Constructional Steel Research,* pp. 1030-1045, 2008.

[40] S. W. Legg, A. J. Benavides-Serrano, J. D. Siirola, J. P. Watson, S. G. Davis, A. Bratteteig, and C. D. Laird, "A stochastic programming approach for gas detector placement using CFD-based dispersion simulations," *Computers and Chemical Engineering,* pp. 194-201, 2012.

[41] A. J. Benavides-Serrano, S. W. Legg, R. Vazquez-Roman, M. S. Mannan, and C. D. Laird, "A Stochastic Programming Approach for the Optimal Placement of

Gas Detectors: Unavailability and Voting Strategies," *Industrial & Engineering Chemistry Research,* pp. 5355-5365, 2013.

[42] G. K. Schleyer, M. J. Lowak, M. A. Polcyn, and G. S. Langdon, "Experimental investigation of blast wall panels under shock pressure loading," *International Journal of Impact Engineering,* pp. 1095-1118, 2007.

[43] A. Ahmad, S. A. Hassan, A. Ripin, M. W. Ali, and S. Haron, "A risk-based method for determining passive fire protection adequcy," *Fire Safety Journal*, pp. 160-169, 2013.

[44] American Petroleum Institute, "Recommended Practice for Fire Prevention and Control on Fixed Open-type Offshore Production Platforms, 4th edition," vol. 14G, ed: API, 2007.

[45] L. A. Louca, J. W. Boh, and Y. S. Choo, "Response of profiled barriers subject to hydrocarbon explosions," *Proceedings of the Institution of Civil Engineers*, pp. 319-331, 2004.

[46] *FLACS v9.1 User's Manual*: GexCon AS, 2010.

[47] O. R. Hansen, S. G. Davis, F. Gavelli, and J. P. Richardson, "Benefits of CFD for Onshore Facilities," in *8th Global Congress on Process Safety*, Houston, TX, 2012.

[48] F. A. Gifford, "Use of Routine Meteorological Observations for Estimating Atmospheric Dispersion," *Nuclear Safety,* vol. 2, 1961.

[49] *FLACS v10.2 User's Manual*: GexCon AS, 2014.

[50] "Vulnerability of Humans," International Association of Oil and Gas Producers Report No. 434-14.1, 2010.

[51] F. P. Lees, "Lees' Loss Prevention in the Process Industries, 4th Edition," M. S. Mannan, Ed., ed, 2013.

[52] "Methods of approximation and determination of human vulnerability for offshore major hazard assessment," United Kingdom Health and Safety Executive2010.

[53] *Occupational Safety and Health Standards, Subpart I, Personal Protective Equipment,* United States Occupational Safety and Health Administration 29 CFR 1910.134, 2011.

[54] "Immediately Dangerous to Life or Health Concentrations (IDLH): Hydrogen Sulfide," National Institute for Occupational Health and Safety, Ed., ed, 1994.

[55] W. P. Yant, "Hydrogen sulfide in industry: occurrence, effects and treatment," *American Journal of Public Health,* pp. 598-608, 1930.

[56] *Guidelines for Consequence Analysis of Chemical Releases*. New York City: Center for Chemical Process Safety, 1999.

[57] Task Committee on Blast-Resistant Design of the Petrochemical Committee of the Energy Division ASCE, *Design of Blast-Resistant Buildings in Petrochemical Facilities (2nd Edition)*: American Society of Civil Engineers, 2010.

[58] R. Horst, P. M. Pardalos, and N. V. Thoai, *Introduction to Global Optimization* vol. 48. Boston, MA: Kluwer Academic Publishers, 2000.

[59] A. Brooke, D. Kendrick, A. Meeraus, R. Raman, and R. E. Rosenthal, "GAMS: A User's Guide," ed: GAMS Development Corporation, 1998.

[60] G. R. Kocis and I. E. Grossman, "Global Optimization of Nonconvex Mixed-Integer Nonlinear Programming Problems in Process Syntesis," *Industrial & Engineering Chemistry Research,* vol. 27, pp. 1407-1421, 1988.

[61] A. H. G. Rinnooy-Kan and G. T. Timmer, "Stochastic Methods for Global Optimization," *American Journal of Mathematical and Management Sciences,* vol. 4, pp. 7-40, 1984.

[62] Dow Chemical Company, "Gas Sweetening," vol. Form No. 170-01395, ed, 1998.

[63] U. Kjellen, "Safety in the design of offshore platforms: integrated safety versus safety as an add-on characteristic," *Safety Science,* vol. 45, pp. 107-127, 2007.

[64] F. P. Lees, *Loss Prevention in the Process Industries. First Edition*: Elsevier, 1980.

[65] V. Cozzani, G. Gubinelli, and E. Salzano, "Escalation thresholds in the assessment of domino accidental events," *Journal of Hazardous Materials,* vol. 129, pp. 1-21, 2006.

[66] R. M. Darbra, A. Palacios, and J. Casal, "Domino effect in chemical accidents: Main features and accident sequences," *Journal of Hazardous Materials,* vol. 183, pp. 565-573, 2010.

[67] B. Abdolhamidzadeh, T. Abbasi, D. Rashtchian, and S. A. Abbasi, "Domino effect in process-industry accidents - An inventory of past events and identification of some patterns," *Journal of Loss Prevention in the Process Industries,* vol. 24, pp. 575-593, 2011.

[68] G. A. Chamberlain, "The Hazards Posed by Large-Scale Pool Fires in Offshore Platforms," *Process Safety and Environmental Protection,* vol. 74, pp. 81-87, 1995.

[69] V. Babrauskas, "Pool fires: burning rates and heat fluxes," in *Fire Protection Handbook, 16th Edition*, A. E. Cote and J. M. Linville, Eds., ed, 1986, pp. 21-36.

[70] R. B. Corr and V. H. Y. Tam, "Gas explosion generated drag loads in offshore installations," *Journal of Loss Prevention in the Process Industries,* vol. 11, pp. 43-48, 1998.

[71] K. v. Wingerden, O. R. Hansen, and P. Foisselon, "Predicting blast overpressures caused by vapor cloud explosions in the vicinity of control rooms," *Process Safety Progress,* vol. 18, pp. 17-24, 1999.

[72] O. R. Hansen, P. Hinze, D. Engel, and S. Davis, "Using computational fluid dynamics (CFD) for blast wave predictions," *Journal of Loss Prevention in the Process Industries,* vol. 23, pp. 885-906, 2010.

[73] I. Sutton, *Offshore Safety Management - Implementing a SEMS Program*: Elsevier, 2012.

[74] J. Radianti and O. C. Granmo, "A Framework for Assessing the Condition of Crowds Exposed to a Fire Hazard Using a Probabilistic Model," *International Journal of Machine Learning and Computing,* vol. 4, pp. 14-20, 2014.

[75] T. Jin, "Visibility and human behavior in fire smoke," in *The SPFE Handbook of Fire Protection Engineering*, P. J. DiNenno, Ed., ed Quincy, Massachusetts: National Fire Protection Association, 2008.

[76] G. W. Mulholland and C. Croarkin, "Specific Extinction Coefficient of Flame Generated Smoke," *Fire and Materials*, vol. 24, pp. 227-230, 2000.

[77] T. Jin, "Visibility through Fire Smoke - Part 5, Allowable Smoke Density for Escape from Fire," Fire Research Institute of Japan,1976.

[78] K. M. Butler and G. W. Mulholland, "Generation and Transport of Smoke Components," *Fire Technology*, vol. 40, pp. 149-176, 2004.

[79] A. Tewarson, "Generation of Heat and Chemical Compounds in Fires," in *The SPFE Handbook of Fire Protection Engineering*, P. J. DiNenno, Ed., 3rd ed Quincy, Massachusetts: National Fire Protection Association, 2002.

[80] D. A. Purser, "Toxicity Assessment of Combustion Products," in *The SPFE Handbook of Fire Protection Engineering*, P. J. DiNenno, Ed., 3rd ed Quincy, Massachusetts: National Fire Protection Association, 2002.

[81] Wood Group Mustang. (August 2012) 2012 Worldwide Survey of Floating Production, Storage, and Offloading (FPSO) Units. *Offshore Magazine*.

[82] J. K. Paik and A. K. Thayamballi, "Ship-Shaped Offshore Installations - Design, Building, and Operation," ed: Cambridge University Press.

[83] Bechtel Corporation. (Accessed February 20, 2015). *Offshore Facilities*. http://www.bechtel.com/expertise/oil-gas-chemicals/offshore/facilities/

[84] P. J. Nardone, *Well Testing Project Management - Offshore and Onshore Operations*: Elsevier, 2009.

[85] O. R. Hansen, P. Hinze, D. Engel, and S. Davis, "Using CFD for Blast Wave Prediction," presented at the Mary Kay O'Connor Process Safety Center 2009 International Symposium, College Station, TX, 2009.

[86] E&P Forum, "Quantitative Risk Assessment Datasheet Directory," E&P Forum, London, UK, 1996.

[87] C. Selby and B. Burgan, "Blast and fire engineering for topside structures, Phase II: Final summary report," Steel Construction Institute, UK, 1998.

[88] A. J. Benavides-Serrano, "Mathematical Programming Formulations for the Optimal Placement of Imperfect Detectors with Applications to Flammable Gas Detection and Mitigation Systems," Doctor of Philosophy, Chemical Engineering, Texas A&M Universtiy, College Station, TX, 2014.

APPENDIX A: SAMPLE GAMS CODE FOR OFFSHORE FLP

```
*###############################################################################
*                                                                              #
* Josh Richardson                                                              #
* 25-Feb-2015                                                                  #
* Constrained FLP                                                              #
* Fire, Explosion, Toxic, Smoke All Dispersion Effects                         #
*                                                                              #
*###############################################################################

$eolcom #
$inlinecom

*###############################################################################
*Set, Scalar, and Parameter Definition#########################################
*###############################################################################

Sets
        s        sections        /       Wellhead, Quarters, Compressors, Storage,
                                         Utilities, Process, Risers, Shop        /

        m        musters         /       M1, M2, M3, M4  /

        f        floors          /       1, 2      /

        h        monitor dir     /       PosX, NegX, PosY, NegY, Top, Bottom     /;

        Alias (s,k);
        Alias (s,j);
        Alias (m,r);
        Alias (f,l);
        Alias (h,g);                                                            #h is the monitor
direction, g is the release direction

Scalars
```

```
        Wx              x-direction size of the platform                        /110/
        Wy              y-direction size of the platform                        /150/
        sep             minimum separation distance between sections            /0/
        FloorSpacing    spacing in between floors                               /20/
        N               Big M scalar for disjunction relation
        T               Big M scalar for toxic relation
        Patm            Atmospheric pressure (Pa)                               /101300/
        epsilon         A small number                                          /0.001/
        time            response time to a leak (s)                             /100/
        CD              discharge coefficient                                   /0.85/
        AmbDensity      density of ambient air [kg per m3]                      /1.2/
        ExpansionFactor Isentropic expansion factor                             /1.4/
        MWalls          Maximum number of blast walls                           /1/
        MaxPop          Maximum number of people at a muster                    /40/
        WindSpeed       Wind speed (m per s)                                    /5/
        IDLH            IDLH of interest (ppm)                                  /100/
        IDLHConc        IDLH of interest (kg per m3)
        FireM           Big M value for fire-muster exclusion interaction       /10/
        FtExposure      Time of exposure to fire (s)                            /3/
        TtExposure      Time of exposure to toxic (min)                         /3/

Parameters
        Stories(s) Number of floors a section takes up

                        /       Wellhead        2
                                Quarters        1
                                Compressors     2
                                Storage         1
                                Utilities       1
                                Process         1
                                Risers          2
                                Shop            1       /

        Area(s) Area allowed for section s

                         /      Wellhead        4950
                                Quarters        1800
                                Compressors     2376
```

```
                        Storage          825
                        Utilities        330
                        Process          900
                        Risers           150
                        Shop             1800   /

AR(s) Maximum aspect ratio between longest and shortest side

                /       Wellhead         2.5
                        Quarters         1.4
                        Compressors      1.9
                        Storage          1.4
                        Utilities        3.3
                        Process          1.5
                        Risers           6.0
                        Shop             1.4    /

SectionCost(s) A cost to put in the objective function

                /       Wellhead         5
                        Quarters         30
                        Compressors      0
                        Storage          0
                        Utilities        0
                        Process          0
                        Risers           0
                        Shop             10     /

Const(s) Explosion intercept constant

                /       Wellhead         0.35
                        Quarters         0
                        Compressors      0.12
                        Storage          0
                        Utilities        0.075
                        Process          0.12
                        Risers           0.12
                        Shop             0      /
```

```
MIE(s) Minimum ignition energy of the material in section s (mJ)

                /       Wellhead         0.28
                        Quarters         0.28
                        Compressors      0.80
                        Storage          0.28
                        Utilities        0.28
                        Process          0.28
                        Risers           0.80
                        Shop             0.28   /

AIT(s) Autoignition temperature of the material in section s (F)

                /       Wellhead         1112
                        Quarters         1112
                        Compressors      406
                        Storage          1112
                        Utilities        1112
                        Process          1112
                        Risers           406
                        Shop             1112   /

ProcessT(s) Process temperature of the material in section s (F)

                /       Wellhead         200
                        Quarters         1
                        Compressors      500
                        Storage          1
                        Utilities        200
                        Process          200
                        Risers           200
                        Shop             1      /

ProcessP(s) Process pressure of the material in section s (psig)

                /       Wellhead         1000
                        Quarters         500
```

```
                        Compressors      200
                        Storage          500
                        Utilities        100
                        Process          100
                        Risers           100
                        Shop             500    /

FR(s) Flowrate of the material in section s (lb per s)

                 /      Wellhead         225
                        Quarters         1
                        Compressors      225
                        Storage          1
                        Utilities        225
                        Process          225
                        Risers           225
                        Shop             1      /

Reactivity(s) Reactivity of the material in section s

                 /      Wellhead         1
                        Quarters         0.3
                        Compressors      1
                        Storage          0.3
                        Utilities        0.3
                        Process          0.3
                        Risers           1
                        Shop             0.3   /

GasHoC(s) Heat of Combustion of the material in section s for a gas leak [kJ per kg]

                 /      Wellhead         55700
                        Quarters         55700
                        Compressors      46800
                        Storage          55700
                        Utilities        55700
                        Process          55700
                        Risers           46800
```

```
                        Shop            55700  /

MassCloud(s) Mass of the stoichiometric vapor cloud in section s [kg]

                /       Wellhead        50
                        Quarters        0
                        Compressors     40
                        Storage         0
                        Utilities       15
                        Process         15
                        Risers          15
                        Shop            0       /

HoleD(s) Leak Diameter [in]

                /       Wellhead        1
                        Quarters        0
                        Compressors     1
                        Storage         0
                        Utilities       1
                        Process         1
                        Risers          1
                        Shop            0        /

PoolHoC(s) Heat of Combustion of the material in section s for a pool fire [kJ per kg]

                /       Wellhead        42800
                        Quarters        42800
                        Compressors     42800
                        Storage         42800
                        Utilities       42800
                        Process         42800
                        Risers          42800
                        Shop            42800     /

MassPool(s) Mass flowrate of material in pool [kg per s]

                /       Wellhead        1
```

```
                        Quarters         1
                        Compressors      1
                        Storage          1
                        Utilities        1
                        Process          1
                        Risers           1
                        Shop             1          /

LeakSource(s) Denotes whether a section is a source of fuel

                /       Wellhead         1
                        Quarters         0
                        Compressors      1
                        Storage          1
                        Utilities        0
                        Process          0
                        Risers           1
                        Shop             0           /

IgnSource(s) Denotes whether a section is a source of fuel

                /       Wellhead         1
                        Quarters         0
                        Compressors      1
                        Storage          0
                        Utilities        0
                        Process          1
                        Risers           0
                        Shop             1           /

Table te(g,h) Release in g direction and monitor in h direction (x10^-5)

                  PosX      NegX      PosY      NegY      Top       Bottom
        PosX      9.75      2.71      5.80      6.46      9.75      9.75
        NegX      3.63      7.14      5.68      6.37      3.63      3.63
        PosY      6.19      5.92      9.18      3.15      6.19      6.19
        NegY      6.19      5.92      3.15      9.18      6.19      6.19
        Top       9.75      2.71      5.80      6.46      9.75      9.75
```

Bottom	9.75	2.71	5.80	6.46	9.75	9.75 ;

Table tfi(g,h) Release in g direction and monitor in h direction (x10^-5)

	PosX	NegX	PosY	NegY	Top	Bottom
PosX	0.125	-0.298	-0.0922	-0.0971	0.125	0.125
NegX	-0.0977	-0.759	-0.602	-0.617	-0.0977	-0.0977
PosY	0.339	-0.630	-0.307	-0.0328	0.339	0.339
NegY	0.339	-0.630	-0.0328	-0.307	0.339	0.339
Top	0.125	-0.298	-0.0922	-0.0971	0.125	0.125
Bottom	0.125	-0.298	-0.0922	-0.0971	0.125	0.125 ;

Table tg(g,h) Release in g direction and monitor in h direction (x10^-5)

	PosX	NegX	PosY	NegY	Top	Bottom
PosX	-24.1	5.04	-8.92	-9.04	-24.1	-24.1
NegX	59.9	-38.2	29.0	24.6	59.9	59.9
PosY	-0.591	-13.6	-16.0	1.80	-0.591	-0.591
NegY	-0.591	-13.6	1.80	-16.0	-0.591	-0.591
Top	-24.1	5.04	-8.92	-9.04	-24.1	-24.1
Bottom	-24.1	5.04	-8.92	-9.04	-24.1	-24.1 ;

Table tac(g,h) Release in g direction and monitor in h direction (x10^-5)

	PosX	NegX	PosY	NegY	Top	Bottom
PosX	112	-50.9	32.3	29.7	112	112
NegX	-89.0	129	71.7	70.6	-89.0	-89.0
PosY	59.6	32.2	143	-49.9	59.6	59.6
NegY	59.6	32.2	-49.9	143	59.6	59.6
Top	112	-50.9	32.3	29.7	112	112
Bottom	112	-50.9	32.3	29.7	112	112 ;

Table ee(g,h) Release in g direction and monitor in h direction (x10^-5)

	PosX	NegX	PosY	NegY	Top	Bottom
PosX	9.75	2.71	5.80	6.46	9.75	9.75
NegX	3.63	7.14	5.68	6.37	3.63	3.63
PosY	6.19	5.92	9.18	3.15	6.19	6.19

```
          NegY      6.19      5.92      3.15      9.18      6.19      6.19
          Top       9.75      2.71      5.80      6.46      9.75      9.75
          Bottom    9.75      2.71      5.80      6.46      9.75      9.75      ;

      Table efi(g,h) Release in g direction and monitor in h direction (x10^-5)

                    PosX      NegX      PosY      NegY      Top       Bottom
          PosX      0.125     -0.298    -0.0922   -0.0971   0.125     0.125
          NegX      -0.0977   -0.759    -0.602    -0.617    -0.0977   -0.0977
          PosY      0.339     -0.630    -0.307    -0.0328   0.339     0.339
          NegY      0.339     -0.630    -0.0328   -0.307    0.339     0.339
          Top       0.125     -0.298    -0.0922   -0.0971   0.125     0.125
          Bottom    0.125     -0.298    -0.0922   -0.0971   0.125     0.125          ;

      Table eg(g,h) Release in g direction and monitor in h direction (x10^-5)

                    PosX      NegX      PosY      NegY      Top       Bottom
          PosX      -24.1     5.04      -8.92     -9.04     -24.1     -24.1
          NegX      59.9      -38.2     29.0      24.6      59.9      59.9
          PosY      -0.591    -13.6     -16.0     1.80      -0.591    -0.591
          NegY      -0.591    -13.6     1.80      -16.0     -0.591    -0.591
          Top       -24.1     5.04      -8.92     -9.04     -24.1     -24.1
          Bottom    -24.1     5.04      -8.92     -9.04     -24.1     -24.1        ;

      Table eac(g,h) Release in g direction and monitor in h direction (x10^-5)

                    PosX      NegX      PosY      NegY      Top       Bottom
          PosX      112       -50.9     32.3      29.7      112       112
          NegX      -89.0     129       71.7      70.6      -89.0     -89.0
          PosY      59.6      32.2      143       -49.9     59.6      59.6
          NegY      59.6      32.2      -49.9     143       59.6      59.6
          Top       112       -50.9     32.3      29.7      112       112
          Bottom    112       -50.9     32.3      29.7      112       112       ;

$onecho>a
      Table se(g,h) Release in g direction and monitor in h direction (x10^-5)

                    PosX      NegX      PosY      NegY      Top       Bottom
```

```
            PosX      9.75      2.71      5.80      6.46      9.75      0
            NegX      3.63      7.14      5.68      6.37      3.63      0
            PosY      6.19      5.92      9.18      3.15      6.19      0
            NegY      6.19      5.92      3.15      9.18      6.19      0
            Top       9.75      2.71      5.80      6.46      9.75      0
            Bottom    0         0         0         0         0         0    ;

      Table sfi(g,h) Release in g direction and monitor in h direction (x10^-5)

                      PosX      NegX      PosY      NegY      Top       Bottom
            PosX      0.125     -0.298    -0.0922   -0.0971   0.125     0
            NegX      -0.0977   -0.759    -0.602    -0.617    -0.0977   0
            PosY      0.339     -0.630    -0.307    -0.0328   0.339     0
            NegY      0.339     -0.630    -0.0328   -0.307    0.339     0
            Top       0.125     -0.298    -0.0922   -0.0971   0.125     0
            Bottom    0         0         0         0         0         0     ;

      Table sg(g,h) Release in g direction and monitor in h direction (x10^-5)

                      PosX      NegX      PosY      NegY      Top       Bottom
            PosX      -24.1     5.04      -8.92     -9.04     -24.1     0
            NegX      59.9      -38.2     29.0      24.6      59.9      0
            PosY      -0.591    -13.6     -16.0     1.80      -0.591    0
            NegY      -0.591    -13.6     1.80      -16.0     -0.591    0
            Top       -24.1     5.04      -8.92     -9.04     -24.1     0
            Bottom    0         0         0         0         0         0    ;

      Table sac(g,h) Release in g direction and monitor in h direction (x10^-5)

                      PosX      NegX      PosY      NegY      Top       Bottom
            PosX      112       -50.9     32.3      29.7      112       0
            NegX      -89.0     129       71.7      70.6      -89.0     0
            PosY      59.6      32.2      143       -49.9     59.6      0
            NegY      59.6      32.2      -49.9     143       59.6      0
            Top       112       -50.9     32.3      29.7      112       0
            Bottom    0         0         0         0         0         0    ;
$offecho
```

```
Parameters
         se(h)
                  /       PosX            9.75
                          NegX            3.63
                          PosY            6.19
                          NegY            6.19
                          Top             9.75
                          Bottom          9.75         /

         sfi(h)
                  /       PosX            0.125
                          NegX            -0.0977
                          PosY            0.339
                          NegY            0.339
                          Top             0.125
                          Bottom          0.125        /

         sg(h)
                  /       PosX            -24.1
                          NegX            59.9
                          PosY            -0.591
                          NegY            -0.591
                          Top             -24.1
                          Bottom          -24.1        /

         sac(h)
                  /       PosX            112
                          NegX            -89.0
                          PosY            59.6
                          NegY            59.6
                          Top             112
                          Bottom          112          /


        UBx(s)                            Upper bound for the length of section s in the x direction
        LBx(s)                            Lower bound for the length of section s in the x direction
        UBy(s)                            Upper bound for the length of section s in the y direction
        LBy(s)                            Lower bound for the length of section s in the y direction
```

```
        ImmIgnFactor(s)             Determination of T-AIT factor
        DelIgnFactor(s)             Scaling factor for delayed ignition
        PImmIgn(s)                  Probability of immediate ignition
        PDelIgn(s)                  Probability of delayed ignition
        PExp(s)                     Probability of an explosion given delayed ignition
        TotalPExp(s)                Total probability of an explosion event
        TotalPFire(s)               Total probability of a fire event
        TotalPEnv(s)                Total probability of an environmental event
        FireballE(s)                Total energy available for fireball event [J]
        E(s)                        Total energy available for vapor cloud event [kJ]
        FireballSize(s)             Size of fireball in section s [ft]
        FireballDuration(s)         Duration of Fireball [s]
        LeakA(s)                    Leak Area [m2]
        JetFireMassFlow(s)          Mass released for jet fire [kg per s]
        JetFireQ(s)                 Heat released for jet fire [kW]
        JetFireL(s)                 Length of jet fire flame [m]
        MassBurning(s)              Mass burning rate [kg per s m2]
        PoolD(s)                    Pool diameter [m]
        PoolFireQ(s)                Heat released from pool fire [kW]
        PoolFireH(s)                Pool fire height [m]
        PoolFireE(s)                Pool fire emission [kW]
        TotalArea                   Total area of the platform
        AreaRatio                   Ratio of occupied area to total area of platform
        Qk(s)                       Unused
        LFLVol                      Lower flammability fraction by volume
        FlammableDensity            Density of flammable gas in [kg per m3]
        LFLMass                     Lower flammability fraction by mass
        MassFracFlam                Mass fraction of flammable material in jet fire
        MassFracToxic               Mass fraction of toxic material in jet fire
        FireScale                   Scaling factor for heat radiation (facilitates solution of
model)
        Eexp(s)                     Explosion energy [J]
        random(s)                   Random number
        Ustar(s)                    Scaled wind speed
        FlameAngle(s)               Pool fire angle
        xprime(s)                   Height modification of fire radiation
        MaxWalls                    Maximum number of walls available;
```

```
**General Parameters and Scalars
        UBx(s) = min((Area(s)*AR(s))**(1/2), Wx);
        UBy(s) = min((Area(s)*AR(s))**(1/2), Wy);
        LBx(s) = Area(s)/UBx(s);
        LBy(s) = Area(s)/UBy(s);
        N = max(Wx,Wy);
        T = 100;
        TotalArea = sum(s,Stories(s)*Area(s));
        AreaRatio = TotalArea/(Wx*Wy)/card(f);

**Fireball Parameters
        FireScale = 10000;
        FireballE(s) = GasHoC(s)*MassCloud(s)/FireScale;                        #kJ of available
energy
        FireballSize(s) = (5.8*MassCloud(s)**(1/3))/0.3048;
        FireballDuration(s) = 0.45*MassCloud(s)**(1/3);

**Jet Fire Parameters
        LeakA(s) = 3.14*(HoleD(s)*0.3048/12/2)**2;
        JetFireMassFlow(s) =
CD*LeakA(s)*sqrt((2*(ProcessP(s)*101325/14.7)/AmbDensity)*(ExpansionFactor/(ExpansionFactor-1))*(1-
(Patm/(ProcessP(s)*101325/14.7))**((ExpansionFactor-1)/ExpansionFactor)));
        JetFireQ(s) = JetFireMassFlow(s)*GasHoC(s)/FireScale;                   #kJ of available
energy
        JetFireL(s) = 0.2*JetFireQ(s)**0.4;

**Pool Fire Parameters
        MassBurning(s) = 0.05;
        PoolD(s) = ((4*MassPool(s))/(3.14*MassBurning(s)))**(1/2);
        PoolFireQ(s) = PoolHoC(s)*((0.5*PoolD(s))**2)*3.14*MassBurning(s)/FireScale;
        PoolFireH(s) = 0.23*(PoolFireQ(s)*FireScale)**(2/5)-1.02*PoolD(s);
        PoolFireE(s) = (58*(10**(-0.00823*PoolD(s))))*(MassPool(s)/(MassPool(s)+epsilon));
        FlammableDensity = 0.6;
        Ustar(s)$(LeakSource(s) ne 0) =
max(1,(WindSpeed/((9.81*MassBurning(s)*PoolD(s)/FlammableDensity)**(1/3))));
```

```
        FlameAngle(s)$(LeakSource(s) ne 0) = (pi/2) - arctan((1/sqrt(Ustar(s)))/(sqrt(1-
((1/sqrt(Ustar(s)))*(1/sqrt(Ustar(s)))))+0.0001));  #arccos found using arccos(y) = pi/2 -
arctan(y/sqrt(1-y*y)), y in (-1,1)
        xprime(s) = 0;
        xprime(s)$(PoolFireE(s) gt max(JetFireQ(s),FireballE(s))) = FloorSpacing/(sin(pi/2-
FlameAngle(s))/cos(pi/2-FlameAngle(s)));

**Fire Overall Parameters
        E(s) = max(FireballE(s),PoolFireE(s),JetFireQ(s));

**Explosion Parameters
        Eexp(s) = FireballE(s)*1000;                                          #J of available
energy

**Dispersed Vapor Cloud Explosion Parameters
        LFLVol = 0.05;
        LFLMass = LFLVol*(AmbDensity/FlammableDensity);
        MassFracFlam = 0.95;

**Dispersed Toxic Parameters
        Qk(s) = (JetFireMassFlow(s)+uniform(0.1,0.2))/2.25;
        IDLHConc = (IDLH/1000000)*AmbDensity;
        MassFracToxic = 1-MassFracFlam;

**Probability Parameters
        ImmIgnFactor(s) = ProcessT(s)/AIT(s);
        DelIgnFactor(s) = (0.6-log10(MIE(s)))*(7*exp(0.642*log(FR(s))-4.67))*(1-(1-
LeakSource(s))*exp(-0.015*LeakSource(s)*time));
        PImmIgn(s)$(ImmIgnFactor(s) < 0.9) = 0;
        PImmIgn(s)$(ImmIgnFactor(s) > 1.2) = 1;
        PImmIgn(s)$(ImmIgnFactor(s) > 0.9 and ImmIgnFactor(s) < 1.2) = (1-5000*exp(-
9.5*ImmIgnFactor(s)))+((0.0024*ProcessP(s)**(1/3))/(MIE(s)**(2/3)));
        PDelIgn(s)$(DelIgnFactor(s) > 1) = 1-(0.7/DelIgnFactor(s));
        PDelIgn(s)$(DelIgnFactor(s) < 1) = 0.3*DelIgnFactor(s);
        PExp(s) = Reactivity(s)*0.024*(FR(s)**0.435);
        TotalPExp(s) = PExp(s)*PDelIgn(s)*(1-PImmIgn(s));
        TotalPFire(s) = PImmIgn(s)+((1-PExp(s))*(PDelIgn(s))*(1-PImmIgn(s)));
        TotalPEnv(s) = (1-PDelIgn(s))*(1-PImmIgn(s));
```

```
**Wall Parameters
        MaxWalls = MWalls;

**Random number
        random(s) = uniform(0.1,0.2);


*#############################################################################
*Variables####################################################################
*#############################################################################


Variables
**Variable declaration_____________________________________________________
***Midpoint and side length
        x(s)                            midpoint in x-direction of section s
        y(s)                            midpoint in y-direction of section s
        Lx(s)                           length in x-direction of section s [ft]
        Ly(s)                           length in y-direction of section s [ft]

***Muster variables
        mx(m)                           x-coordinate of muster point m
        my(m)                           y-coordinate of muster point m
        ex1(s,m)                        half muster x-coordinate for s
        ex2(s,m)                        muster x-coordinate for s
        ey1(s,m)                        half muster y-coordinate for s
        ey2(s,m)                        muster y-coordinate for s
        ma(m)                           binary variable for muster point on left edge of platform
        mb(m)                           binary variable for muster point on right edge of platform
        mc(m)                           binary variable for muster point on bottom edge of platform
        md(m)                           binary variable for muster point on top edge of platform
        SectionMuster(s,m)              binary variable for section s assigned to muster m

***Floor variables
        NF                              number of floors
        Floor(s)                        floor that section s is assigned to
        FO(f)                           binary variable defining whether floor f is occupied
```

```
        V(s,f)                          binary variable for section assignment to floor
        ZZ(s,k,f)                       binary variable for sections s and k allocated to the same
floor

***Non-overlap variables
        a(s,k,f)                        binary variable for non-overlap constraint left
        b(s,k,f)                        binary variable for non-overlap constraint right
        c(s,k,f)                        binary variable for non-overlap constraint below
        d(s,k,f)                        binary variable for non-overlap constraint above
        upstar(s,k,f,l)                 intermediate binary variable to determine non-overlap
constraint up
        downstar(s,k,f,l)               intermediate binary variable to determine non-overlap
constraint down
        up(s,k,f)                       binary variable for non-overlap constraint up floor
        down(s,k,f)                     binary variable for non-overlap constraint down floor
        Dx(s,k)                         minimum separation distance between sections s and k in the
x-direction
        Dy(s,k)                         minimum separation distance between sections s and k in the
y-direction

***Blast wall variables
        wa(s)                           blast wall right of section s
        wb(s)                           blast wall left of section s
        wc(s)                           blast wall above section s
        wd(s)                           blast wall below section s
        BWa(s,k)                        blast from k affected by blast wall on s
        BWb(s,k)                        blast from k affected by blast wall on s
        BWc(s,k)                        blast from k affected by blast wall on s
        BWd(s,k)                        blast from k affected by blast wall on s
        BW(s,k)                         blast from k affected by blast wall on s

***Explosion variables
        P(s,k)                          overpressure on s due to an explosion in k
        EProbit(s,k)                    probit value of s due to an explosion in k
        DestructionProbability(s,k)     calculated probability of destruction
        MitigatedProb(s,k)              mitigated probability of destruction for section s after
considering mitigation
```

```
        eSD(s,h)                          scaled dispersion to the h direction of s on floor f due to
a release in direction g
        dispE(s,k,h)                      dispersed energy in section s lying in monitor region h due
to a release in section k in the g direction
        cprime(s,k,j,h)                   base overpressure from s due to a dispersion from k
        LFLExceed(s,h)                    binary to denote whether the LFL is exceeded in region h by
a release by s

***Fire variables
        I1(s,k,m)                         Top route fire intensity
        I2(s,k,m)                         Bottom route fire intensity
        I3(s,k,m)                         Middle route fire intensity
        I4(s,k)                           Midpoint fire intensity
        I5(s,k,m)                         Radiation at muster point
        I(s,k,m)                          fire intensity of the escape path between s and m due to a
fire in k
        FProbit(s,k,m)                    probit value of the escape path from s to m due to a fire in
k
        FProbitEscape(s,k,m)              probit value of the escape path from s to m due to a fire in
k
        FProbitMidpoint(s,k)              probit value of the section s due to a fire in k
        FProbitMuster(s,k,m)              probit value of the muster point m section s is assigned to
due to a fire in k
        Fa(s,m)                           determines escape path
        Fb(s,m)                           determines escape path
        Fc(s,m)                           determines escape path
        EscapeProbability(s,k,m)          calculated probability of escape blockage
        EscapeProbabilityMidpoint(s,k,m)  calculated probability of escape blockage

***Toxic variables
        BR(s,f,h)                         blockage ratio to the h direction of s on floor f
        tSD(s,f,g,h)                      scaled dispersion to the h direction of s on floor f due to
a release in direction g
        ToxicProbit(s,k,f,g,h)            probit value of a g-direction release in k on floor f
causing toxic effect in section s to the h direction of k
        ToxicProbability(s,k)             calculated probability of toxic effect from a release in k
on s
```

```
***Smoke variables
        sSD(s,f,h)                      scaled dispersion to the h direction of s on floor f due to
a release in direction g
        vesc(s)                         escape speed from section s
        tesc(s,m)                       escape time from section s to muster point m
        tincCO(s)                       time to incapacitation by carbon monoxide
        tincCO2(s)                      time to incapacitation by carbon dioxide
        Incap(s,m)                      whether incapacitation is likely to occur between section s
and muster point m

***Objective
        Prob                            cost to be minimized for FLP;


**Variable definition_____________________________________________________________
***Midpoint and side length
        positive variable x;
        positive variable y;
        positive variable Lx;
        positive variable Ly;

***Muster variables
        positive variable mx;
        positive variable my;
        positive variable ex1;
        positive variable ex2;
        positive variable ey1;
        positive variable ey2;
        binary variable ma;
        binary variable mb;
        binary variable mc;
        binary variable md;
        binary variable SectionMuster;

***Floor variables
        positive variable Floor;
        integer variable NF;
        integer variable TotalFloors;
```

```
        binary variable V;
        binary variable ZZ;
        binary variable FO;

***Non-overlap variables
        binary variable a;
        binary variable b;
        binary variable c;
        binary variable d;
        binary variable up;
        binary variable upstar;
        binary variable downstar;
        binary variable down;
        positive variable Dx;
        positive variable Dy;

***Blast wall variables
        binary variable wa;
        binary variable wb;
        binary variable wc;
        binary variable wd;
        binary variable BWa;
        binary variable BWb;
        binary variable BWc;
        binary variable BWd;
        integer variable BW;

***Explosion variables
        positive variable P;
        variable EProbit;
        positive variable DestructionProbability;
        positive variable MitigatedProb;
        positive variable eSD;
        positive variable dispE;
        positive variable cprime;
        binary variable LFLExceed;

***Fire variables
```

```
        binary variable Fa;
        binary variable Fb;
        binary variable Fc;
        positive variable I1;
        positive variable I2;
        positive variable I3;
        positive variable I4;
        positive variable I5;
        positive variable I;
        variable FProbitEscape;
        variable FProbitMidpoint;
        variable FProbitMuster;
        positive variable EscapeProbability;
        positive variable EscapeProbabilityEscape;
        positive variable EscapeProbabilityMidpoint;

***Toxic variables
        positive variable Conc;
        positive variable BR;
        positive variable tSD;
        variable ToxicProbit;
        positive variable ToxicProbability;

***Smoke variables
        positive variable sSD;
        positive variable vesc;
        positive variable tesc;
        positive variable tincCO;
        positive variable tincCO2;
        binary variable Incap;



*#########################################################################
*Variable Initial Values and Bounds#####################################
*#########################################################################

**Essential Fixed Variables_____________________________________________
```

```
***Muster Points fixed to sides
*$onecho>a
ma.fx('M1') = 1;
mb.fx('M2') = 1;
mc.fx('M3') = 1;
md.fx('M4') = 1;
mx.fx('M1') = 0;
mx.fx('M2') = Wx;
my.fx('M3') = 0;
my.fx('M4') = Wy;
my.lo('M1') = 0;
my.up('M1') = Wy;
my.lo('M2') = 0;
my.up('M2') = Wy;
mx.lo('M3') = 0;
mx.up('M3') = Wx;
mx.lo('M4') = 0;
mx.up('M4') = Wx;
*$offecho

*$onecho > a
**Fixed Variables and Strict Limits_____________________________________________

***Midpoints
x.lo(s) = 0;
x.up(s) = Wx;
y.lo(s) = 0;
y.up(s) = Wy;

***Section length less than length of platform
Lx.lo(s) = 0;
Lx.up(s) = Wx;
Ly.lo(s) = 0;
Ly.up(s) = Wy;

***Exclusion length less than length of platform
Dx.lo(s,k) = 0;
```

```
Dx.up(s,k) = Wx;
Dy.lo(s,k) = 0;
Dy.up(s,k) = Wy;

***Escape Radiation Points
ex1.lo(s,m) = 0;
ex1.up(s,m) = Wx;
ex2.lo(s,m) = 0;
ex2.up(s,m) = Wx;
ey1.lo(s,m) = 0;
ey1.up(s,m) = Wy;
ey2.lo(s,m) = 0;
ey2.up(s,m) = Wy;

***Disjunction Relation Constraints
a.fx(s,s,f) = 0;
b.fx(s,s,f) = 0;
c.fx(s,s,f) = 0;
d.fx(s,s,f) = 0;
up.fx(s,s,f) = 0;
up.l(s,k,f) = 0;
upstar.fx(s,s,f,l) = 0;
upstar.fx(s,k,f,f) = 0;
*upstar.fx(s,k,f,l)$(ord(f) lt ord(l)) = 0;
down.fx(s,s,f) = 0;
down.l(s,k,f) = 0;

***Floor Constraints
NF.lo = 1;
NF.up = card(f);
Floor.lo(s) = 1;
Floor.up(s) = card(f);
ZZ.fx(s,s,f) = 0;

***Blast Walls
BW.up(s,k) = 1;

***Explosion
```

```
****Explosion Effect
P.lo(s,k) = 0;
P.fx(s,s) = 0;

****Explosion Probit
EProbit.lo(s,k) = -100;
EProbit.up(s,k) = 100;

****Explosion Probability
DestructionProbability.fx(s,s) = 0;
DestructionProbability.lo(s,k) = 0;
eSD.lo(s,h) = 0;
eSD.up(s,h) = 1;
cprime.up(s,k,j,h) = 1000000;
LFLExceed.lo(s,h) = 0;
LFLExceed.up(s,h) = 1;

****Mitigated Probability
MitigatedProb.fx(s,s) = 0;
MitigatedProb.lo(s,k) = 0;

****Dispersed Cloud
DispE.lo(s,k,h) = 0;
DispE.up(s,k,h) = 1000000;

***Fire
****Fire Effect
I1.fx(s,s,m) = 0;
I2.fx(s,s,m) = 0;
I3.fx(s,s,m) = 0;
I4.fx(s,s) = 0;
I5.fx(s,s,m) = 0;
I.fx(s,s,m) = 0;
I.up(s,k,m) = 10;
I1.up(s,k,m) = 10;
I2.up(s,k,m) = 10;
I3.up(s,k,m) = 10;
I4.up(s,k) = 10;
```

```
I5.up(s,k,m) = 10;

****Fire Probit
FProbit.lo(s,k,m) = -1000;
FProbit.up(s,k,m) = 1000;
FProbitEscape.lo(s,k,m) = -1000;
FProbitEscape.up(s,k,m) = 1000;
FProbitMidpoint.lo(s,k) = -1000;
FProbitMidpoint.up(s,k) = 1000;

****Escape Probability
EscapeProbability.fx(s,s,m) = 0;
EscapeProbability.lo(s,k,m) = 0;
EscapeProbability.up(s,k,m) = 4;

****Muster Constraints
Fa.lo(s,m) = 0;
Fb.lo(s,m) = 0;
Fc.lo(s,m) = 0;

***Toxic
****Blockage Ratio
BR.lo(s,f,h) = 0;
BR.up(s,f,h) = 2;

****Toxic Effect (Scaled Dispersion)
tSD.lo(s,f,g,h) = 0;
tSD.up(s,f,g,h) = 4;

****Toxic Probit
ToxicProbit.lo(s,k,f,g,h) = -200;
ToxicProbit.up(s,k,f,g,h) = 200;

****Toxic Probability
ToxicProbability.fx(s,s) = 0;
ToxicProbability.lo(s,k) = 0;
ToxicProbability.up(s,k) = 10;
```

```
***Smoke
sSD.lo(s,f,h) = 0;
sSD.up(s,f,h) = 1;
vesc.lo(s) = 0.3;
vesc.up(s) = 1000;
tesc.lo(s,m) = 0;
tesc.up(s,m) = 1000;
tincCO.lo(s) = 0;
tincCO.up(s) = 1000000;
tincCO2.lo(s) = 0;
tincCO2.up(s) = 10000000;
Incap.lo(s,m) = 0;
Incap.up(s,m) = 1;

*$offecho

**Fixes Sections_____________________________________________________________

$onecho > a
x.fx('Wellhead') = 33.81941804;
x.fx('Quarters') = 23.9696637;
x.fx('Compressors') = 88.81941804;
x.fx('Storage') = 16.97781598;
x.fx('Utilities') = 105;
x.fx('Process') = 97.75255129;
x.fx('Risers') = 107.5;
x.fx('Shop') = 23.88984567;
y.fx('Wellhead') = 113.4085957;
y.fx('Quarters') = 18.77373023;
y.fx('Compressors') = 121.9554448;
y.fx('Storage') = 51.05268945;
y.fx('Utilities') = 77.41088961;
y.fx('Process') = 75.53971653;
y.fx('Risers') = 15;
y.fx('Shop') = 18.83645488;
Lx.fx('Wellhead') = 67.63883607;
Lx.fx('Quarters') = 47.93932739;
Lx.fx('Compressors') = 42.36116393;
```

```
Lx.fx('Storage') = 33.95563196;
Lx.fx('Utilities') = 10;
Lx.fx('Process') = 24.49489743;
Lx.fx('Risers') = 5;
Lx.fx('Shop') = 47.77969133;
Ly.fx('Wellhead') = 73.18280869;
Ly.fx('Quarters') = 37.54746047;
Ly.fx('Compressors') = 56.08911039;
Ly.fx('Storage') = 24.2964113;
Ly.fx('Utilities') = 33;
Ly.fx('Process') = 36.74234614;
Ly.fx('Risers') = 30;
Ly.fx('Shop') = 37.67290976;
$offecho

$onecho > a
Lx.fx('Wellhead') = 110;
Ly.fx('Wellhead') = 45;
x.fx('Wellhead') = 55;
y.fx('Wellhead') = 88.5;
Lx.fx('Quarters') = 50;
Ly.fx('Quarters') = 36;
x.fx('Quarters') = 55;
y.fx('Quarters') = 132;
Lx.fx('Compressors') = 36;
Ly.fx('Compressors') = 66;
x.fx('Compressors') = 18;
y.fx('Compressors') = 33;
Lx.fx('Storage') = 25;
Ly.fx('Storage') = 33;
x.fx('Storage') = 67.5;
y.fx('Storage') = 16.5;
Lx.fx('Utilities') = 10;
Ly.fx('Utilities') = 33;
x.fx('Utilities') = 105;
y.fx('Utilities') = 16.5;
Lx.fx('Process') = 36;
Ly.fx('Process') = 25;
```

```
x.fx('Process') = 67.5;
y.fx('Process') = 53;
Lx.fx('Risers') = 5;
Ly.fx('Risers') = 30;
x.fx('Risers') = 95;
y.fx('Risers') = 15;
Lx.fx('Shop') = 50;
Ly.fx('Shop') = 36;
x.fx('Shop') = 55;
y.fx('Shop') = 132;

V.fx('Wellhead','1') = 1;
V.fx('Wellhead','2') = 1;
V.fx('Quarters','1') = 0;
V.fx('Quarters','2') = 1;
V.fx('Compressors','1') = 1;
V.fx('Compressors','2') = 1;
V.fx('Storage','1') = 1;
V.fx('Storage','2') = 0;
V.fx('Utilities','1') = 1;
V.fx('Utilities','2') = 0;
V.fx('Process','1') = 1;
V.fx('Process','2') = 0;
V.fx('Risers','1') = 1;
V.fx('Risers','2') = 1;
V.fx('Shop','1') = 1;
V.fx('Shop','2') = 0;
$offecho

*#############################################################################
*Equation Initialization#####################################################
*#############################################################################

Equations
**Area, AR, and Side Length Equations_____________________________________________
        AreaConstraint(s)                       constrains the side lengths of section s to fit the
area parameter
```

```
        LengthConstraintXLo(s)                  constrains the length of the x side to be within
lower aspect ratio limits
        LengthConstraintXHi(s)                  constrains the length of the x side to be within
upper aspect ratio limits
        LengthConstraintYLo(s)                  constrains the length of the y side to be within
lower aspect ratio limits
        LengthConstraintYHi(s)                  constrains the length of the y side to be within
upper aspect ratio limits

**Separation Distance_____________________________________________________
        DefineDx(s,k)                           defines Dx of section s
        DefineDy(s,k)                           defines Dy of section s

**Boundary Constraints___________________________________________________
        BoundaryX1(s)                           constrains the sections to be within the lower x
boundary of the platform
        BoundaryX2(s)                           constrains the sections to be within the upper x
boundary of the platform
        BoundaryY1(s)                           constrains the sections to be within the lower y
boundary of the platform
        BoundaryY2(s)                           constrains the sections to be within the upper y
boundary of the platform

**Non-Overlap Constraints________________________________________________
        LeftConstraint(s,k,f)                   non-overlapping constraint bounds section s to the
left of section k
        RightConstraint(s,k,f)                  non-overlapping constraint bounds section s to the
right of section k
        BelowConstraint(s,k,f)                  non-overlapping constraint bounds section s to be
below section k
        AboveConstraint(s,k,f)                  non-overlapping constraint bounds section s to be
above section k
        DisjunctionCheck1(s,k,f)                if a is left of b then b must be right of a and
vice-versa
        DisjunctionCheck2(s,k,f)                if a is above b then b must be below a and vice-
versa

*Decision Variables to Select Non-Overlap Constraint_____________________
```

```
        DecisionConstraint(s,k,f)               decides which non-overlapping constraint to use
        DecisionConstraint2(s,k)                makes sure that ZZ is only defined for stories that
s and k occupy
        DecisionConstraint3(s,k,f)              makes sure that ZZ is equal for both s and k on a
certain floor

**Muster Point Constraints_____________________________________________________
        MusterAssign(s)                         assigns one muster to a section
        EscapeX1(s,m)                           defines ex1 - a point of fire impact on escape
        EscapeY1(s,m)                           defines ey1 - a point of fire impact on escape
        EscapeX2(s,m)                           defines ex2 - a point of fire impact on escape
        EscapeY2(s,m)                           defines ey2 - a point of fire impact on escape
        MusterLimit(m)                          assigns at most two sections to one muster

**Blast Wall Constraints_______________________________________________________
        BlastWallA(s,k)                         Defines BW (whether blast wall s affects blast from
k)
        BlastWallB(s,k)                         Defines BW (whether blast wall s affects blast from
k)
        BlastWallC(s,k)                         Defines BW (whether blast wall s affects blast from
k)
        BlastWallD(s,k)                         Defines BW (whether blast wall s affects blast from
k)
        BlastWall(s,k)                          Defines BW (whether blast wall s affects blast from
k)
        MaxBlastWalls                           Defines maximum number of blast walls

**Floor Constraints____________________________________________________________
        OneFloor(s)                             assigns a section to only one floor
        FloorConstraint1(s,k,f)                 defines ZZ (sections s and k allocated to same
floor)
        FloorConstraint2(s,k,f)                 defines ZZ (sections s and k allocated to same
floor)
        FloorConstraint3(s,k,f)                 defines ZZ (sections s and k allocated to same
floor)
        FloorOccupied1(f)                       defines FO (1 if floor occupied 0 if not)
        FloorOccupied2(s,f)                     defines FO (1 if floor occupied 0 if not)
```

```
        FloorOrder(f,l)                         floor f must be occupied before any floors above it
can be occupied
        NumberOfFloors(f)                       defines NF - the number of floors in the platform
        NumberOfFloors2                         defines NF - the number of floors in the platform
        FloorNumber(s)                          defines Floor - the effective floor number of
section s
        FloorAdjacent(f,l,s)                    Forces floors to be adjacent for a multi-story
section
*$onecho>a
        RelativeFloor1(s,k,f,l)                 Defines up*
        RelativeFloor2(s,k,f,l)                 Defines up*
        RelativeFloor3(s,k,f,l)                 Defines up*
        RelativeFloor4(s,k,f,l)                 Defines up
        RelativeFloor5(s,k,f,l)                 Defines up
        RelativeFloor6(s,k,f,l)                 Defines down
        RelativeFloor7(s,k,f,l)                 a
        RelativeFloor8(s,k,f)                   a
        RelativeFloor9(s,k,f,l)                 Defines down
        RelativeFloor10(s,k,f,l)                 a
        RelativeFloor11(s,k,f)                   a
*$offecho

**Explosion_____________________________________________________________________
***Explosion Effect
        ExpPressure(s,k)                        Determines pressure from explosion in s on k

**Explosion Probit
        ExpProbit(s,k)                          Determines probit value of explosion overpressure

**Explosion Probability
        DestProbability(s,k)                    Determines the probability of destruction of s due
to explosion in k
        ModifiedProbability(s,k)                Defines the mitigated probability after blast walls
intergrated

**Dispersed Cloud Explosion
        eScaledDispersion(s,f,g,h)              Defines the mass fraction of flammable material in
monitor region h due to a g-direction release in s on floor f
```

```
        DispersedEnergy(s,k,f,h)                Defines the amount of energy available for a
dispersed cloud explosion
        DispersedBase(s,k,j,h)                  Defines the base pressure of a dispersed cloud
explosion
        LFLExceedance(s,k,h)                    Determines whether the LFL is exceeded in the
potential explosion domain

*$onecho>a
        DispersedEProbitPosX(s,k,j,f,h)         Determines the probit value for a dispersed cloud in
the positive x monitor region
        DispersedEProbitNegX(s,k,j,f,h)         Determines the probit value for a dispersed cloud in
the negative x monitor region
        DispersedEProbitPosY(s,k,j,f,h)         Determines the probit value for a dispersed cloud in
the positive y monitor region
        DispersedEProbitNegY(s,k,j,f,h)         Determines the probit value for a dispersed cloud in
the negative y monitor region
        DispersedEProbitTop(s,k,j,f,h)          Determines the probit value for a dispersed cloud in
the top monitor region
        DispersedEProbitBottom(s,k,j,f,h)       Determines the probit value for a dispersed cloud in
the bottom monitor region
*$offecho

**Fire_____________________________________________________________________________
***Fire Intensity Equations
        FireIntensity1(s,k,m)                   Determines flash fire intensity from fire in k on
key escape points
        FireIntensity2(s,k,m)                   Determines flash fire intensity from fire in k on
key escape points
        FireIntensity3(s,k,m)                   Determines flash fire intensity from fire in k on
key escape points
        FireIntensity4(s,k,m)                   Determines flash fire intensity from fire in k on
key escape points
        FireIntensity5(s,k,m)                   Determines flash fire intensity from fire in k on
key escape points
        FireIntensity6(s,k,m)                   Determines flash fire intensity from fire in k on
key escape points
        FireIntensity7(s,k,m)                   Determines flash fire intensity from fire in k on
key escape points
```

```
        FireIntensity8(s,k)                     Determines flash fire intensity from fire in k on
key escape points
        FireIntensity9(s,k,m)                   Determines flash fire intensity from fire in k on
key escape points

***Escape Path Equations
        PathChoice(s,k,m)                       Determines escape path
        PathConstraint(s,m)                     Constrains escape path

***Fire Probit
        FireProbitEscape(s,k,m)                 Determines probit value of fire
        FireProbitMuster(s,k,m)                 Determines probit value of fire
        FireProbitMidpoint(s,k)                 Determines probit value of fire

***Fire Probability
        EscProbability(s,k,m)                   Determines the probability of failure of escape from
s to m

**Toxic_____________________________________________________________________
***Blockage
        LeftBlockage(s,f)                       Defines blockage ratio BR to the left of s on floor
f
        RightBlockage(s,f)                      Defines blockage ratio BR to the right of s on floor
f
        BelowBlockage(s,f)                      Defines blockage ratio BR above on floor f
        AboveBlockage(s,f)                      Defines blockage ratio BR below s on floor f
        UpBlockage(s,f)                         Defines blockage ratio BR on top of s on floor f
        DownBlockage(s,f)                       Defines blockage ratio BR under s on floor f

***Scaled Dispersion
        tScaledDispersion(s,f,g,h)              Defines the mass fraction of toxic material in
monitor region h due to a g-direction release in s on floor f

***Toxic Probit
        RightToxicProbit(s,k,f,g)               Defines the toxic probit of section k due to a g-
direction release on floor f from section s in the positive-x monitor direction
        LeftToxicProbit(s,k,f,g)                Defines the toxic probit of section k due to a g-
direction release on floor f from section s in the negative-x monitor direction
```

```
        AboveToxicProbit(s,k,f,g)                Defines the toxic probit of section k due to a g-
direction release on floor f from section s in the positive-y monitor direction
        BelowToxicProbit(s,k,f,g)                Defines the toxic probit of section k due to a g-
direction release on floor f from section s in the negative-y monitor direction
        TopToxicProbit(s,k,f,g)                  Defines the toxic probit of section k due to a g-
direction release on floor f from section s in the top monitor direction
        BottomToxicProbit(s,k,f,g)               Defines the toxic probit of section k due to a g-
direction release on floor f from section s in the bottom monitor direction

***Toxic Probability
        CombinedToxicEffect(s,k)                 Defines the combined probability of all release
directions and monitor regions and floors that a release from section k affects section s

**Smoke_____________________________________________________________________
        sScaledDispersion(s,f,h)                 Scaled dispersion of smoke in region h from a fire
in s on floor f due to a release in the g direction
        EscapeSpeed(s,k,f,h)
        EscapeTime(s,m)
        IncapacitationCO(s,k,f,h)
        IncapacitationCO2(s,k,f,h)
        IncapacitatedCO(s,m)
        IncapacitatedCO2(s,m)

**Objective Function________________________________________________________
        Objective                                Defines objective function for FLP;


*#############################################################################
*Equation Definition##########################################################
*#############################################################################

**Objective Function_____________________________________________________
*$onecho>a
         Objective ..                                                    Prob =e=
sum(s$(SectionCost(s) ne 0),SectionCost(s)*sum(k$(LeakSource(k) ne 0),
sum(m,EscapeProbability(s,k,m))))+0.001*sum((s,k,m),SectionMuster(s,m)*(I(s,k,m)+I4(s,k)+I5(s,k,m)))

+sum(s$(SectionCost(s) ne 0),((SectionCost(s))*(sum(k$(LeakSource(k) ne 0), MitigatedProb(s,k)))))
```

```
+sum(s$(SectionCost(s) ne 0),SectionCost(s)*sum(k$(LeakSource(k) ne 0),
ToxicProbability(s,k)))+0.0001*sum((s,f,g,h),tSD(s,f,g,h));

*$offecho
*        Objective ..                                                    Prob =e=
sum((s,k,f),up(s,k,f)+down(s,k,f));
*        Objective ..                                                    Prob =e= 1;

**Area, AR, and Side Length Equations_____________________________________
         AreaConstraint(s) ..                                           Area(s) =e=
Lx(s)*Ly(s);
         LengthConstraintXLo(s) ..                                      Lx(s) =g= LBx(s);
         LengthConstraintXHi(s) ..                                      Lx(s) =l= UBx(s);
         LengthConstraintYLo(s) ..                                      Ly(s) =g= LBy(s);
         LengthConstraintYHi(s) ..                                      Ly(s) =l= UBy(s);


*Separation Distance_____________________________________________________
         DefineDx(s,k)$(ord(s) ne ord(k)) ..                            Dx(s,k) =e= (Lx(s) +
Lx(k))/2 + sep;
         DefineDy(s,k)$(ord(s) ne ord(k)) ..                            Dy(s,k) =e= (Ly(s) +
Ly(k))/2 + sep;


*Boundary Constraints____________________________________________________
         BoundaryX1(s) ..                                               x(s) =g= Lx(s)/2;
         BoundaryX2(s) ..                                               x(s) =l= Wx -
Lx(s)/2;
         BoundaryY1(s) ..                                               y(s) =g= Ly(s)/2;
         BoundaryY2(s) ..                                               y(s) =l= Wy -
Ly(s)/2;


*Non-Overlap Constraints_________________________________________________
         LeftConstraint(s,k,f)$(ord(s) gt ord(k)) ..                    x(s) =l= (1-
a(s,k,f))*N + (x(k) - Dx(s,k));
```

```
         RightConstraint(s,k,f)$(ord(s) gt ord(k)) ..                    x(s) =g= (x(k) +
Dx(s,k)) - (1-b(s,k,f))*N;
         BelowConstraint(s,k,f)$(ord(s) gt ord(k)) ..                    y(s) =l= (1-
c(s,k,f))*N + (y(k) - Dy(s,k));
         AboveConstraint(s,k,f)$(ord(s) gt ord(k)) ..                    y(s) =g= (y(k) +
Dy(s,k)) - (1-d(s,k,f))*N;
         DisjunctionCheck1(s,k,f) ..                                     a(s,k,f) =e=
b(k,s,f);
         DisjunctionCheck2(s,k,f) ..                                     c(s,k,f) =e=
d(k,s,f);


*Decision Variables to Select Non-Overlap Constraint_____________________________
         DecisionConstraint(s,k,f)$(ord(s) gt ord(k)) ..                 a(s,k,f) + b(s,k,f)
+ c(s,k,f) + d(s,k,f) - ZZ(s,k,f) =e= 0;
         DecisionConstraint2(s,k)$(ord(s) gt ord(k)) ..                  sum(f,ZZ(s,k,f)) =l=
Stories(s);
         DecisionConstraint3(s,k,f)$(ord(s) gt ord(k))..                 ZZ(s,k,f) =e=
ZZ(k,s,f);


*Muster Point Constraints_____________________________________________________
         MusterAssign(s) ..
sum(m,SectionMuster(s,m)) =e= 2;
         EscapeX1(s,m) ..                                                ex1(s,m) =e=
(mx(m)+x(s))/2;
         EscapeY1(s,m) ..                                                ey1(s,m) =e=
(my(m)+y(s))/2;
         EscapeX2(s,m) ..                                                ex2(s,m) =e= mx(m);
         EscapeY2(s,m) ..                                                ey2(s,m) =e= my(m);
         MusterLimit(m) ..                                               sum(s,
SectionMuster(s,m)) =l= 5;


*Blast Wall___________________________________________________________________
         BlastWallA(s,k)$(LeakSource(k) ne 0 and SectionCost(s) ne 0) ..  BWa(s,k) =l= (1-
(1/(Stories(s)+1)))*(sum(f, a(s,k,f)/Stories(s))+wa(s));
```

```
         BlastWallB(s,k)$(LeakSource(k) ne 0 and SectionCost(s) ne 0) ..         BWb(s,k) =l= (1-
(1/(Stories(s)+1)))*(sum(f, b(s,k,f)/Stories(s))+wb(s));
         BlastWallC(s,k)$(LeakSource(k) ne 0 and SectionCost(s) ne 0) ..         BWc(s,k) =l= (1-
(1/(Stories(s)+1)))*(sum(f, c(s,k,f)/Stories(s))+wc(s));
         BlastWallD(s,k)$(LeakSource(k) ne 0 and SectionCost(s) ne 0) ..         BWd(s,k) =l= (1-
(1/(Stories(s)+1)))*(sum(f, d(s,k,f)/Stories(s))+wd(s));
         BlastWall(s,k)$(LeakSource(k) ne 0 and SectionCost(s) ne 0) ..          BW(s,k) =e=
BWa(s,k)+BWb(s,k)+BWc(s,k)+BWd(s,k);
         MaxBlastWalls ..                                                       MaxWalls =e= sum(s,
wa(s)+wb(s)+wc(s)+wd(s));


*Floor Constraints_____________________________________________________________
         OneFloor(s) ..                                                         sum(f, V(s,f)) =e=
Stories(s);
         FloorConstraint1(s,k,f)$(ord(s) gt ord(k)) ..                          ZZ(s,k,f) =g=
V(s,f)+V(k,f)-1;
         FloorConstraint2(s,k,f)$(ord(s) gt ord(k)) ..                          ZZ(s,k,f) =l= 1-
V(s,f)+V(k,f);
         FloorConstraint3(s,k,f)$(ord(s) gt ord(k)) ..                          ZZ(s,k,f) =l=
1+V(s,f)-V(k,f);
         FloorOccupied1(f) ..                                                   FO(f) =l=
sum(s,V(s,f));
         FloorOccupied2(s,f) ..                                                 FO(f) =g= V(s,f);
         FloorOrder(f,l)$(ord(l) gt ord(f)) ..                                  FO(f) =g= FO(l);
         NumberOfFloors(f) ..                                                   NF =g= ord(f)*FO(f);
         NumberOfFloors2 ..                                                     NF =l= card(f);
*         FloorAdjacent(f,l,s)$(ord(l) gt ord(f)) ..                            ord(f) =g=
V(s,f)*V(s,l)*ord(l)-Stories(s)+1;
         FloorAdjacent(f,l,s)$(ord(l) eq ord(f)-Stories(s)) ..                  V(s,f)+V(s,l) =l= 1;
         FloorNumber(s) ..                                                      Floor(s) =e= sum(f,
ord(f)*V(s,f)/Stories(s));

$onecho>a
         RelativeFloor1(s,k,f,l)$(ord(f) gt ord(l) and ord(s) ne ord(k)) ..     upstar(s,k,f,l) =l=
1+log(V(s,f)+0.61)+log(V(k,l)+0.61);
         RelativeFloor1(s,k,f,l)$(ord(f) gt ord(l) and ord(s) ne ord(k)) ..     upstar(s,k,f,l) =e=
V(s,f)*V(k,l);
```

```
         RelativeFloor2(s,k,f,l)$(ord(f) gt ord(l) and ord(s) ne ord(k)) ..      upstar(s,k,f,l) =l=
1-V(s,f)+V(k,l);
         RelativeFloor3(s,k,f,l)$(ord(f) gt ord(l) and ord(s) ne ord(k)) ..      upstar(s,k,f,l) =g=
V(s,f)+V(k,l)-1;
         RelativeFloor4(s,k,f,l)$(ord(f) gt ord(l) and ord(s) ne ord(k)) ..      up(s,k,f) =g=
upstar(s,k,f,l);
*         RelativeFloor5(s,k,f)$(ord(s) ne ord(k)) ..                             up(s,k,f) =l=
sum(l, upstar(s,k,f,l));
*         RelativeFloor6(s,k,f,l)$(ord(f) gt ord(l) and ord(s) ne ord(k)) ..      up(s,k,f) =e=
down(k,s,l);
*         RelativeFloor7(s,k,f)$(ord(s) ne ord(k)) ..
up(s,k,f)+down(s,k,f) =l= V(s,f);
*         RelativeFloor7(s,k,f,l)$(ord(s) ne ord(k)) ..                             upstar(s,k,f,l)
=l= V(s,f);
*         RelativeFloor7(s,k,f)$(ord(s) ne ord(k)) ..
up(s,k,f)+down(s,k,f)+ZZ(s,k,f) =e= 1;
*         RelativeFloor8(s,k,f,l)$(ord(f) lt ord(l) and ord(s) ne ord(k)) ..      upstar(s,k,f,l) =e=
0;
$offecho

$onecho>a
         RelativeFloor1(s,k,f,l)$(ord(f) gt ord(l) and ord(s) ne ord(k)) ..      upstar(s,k,f,l) =l=
V(s,f);
         RelativeFloor2(s,k,f,l)$(ord(f) gt ord(l) and ord(s) ne ord(k)) ..      upstar(s,k,f,l) =l=
V(k,l);
         RelativeFloor3(s,k,f,l)$(ord(s) ne ord(k) and ord(l) lt ord(f)) ..      upstar(s,k,f,l) =g=
V(s,f)+V(k,l)-1;
         RelativeFloor4(s,k,f,l)$(ord(s) ne ord(k) and ord(l) lt ord(f)) ..      up(s,k,f) =g=
upstar(s,k,f,l);
         RelativeFloor5(s,k,f)$(ord(s) ne ord(k)) ..                             up(s,k,f) =l= sum(l,
upstar(s,k,f,l));
         RelativeFloor6(s,k,f,l)$(ord(s) ne ord(k) and ord(f) gt ord(l)) ..      up(s,k,f) =e=
down(k,s,l);
*         RelativeFloor7(s,k,f)$(ord(s) ne ord(k)) ..
up(s,k,f)+down(s,k,f) =l= ZZ(s,k,f);
$offecho

$onecho>a
```

```
         This works for upstar!
         RelativeFloor1(s,k,f,l)$(ord(f) eq ord(l) and ord(s) ne ord(k)) ..      upstar(s,k,f,l) =l=
(2-ZZ(s,k,f)-ZZ(s,k,l));
         RelativeFloor2(s,k,f,l)$(ord(f) gt ord(l) and ord(s) ne ord(k)) ..      upstar(s,k,f,l) =g=
V(s,f)+V(k,l)-1;
         RelativeFloor3(s,k,f,l)$(ord(s) ne ord(k) and ord(l) lt ord(f)) ..      upstar(s,k,f,l) =l=
1-V(s,f)+V(k,l);
         RelativeFloor4(s,k,f,l)$(ord(s) ne ord(k) and ord(l) lt ord(f)) ..      upstar(s,k,f,l) =l=
V(s,f);
         RelativeFloor5(s,k,f,l)$(ord(s) ne ord(k) and ord(l) lt ord(f)) ..      upstar(s,k,f,l) =l=
1+V(s,f)-V(k,l);
         RelativeFloor6(s,k,f,l)$(ord(s) ne ord(k) and ord(f) lt ord(l)) ..      upstar(s,k,f,l) =e=
0;
$offecho

         RelativeFloor1(s,k,f,l)$(ord(f) eq ord(l) and ord(s) ne ord(k)) ..      upstar(s,k,f,l) =l=
(2-ZZ(s,k,f)-ZZ(s,k,l));
         RelativeFloor2(s,k,f,l)$(ord(f) gt ord(l) and ord(s) ne ord(k)) ..      upstar(s,k,f,l) =g=
V(s,f)+V(k,l)-1;
         RelativeFloor3(s,k,f,l)$(ord(s) ne ord(k) and ord(l) lt ord(f)) ..      upstar(s,k,f,l) =l=
1-V(s,f)+V(k,l);
         RelativeFloor4(s,k,f,l)$(ord(s) ne ord(k) and ord(l) lt ord(f)) ..      upstar(s,k,f,l) =l=
V(s,f);
         RelativeFloor5(s,k,f,l)$(ord(s) ne ord(k) and ord(l) lt ord(f)) ..      upstar(s,k,f,l) =l=
1+V(s,f)-V(k,l);
         RelativeFloor6(s,k,f,l)$(ord(s) ne ord(k) and ord(f) lt ord(l)) ..      upstar(s,k,f,l) =e=
0;
         RelativeFloor7(s,k,f,l)$(ord(s) ne ord(k) and ord(l) lt ord(f)) ..      up(s,k,f) =g=
upstar(s,k,f,l);
         RelativeFloor8(s,k,f)$(ord(s) ne ord(k)) ..                             up(s,k,f) =l=
sum(l$(ord(l) lt ord(f)),upstar(s,k,f,l));
         RelativeFloor9(s,k,f,l)$(ord(s) ne ord(k) and ord(l) lt ord(f)) ..      upstar(s,k,f,l) =e=
downstar(k,s,l,f);
         RelativeFloor10(s,k,f,l)$(ord(s) ne ord(k) and ord(l) gt ord(f)) ..     down(s,k,f) =g=
downstar(s,k,f,l);
         RelativeFloor11(s,k,f)$(ord(s) ne ord(k)) ..                            down(s,k,f) =l=
sum(l$(ord(l) gt ord(f)), downstar(s,k,f,l));
```

```
*Vapor Cloud Explosion Constraints_____________________________________________
**Local Explosion
         ExpPressure(s,k)$(ord(s) ne ord(k) and LeakSource(k) ne 0 and SectionCost(s) ne 0) ..
P(s,k) =e= Const(k)*(Patm*(Eexp(k)/Patm)**(1/3))/((sqrt(sqr((x(s)-x(k))+epsilon)+sqr(y(s)-
y(k))+epsilon)*0.3048));
         ExpProbit(s,k)$(ord(s) ne ord(k) and LeakSource(k) ne 0 and SectionCost(s) ne 0) ..
EProbit(s,k) =g= -23.8+2.92*((log(P(s,k)+epsilon)+(1/3)*log(FireScale)));
         DestProbability(s,k)$(ord(s) ne ord(k) and LeakSource(k) ne 0 and SectionCost(s) ne 0) ..
DestructionProbability(s,k) =e= errorf((EProbit(s,k)-5)/sqrt(2))*TotalPExp(k);
         ModifiedProbability(s,k)$(ord(s) ne ord(k) and LeakSource(k) ne 0 and SectionCost(s) ne 0)
..           MitigatedProb(s,k) =e= (1-BW(s,k))*DestructionProbability(s,k);

**Dispersed Cloud Explosion
*$onecho>a
         eScaledDispersion(s,f,g,h)$(LeakSource(s) ne 0) ..
eSD(s,h) =g= (10**(-
5))*LeakSource(s)*JetFireMassFlow(s)*(100*BR(s,f,h)*(ee(g,h)+efi(g,h)*WindSpeed)+eg(g,h)*WindSpeed+ea
c(g,h));
         DispersedEnergy(s,k,f,h)$(LeakSource(k) ne 0 and IgnSource(s) ne 0) ..
dispE(s,k,h) =g= eSD(k,h)*Area(s)*FloorSpacing*FlammableDensity*GasHoC(k)/(FireScale*10000);
         DispersedBase(s,k,j,h)$(ord(s) ne ord(k) and LeakSource(k) ne 0 and IgnSource(s) ne 0) ..
cprime(s,k,j,h) =g= Const(s)*(Patm*((dispE(s,k,h)+1)/Patm)**(1/3))/((sqrt(sqr((x(s)-
x(j))+epsilon)+sqr(y(s)-y(j))+epsilon)*0.3048));
         LFLExceedance(s,k,h)$(ord(s) ne ord(k) and LeakSource(s) ne 0 and IgnSource(k) ne 0) ..
eSD(s,h) =l= (1-LFLExceed(s,h))*LFLMass;

         DispersedEProbitPosX(s,k,j,f,h)$(ord(s) ne ord(k) and ord(k) ne ord (j)
                 and LeakSource(s) ne 0 and IgnSource(k) ne 0 and SectionCost(j) ne 0) ..
EProbit(s,k) =g= -
23.8+2.92*(log(cprime(s,k,j,'PosX')+0.001)+10*log(b(j,s,f)+0.00001)+10*log(a(s,k,f)+0.00001)+10*log(L
FLExceed(s,'PosX')+0.00001)+(1/3)*log(FireScale*10000));
         DispersedEProbitNegX(s,k,j,f,h)$(ord(s) ne ord(k) and ord(k) ne ord (j)
                 and LeakSource(s) ne 0 and IgnSource(k) ne 0 and SectionCost(j) ne 0) ..
EProbit(s,k) =g= -
23.8+2.92*(log(cprime(s,k,j,'NegX')+0.001)+10*log(a(j,s,f)+0.00001)+10*log(b(s,k,f)+0.00001)+10*log(L
FLExceed(s,'NegX')+0.00001)+(1/3)*log(FireScale*10000));
         DispersedEProbitPosY(s,k,j,f,h)$(ord(s) ne ord(k) and ord(k) ne ord (j)
```

```
                and LeakSource(s) ne 0 and IgnSource(k) ne 0 and SectionCost(j) ne 0) ..
EProbit(s,k) =g= -
23.8+2.92*(log(cprime(s,k,j,'PosY')+0.001)+10*log(c(j,s,f)+0.00001)+10*log(d(s,k,f)+0.00001)+10*log(L
FLExceed(s,'PosY')+0.00001)+(1/3)*log(FireScale*10000));
        DispersedEProbitNegY(s,k,j,f,h)$(ord(s) ne ord(k) and ord(k) ne ord (j)
                and LeakSource(s) ne 0 and IgnSource(k) ne 0 and SectionCost(j) ne 0) ..
EProbit(s,k) =g= -
23.8+2.92*(log(cprime(s,k,j,'NegY')+0.001)+10*log(d(j,s,f)+0.00001)+10*log(c(s,k,f)+0.00001)+10*log(L
FLExceed(s,'NegY')+0.00001)+(1/3)*log(FireScale*10000));
        DispersedEProbitTop(s,k,j,f,h)$(ord(s) ne ord(k) and ord(k) ne ord (j)
                and LeakSource(s) ne 0 and IgnSource(k) ne 0 and SectionCost(j) ne 0) ..
EProbit(s,k) =g= -
23.8+2.92*(log(cprime(s,k,j,'Top')+0.001)+10*log(down(j,s,f)+0.00001)+10*log(up(s,k,f)+0.00001)+10*lo
g(LFLExceed(s,'Top')+0.00001)+(1/3)*log(FireScale*10000));
        DispersedEProbitBottom(s,k,j,f,h)$(ord(s) ne ord(k) and ord(k) ne ord (j)
                and LeakSource(s) ne 0 and IgnSource(k) ne 0 and SectionCost(j) ne 0) ..
EProbit(s,k) =g= -
23.8+2.92*(log(cprime(s,k,j,'Bottom')+0.001)+10*log(up(j,s,f)+0.00001)+10*log(down(s,k,f)+0.00001)+10
*log(LFLExceed(s,'Bottom')+0.00001)+(1/3)*log(FireScale*10000));
*$offecho
$onecho>a
        eScaledDispersion(s,f,g,h)$(LeakSource(s) ne 0) ..
eSD(s,h) =g= 0;
        DispersedEnergy(s,k,f,h)$(LeakSource(k) ne 0 and IgnSource(s) ne 0) ..
dispE(s,k,h) =g= 0;
        DispersedBase(s,k,j,h)$(ord(s) ne ord(k) and LeakSource(k) ne 0 and IgnSource(s) ne 0) ..
cprime(s,k,j,h) =g= 0;
        LFLExceedance(s,k,h)$(ord(s) ne ord(k) and LeakSource(s) ne 0 and IgnSource(k) ne 0) ..
(1-LFLExceed(s,h))*LFLMass =l= eSD(s,h);

        DispersedEProbitPosX(s,k,j,f,h)$(ord(s) ne ord(k) and ord(k) ne ord (j)
                and LeakSource(s) ne 0 and IgnSource(k) ne 0 and SectionCost(j) ne 0) ..
EProbit(s,k) =g= -100;
        DispersedEProbitNegX(s,k,j,f,h)$(ord(s) ne ord(k) and ord(k) ne ord (j)
                and LeakSource(s) ne 0 and IgnSource(k) ne 0 and SectionCost(j) ne 0) ..
EProbit(s,k) =g= -100;
        DispersedEProbitPosY(s,k,j,f,h)$(ord(s) ne ord(k) and ord(k) ne ord (j)
```

```
                and LeakSource(s) ne 0 and IgnSource(k) ne 0 and SectionCost(j) ne 0) ..
EProbit(s,k) =g= -100;
        DispersedEProbitNegY(s,k,j,f,h)$(ord(s) ne ord(k) and ord(k) ne ord (j)
                and LeakSource(s) ne 0 and IgnSource(k) ne 0 and SectionCost(j) ne 0) ..
EProbit(s,k) =g= -100;
        DispersedEProbitTop(s,k,j,f,h)$(ord(s) ne ord(k) and ord(k) ne ord (j)
                and LeakSource(s) ne 0 and IgnSource(k) ne 0 and SectionCost(j) ne 0) ..
EProbit(s,k) =g= -100;
        DispersedEProbitBottom(s,k,j,f,h)$(ord(s) ne ord(k) and ord(k) ne ord (j)
                and LeakSource(s) ne 0 and IgnSource(k) ne 0 and SectionCost(j) ne 0) ..
EProbit(s,k) =g= -100;
$offecho

*Fire Constraints_____________________________________________________________
**Fire Effect
        FireIntensity1(s,k,m)$(ord(s) ne ord(k) and LeakSource(k) ne 0 and SectionCost(s) ne 0) ..
I1(s,k,m) =g= LeakSource(k)*((E(k))/((4*3.14*(1+(sqr((x(s)-(x(k)+(Floor(s)-
Floor(k))*xprime(k)))*0.3048)+sqr((ey1(s,m)-y(k))*0.3048)+sqr(((Floor(s)-
Floor(k))*FloorSpacing)*0.3048))))));
        FireIntensity2(s,k,m)$(ord(s) ne ord(k) and LeakSource(k) ne 0 and SectionCost(s) ne 0) ..
I1(s,k,m) =g= LeakSource(k)*((E(k))/((4*3.14*(1+(sqr((x(s)-(x(k)+(Floor(s)-
Floor(k))*xprime(k)))*0.3048)+sqr((ey2(s,m)-y(k))*0.3048)+sqr(((Floor(s)-
Floor(k))*FloorSpacing)*0.3048))))));
        FireIntensity3(s,k,m)$(ord(s) ne ord(k) and LeakSource(k) ne 0 and SectionCost(s) ne 0) ..
I1(s,k,m) =g= LeakSource(k)*((E(k))/((4*3.14*(1+(sqr((ex1(s,m)-(x(k)+(Floor(s)-
Floor(k))*xprime(k)))*0.3048)+sqr((ey2(s,m)-y(k))*0.3048)+sqr(((Floor(s)-
Floor(k))*FloorSpacing)*0.3048))))));

        FireIntensity4(s,k,m)$(ord(s) ne ord(k) and LeakSource(k) ne 0 and SectionCost(s) ne 0) ..
I2(s,k,m) =g= LeakSource(k)*((E(k))/((4*3.14*(1+(sqr((ex1(s,m)-(x(k)+(Floor(s)-
Floor(k))*xprime(k)))*0.3048)+sqr((y(s)-y(k))*0.3048)+sqr(((Floor(s)-
Floor(k))*FloorSpacing)*0.3048))))));
        FireIntensity5(s,k,m)$(ord(s) ne ord(k) and LeakSource(k) ne 0 and SectionCost(s) ne 0) ..
I2(s,k,m) =g= LeakSource(k)*((E(k))/((4*3.14*(1+(sqr((ex2(s,m)-(x(k)+(Floor(s)-
Floor(k))*xprime(k)))*0.3048)+sqr((y(s)-y(k))*0.3048)+sqr(((Floor(s)-
Floor(k))*FloorSpacing)*0.3048))))));
        FireIntensity6(s,k,m)$(ord(s) ne ord(k) and LeakSource(k) ne 0 and SectionCost(s) ne 0) ..
I2(s,k,m) =g= LeakSource(k)*((E(k))/((4*3.14*(1+(sqr((ex2(s,m)-(x(k)+(Floor(s)-
```

```
Floor(k))*xprime(k)))*0.3048)+sqr((ey1(s,m)-y(k))*0.3048)+sqr(((Floor(s)-
Floor(k))*FloorSpacing)*0.3048))))));

         FireIntensity7(s,k,m)$(ord(s) ne ord(k) and LeakSource(k) ne 0 and SectionCost(s) ne 0) ..
I3(s,k,m) =e= LeakSource(k)*((E(k))/((4*3.14*(1+(sqr((ex1(s,m)-x(k))*0.3048)+sqr((ey1(s,m)-
y(k))*0.3048)+sqr((Floor(s)-Floor(k))*FloorSpacing*0.3048))))));
         FireIntensity8(s,k)$(ord(s) ne ord(k) and LeakSource(k) ne 0 and SectionCost(s) ne 0) ..
I4(s,k) =e= (LeakSource(k)*((E(k))/((4*3.14*(1+(sqr((x(s)-(x(k)+(Floor(s)-
Floor(k))*xprime(k)))*0.3048)+sqr((y(s)-y(k))*0.3048)+sqr(((Floor(s)-
Floor(k))*FloorSpacing)*0.3048)))))))*(1-BW(s,k))+0.0001;
         FireIntensity9(s,k,m)$(LeakSource(k) ne 0 and SectionCost(s) ne 0) ..
I5(s,k,m) =e= LeakSource(k)*((E(k))/((4*3.14*(1+(sqr((ex2(s,m)-(x(k)+(Floor(s)-
Floor(k))*xprime(k)))*0.3048)+sqr((ey2(s,m)-y(k))*0.3048)+sqr(((Floor(s)-
Floor(k))*FloorSpacing)*0.3048))))));

**Muster Choice
         PathChoice(s,k,m)$(ord(s) ne ord(k) and LeakSource(k) ne 0) ..
I(s,k,m) =e= LeakSource(k)*(Fa(s,m)*I1(s,k,m)+Fb(s,m)*I2(s,k,m)+Fc(s,m)*I3(s,k,m));
         PathConstraint(s,m) ..
Fa(s,m) + Fb(s,m) + Fc(s,m) =e= 1;


**Fire Probit and Probability
         FireProbitEscape(s,k,m)$(ord(s) ne ord(k) and LeakSource(k) ne 0 and SectionCost(s) ne 0) ..
FProbitEscape(s,k,m) =e= -
14.9+2.56*(log((tesc(s,m)*((I(s,k,m))**(4/3))+0.0001))+(4/3)*log(FireScale));
         FireProbitMidpoint(s,k)$(ord(s) ne ord(k) and LeakSource(k) ne 0 and SectionCost(s) ne 0) ..
FProbitMidpoint(s,k) =e= -14.9+2.56*(log(FtExposure*((I4(s,k))**(4/3))+0.0001)+(4/3)*log(FireScale));
         FireProbitMuster(s,k,m)$(ord(s) ne ord(k) and LeakSource(k) ne 0 and SectionCost(s) ne 0) ..
FProbitMuster(s,k,m) =e= -
14.9+2.56*(log(FtExposure*((I5(s,k,m))**(4/3)+0.0001))+(4/3)*log(FireScale));
         EscProbability(s,k,m)$(ord(s) ne ord(k) and LeakSource(k) ne 0 and SectionCost(s) ne 0) ..
EscapeProbability(s,k,m) =e= SectionMuster(s,m)*TotalPFire(k)*((((errorf((FProbitEscape(s,k,m)-
5)/sqrt(2)))

+(errorf((FProbitMuster(s,k,m)-5)/sqrt(2))))+(errorf((FProbitMidpoint(s,k)-
5)/sqrt(2))))/4+Incap(s,m));
```

```
*         EscProbability(s,k,m)$(ord(s) ne ord(k) and LeakSource(k) ne 0 and SectionCost(s) ne 0) ..
EscapeProbability(s,k,m) =e= 0.5;

*Toxic Constraints_____________________________________________________________
**Blockage Ratios
         RightBlockage(s,f)$(LeakSource(s) ne 0) ..
BR(s,f,'PosX') =e= LeakSource(s)*sum(k, a(s,k,f)*Area(k))/((Wx-x(s)+epsilon)*Wy);
         LeftBlockage(s,f)$(LeakSource(s) ne 0) ..
BR(s,f,'NegX') =e= LeakSource(s)*sum(k, b(s,k,f)*Area(k))/((x(s)+epsilon)*Wy);
         AboveBlockage(s,f)$(LeakSource(s) ne 0) ..
BR(s,f,'PosY') =e= LeakSource(s)*sum(k, c(s,k,f)*Area(k))/((Wy-y(s)+epsilon)*Wx);
         BelowBlockage(s,f)$(LeakSource(s) ne 0) ..
BR(s,f,'NegY') =e= LeakSource(s)*sum(k, d(s,k,f)*Area(k))/((y(s)+epsilon)*Wx);
         UpBlockage(s,f)$(LeakSource(s) ne 0) ..
BR(s,f,'Top') =e= V(s,f)*LeakSource(s)*sum(k, up(s,k,f)*Area(k)/(Wx*Wy));
         DownBlockage(s,f)$(LeakSource(s) ne 0) ..
BR(s,f,'Bottom') =e= V(s,f)*LeakSource(s)*sum(k, down(s,k,f)*Area(k)/(Wx*Wy));


**Scaled Dispersion
         tScaledDispersion(s,f,g,h)$(LeakSource(s) ne 0) ..
tSD(s,f,g,h) =g= (10**(-
5))*LeakSource(s)*JetFireMassFlow(s)*(100*BR(s,f,h)*(te(g,h)+tfi(g,h)*WindSpeed)+tg(g,h)*WindSpeed+ta
c(g,h));


**Toxic Probit and Probability
         RightToxicProbit(s,k,f,g)$(ord(s) ne ord(k) and LeakSource(s) ne 0 and SectionCost(k) ne
0)..           ToxicProbit(s,k,f,g,'PosX') =e= (1-a(s,k,f))*(-T)+(-
31.42+3.008*1.43*log(epsilon+tSD(s,f,g,'PosX'))+3.008*1.43*log(1000000)+3.008*log(TtExposure));
         LeftToxicProbit(s,k,f,g)$(ord(s) ne ord(k) and LeakSource(s) ne 0 and SectionCost(k) ne 0)..
ToxicProbit(s,k,f,g,'NegX') =e= (1-b(s,k,f))*(-T)+(-
31.42+3.008*1.43*log(epsilon+tSD(s,f,g,'NegX'))+3.008*1.43*log(1000000)+3.008*log(TtExposure));
         AboveToxicProbit(s,k,f,g)$(ord(s) ne ord(k) and LeakSource(s) ne 0 and SectionCost(k) ne
0)..           ToxicProbit(s,k,f,g,'PosY') =e= (1-c(s,k,f))*(-T)+(-
31.42+3.008*1.43*log(epsilon+tSD(s,f,g,'PosY'))+3.008*1.43*log(1000000)+3.008*log(TtExposure));
```

```
         BelowToxicProbit(s,k,f,g)$(ord(s) ne ord(k) and LeakSource(s) ne 0 and SectionCost(k) ne
0)..           ToxicProbit(s,k,f,g,'NegY') =e= (1-d(s,k,f))*(-T)+(-
31.42+3.008*1.43*log(epsilon+tSD(s,f,g,'NegY'))+3.008*1.43*log(1000000)+3.008*log(TtExposure));
         TopToxicProbit(s,k,f,g)$(ord(s) ne ord(k) and LeakSource(k) ne 0 and SectionCost(k) ne 0)..
ToxicProbit(s,k,f,g,'Top') =e= (1-up(s,k,f))*(-T)+(-
31.42+3.008*1.43*log(epsilon+tSD(s,f,g,'Top'))+3.008*1.43*log(1000000)+3.008*log(TtExposure));
         BottomToxicProbit(s,k,f,g)$(ord(s) ne ord(k) and LeakSource(k) ne 0 and SectionCost(k) ne
0)..          ToxicProbit(s,k,f,g,'Bottom') =e= (1-down(s,k,f))*(-T)+(-
31.42+3.008*1.43*log(epsilon+tSD(s,f,g,'Bottom'))+3.008*1.43*log(1000000)+3.008*log(TtExposure));
         CombinedToxicEffect(s,k)$(ord(s) ne ord(k) and LeakSource(k) ne 0 and SectionCost(s) ne 0)..
ToxicProbability(s,k) =e= LeakSource(k)*TotalPEnv(k)*sum(f,sum(g,sum(h,
errorf((ToxicProbit(k,s,f,g,h)-5)/sqrt(2)))))/5;


*Smoke Modeling Constraints_____________________________________________________
$onecho>a
**Escape
         sScaledDispersion(s,f,h)$(LeakSource(s) ne 0) ..
sSD(s,f,h) =g= (10**(-
5))*LeakSource(s)*JetFireMassFlow(s)*(100*BR(s,f,h)*(se(h)+sfi(h)*WindSpeed)+sg(h)*WindSpeed+sac(h));
         EscapeSpeed(s,k,f,h)$(LeakSource(k) ne 0 and SectionCost(s) ne 0) ..
vesc(s) =l= 1.2-1.8*sSD(k,f,h);
         EscapeTime(s,m)$(SectionCost(s) ne 0) ..
tesc(s,m) =e= SectionMuster(s,m)*((sqrt(sqr(x(s)-mx(m)))+sqrt(sqr(y(s)-my(m))))/(vesc(s)+0.01));

**Toxic
         IncapacitationCO(s,k,f,h)$(ord(s) ne ord(k) and LeakSource(s) ne 0 and SectionCost(k) ne 0)
..          tincCO(s) =l= 30/((3.317E-5)*sSD(s,f,h)*50+0.001);
         IncapacitationCO2(s,k,f,h)$(ord(s) ne ord(k) and LeakSource(s) ne 0 and SectionCost(k) ne 0)
..         tincCO2(s) =l= exp(6.1623-0.5189*sSD(s,f,h));
         IncapacitatedCO(s,m) ..
tesc(s,m) =g= (Incap(s,m))*tincCO(s);
         IncapacitatedCO2(s,m) ..
tesc(s,m) =g= (Incap(s,m))*tincCO2(s);
$offecho
*$onecho>a
**Escape
```

```
         sScaledDispersion(s,f,h)$(LeakSource(s) ne 0) ..
sSD(s,f,h) =g= (10**(-
7))*LeakSource(s)*JetFireMassFlow(s)*(100*BR(s,f,h)*(se(h)+sfi(h)*WindSpeed)+sg(h)*WindSpeed+sac(h));
         EscapeSpeed(s,k,f,h)$(LeakSource(k) ne 0 and SectionCost(s) ne 0) ..
vesc(s) =l= 1.2-1.8*sSD(k,f,h);
         EscapeTime(s,m)$(SectionCost(s) ne 0) ..
tesc(s,m) =e= SectionMuster(s,m)*((sqrt(sqr(x(s)-mx(m))+0.01)+sqrt(sqr(y(s)-
my(m))+0.01))/(vesc(s)+0.01));

**Toxic
         IncapacitationCO(s,k,f,h)$(ord(s) ne ord(k) and LeakSource(s) ne 0 and SectionCost(k) ne 0)
..          tincCO(s) =l= 30/((3.317E-5)*sSD(s,f,h)*50+0.1);
         IncapacitationCO2(s,k,f,h)$(ord(s) ne ord(k) and LeakSource(s) ne 0 and SectionCost(k) ne 0)
..         tincCO2(s) =l= exp(6.1623-0.5189*sSD(s,f,h));
         IncapacitatedCO(s,m) ..
1000*(Incap(s,m))+tincCO(s) =g= tesc(s,m);
         IncapacitatedCO2(s,m) ..
1000*(Incap(s,m))+tincCO2(s) =g= tesc(s,m);
*$offecho


*###############################################################################
*Model##########################################################################
*###############################################################################

Model
$onecho>a
      Initialization      /First,
AreaConstraint1,LengthConstraintXLo,LengthConstraintXHi,LengthConstraintYLo,LengthConstraintYHi,
                           DefineDx, DefineDy, BoundaryX1, BoundaryX2, BoundaryY1, BoundaryY2,
LeftConstraint, RightConstraint,
                           AboveConstraint, BelowConstraint, DecisionConstraint, OneFloor,
FloorConstraint1, FloorConstraint2,
                           FloorConstraint3, FloorOccupied1, FloorOccupied2, FloorOrder,
NumberOfFloors, NumberOfFloors2,
                           MusterAssign, MusterLimit, FloorNumber/
$offecho
      Initialization      /all/
```

```
      FLP                 /all/


*###########################################################################
*Options###################################################################
*###########################################################################

Option iterlim = 100000000;
Option sysout = on;
Option subsystems;
*Option minlp = Convert;
FLP.OPTFILE = 1;
FLP.reslim = 100000000;
*FLP.SCALEOPT = 1;
$onecho > cplex.opt
printoptions yes
quality yes
scaind 0
simdisplay 2
names yes
*epgap 0.0003
*optcr = 0.4
$offecho
$onecho > dicopt.opt
stop 0
*nlptracefile nlptrace
*maxcycles 10
*maxcycles 5
*maxcycles 4
maxcycles 3
*maxcycles 2
*maxcycles 1
NLPSolver CONOPT
MIPSolver CPLEX
mipoptfile cplex.opt
nlpoptfile conopt.opt
epsmip 1e-4
```

```
$offecho
$onecho > conopt.opt
*lstcrs = t
*lsanrm = t
*rtnwmi = 1
*rtnwma = 1
*rtnwtr = 1
*rtobjr = 1
$offecho

*###########################################################################
*Solve#####################################################################
*###########################################################################

*solve Initialization using minlp minimizing z;
*solve FLP using minlp minimizing Prob;
scalar q;
scalar globiter;
scalar globmin ; globmin = inf ;
scalar globscale; globscale = inf;
parameter globx(s);
parameter globy(s);
parameter globLx(s);
parameter globLy(s);
parameter globmx(m);
parameter globmy(m);
parameter globFloor(s);
parameter globSectionMuster(s,m);
parameter globMitigatedProb(s,k);
parameter globEscapeProbability(s,k,m);
parameter globToxicProbability(s,k);
parameter globBW(s,k);

option bratio = 1;

for (q = 1 to 100,
         x.l(s) = uniform(0.2*Wx,0.8*Wx);
         y.l(s) = uniform(0.2*Wy,0.8*Wy);
```

```
        solve FLP using minlp minimizing Prob;
        if (FLP.modelstat ne 9 and FLP.solvestat eq 1,
                if (Prob.l le globmin,
                        globmin = Prob.l;
                        globiter = q;
                        globx(s) = x.l(s);
                        globy(s) = y.l(s);
                        globLx(s) = Lx.l(s);
                        globLy(s) = Ly.l(s);
                        globmx(m) = mx.l(m);
                        globmy(m) = my.l(m);
                        globFloor(s) = Floor.l(s);
                        globSectionMuster(s,m) = SectionMuster.l(s,m);
                        globMitigatedProb(s,k) = MitigatedProb.l(s,k);
                        globEscapeProbability(s,k,m) = EscapeProbability.l(s,k,m);
                        globToxicProbability(s,k) = ToxicProbability.l(s,k);
                        globBW(s,k) = BW.l(s,k);
                    );
            );
    );

$onecho>a
Display Prob.l, BW.l, BWa.l, BWb.l, BWc.l, BWd.l, wa.l, wb.l, wc.l, wd.l, a.l, b.l, c.l, d.l, x.l,
y.l,
        Floor.l, ZZ.l, TotalPExp, P.l, EProbit.l, random, JetFireMassFlow, BR.l, SD.l, mx.l, my.l,
        I.l, TotalArea, AreaRatio, DestructionProbability.l,MitigatedProb.l, EscapeProbability.l,
        ToxicProbability.l, ToxicProbit.l, SectionMuster.l,TotalPFire,TotalPExp,TotalPEnv,I4.l;
$offecho

Display Prob.l, SectionMuster.l, mx.l, my.l, I.l, I4.l, I5.l, Fa.l, Fb.l, Fc.l, FProbitEscape.l,
FProbitMidpoint.l, FProbitMuster.l, EscapeProbability.l,
         DestructionProbability.l, MitigatedProb.l, P.l, EProbit.l, wa.l, wb.l, wc.l, wd.l, BWa.l,
BWb.l, BWc.l, BWd.l, BW.l,
         JetFireMassFlow, tac, tfi, te, tg, a.l, b.l, c.l, d.l, BR.l, tSD.l, ToxicProbit.l,
ToxicProbability.l, FireScale, globscale, globmin, globiter,
         globx, globy, globLx, globLy, globmx, globmy, globFloor, globSectionMuster,
globMitigatedProb, globEscapeProbability, globToxicProbability, globBW
```

```
         UStar, FlameAngle, PoolD, PoolFireQ, PoolFireH, xprime, sSD.l, Incap.l, Floor.l, up.l,
down.l, dispE.l, upstar.l;

$onecho > a
execute_unload "DebugCMPModel.gdx" x.l, y.l, Lx.l, Ly.l, Floor.l, mx.l, my.l, SectionMuster.l

execute 'gdxxrw.exe DebugCMPModel.gdx SQ=N var=Ly.l rng=NewSheet!a4:i4'
execute 'gdxxrw.exe DebugCMPModel.gdx SQ=N var=Lx.l rng=NewSheet!a3:i3'
execute 'gdxxrw.exe DebugCMPModel.gdx SQ=N var=y.l rng=NewSheet!a2:i2'
execute 'gdxxrw.exe DebugCMPModel.gdx SQ=N var=x.l rng=NewSheet!a1:i1'

execute 'gdxxrw.exe DebugCMPModel.gdx SQ=N var=Floor.l rng=NewSheet!a10:i10'

execute 'gdxxrw.exe DebugCMPModel.gdx SQ=N var=my.l rng=NewSheet!a15:i15'
execute 'gdxxrw.exe DebugCMPModel.gdx SQ=N var=mx.l rng=NewSheet!a14:i14'
execute 'gdxxrw.exe DebugCMPModel.gdx SQ=N var=SectionMuster.l rng=NewSheet!a18:i30'
$offecho

$onecho>a
execute_unload "UpwardDispersionCMPModelGlobal.gdx" globx, globy, globLx, globLy, globFloor, globmx,
globmy, globSectionMuster

execute 'gdxxrw.exe UpwardDispersionCMPModelGlobal.gdx SQ=N par=globLy rng=NewSheet!a4:i4'
execute 'gdxxrw.exe UpwardDispersionCMPModelGlobal.gdx SQ=N par=globLx rng=NewSheet!a3:i3'
execute 'gdxxrw.exe UpwardDispersionCMPModelGlobal.gdx SQ=N par=globy rng=NewSheet!a2:i2'
execute 'gdxxrw.exe UpwardDispersionCMPModelGlobal.gdx SQ=N par=globx rng=NewSheet!a1:i1'

execute 'gdxxrw.exe UpwardDispersionCMPModelGlobal.gdx SQ=N par=globFloor rng=NewSheet!a10:i10'

execute 'gdxxrw.exe UpwardDispersionCMPModelGlobal.gdx SQ=N par=globmy rng=NewSheet!a15:i15'
execute 'gdxxrw.exe UpwardDispersionCMPModelGlobal.gdx SQ=N par=globmx rng=NewSheet!a14:i14'
execute 'gdxxrw.exe UpwardDispersionCMPModelGlobal.gdx SQ=N par=globSectionMuster
rng=NewSheet!a18:i30'
$offecho
```